Report on Local Seismicity for Lusitanian & Ebro Basins, including Earthquake Catalog.

Deliverable 2.5

Release Status: FINAL
Authors: Antonio Olaiz, Jorge Diez, Germán Ocampo, José Fernando Borges, João Cartaxo, Guillermo Marro, Francisco Pángaro, Manuel Ron, Paula Canteli, José Mediato, Iván Moreno
Edited by Mark Wilkinson
Date: October 2024
Filename and Version: PilotSTRATEGY_WP_2_D2_5_Report on Local Seismicity for Lusitania Ebro Basin_FINAL
Project ID Number: 101022664

PilotSTRATEGY (H2020- Topic LC-SC3-NZE-6-2020 - RIA)

Document History

Location

This document is stored in the following location:

Filename	Deliverable 2.5 – Report on Local Seismicity for Lusitania & Ebro Basin, including Earthquake Catalog
Location	Local Folder:

Revision History

This document has been through the following revisions:

Version No.	Revision Date	Filename/Location stored:	Brief Summary of Changes
1.0 – FINAL	October 2024		

Authorization

This document requires the following approvals:

AUTHORISATION	Name	Signature	Date
WP Leader	Mark Wilkinson	MW	17/10/2024
Project Coordinator	Isaline Gravaud	IG	23/10/2024

Distribution

This document has been distributed to:

Name	Title	Version Issued	Date of Issue
		PUBLIC	23/10/2024

The PilotSTRATEGY project has received funding from the European Union's Horizon 2020 research and innovation programme under grant agreement No. 101022664

Olaiz, A., Diez, J., Ocampo, G., Borges, J.F., Cartaxo, J., Marro, G., Pángaro, F., Ron, M., Canteli, P., Mediato, J., Moreno, I., 2024. Report on Local Seismicity for Lusitania & Ebro Basin, including Earthquake Catalog. WP2-Deliverable D2.5, EU H2020 PilotSTRATEGY project 101022664, 86 pp.

Disclaimer

The information and views set out in this report are those of the author(s) and do not necessarily reflect the official opinion of the European Union. Neither the European Union institutions and bodies nor any person acting on their behalf may be held responsible for the use which may be made of the information contained therein.

The PilotSTRATEGY project has received funding from the European Union's Horizon 2020 research and innovation programme under grant agreement No. 101022664

Executive summary

This deliverable reports on the assessment and monitoring of local seismicity in the PilotSTRATEGY target areas of Lopin (Spain) and the Lusitanian basin, offshore from Figueira da Foz (Portugal). Pre-injection monitoring is an essential task for any CO_2 injection project, to establish a baseline of natural and any man-made seismicity (such as explosions associated with quarrying). If CO_2 injection were to induce a seismic event, then knowing the natural pattern and intensity of seismic activity would be essential.

The seismic activity in the Lopín area (Spain, Ebro Basin) and the offshore Lusitanian Basin (Bacia Lusitaniana; Portugal) has been thoroughly analyzed. Both areas utilized existing earthquake catalogues: the IGN catalogue (1373 to 2024) for Spain and the "National Seismic Catalog," (2000 to 2023) for Portugal. The number, magnitude and spatial distribution of events has been reviewed for both areas. In the case of the Ebro area, events reported between 2003 and 2022 have been re-evaluated using accurate velocity models and advanced software, resulting in the relocation of 13 events. For Portugal, this time period was chosen due to the improved capabilities of Portugal's national seismic network, which has higher station density and uniformity than previously. This analysis was done in collaboration with the Institute for Sea and Atmosphere (IPMA), which supplied the seismicity data.

Both areas deployed bespoke, temporary networks of seismometers as part of the PilotSTRATEGY project. In August 2023, five seismic stations were deployed in the Lopín area. These stations have performed optimally, recording over 99% of the possible data and maintaining continuous 4G connectivity to the server. After a year of recording (ending in August 2024) five low-magnitude events have been detected within the Lopín monitoring area. Calculated local magnitudes vary between 1.3 and -0.7. Depth range are from 4.9 km to 10.1 km, believed to be located in the upper crust. None of these events have been reported by the population. Focal mechanisms cannot be calculated due to the low magnitude of the events.

For Portugal, the seismic monitoring network was deployed between January and December 2023. The detection and precise location of seismic events was achieved using waveform data from the bespoke PilotSTRATEGY network, combined with waveform data and bulletins provided by IPMA. In total 183 events were detected of which 117 events coincided with the IPMA catalog. The remaining events are predominantly of magnitude less than 1 and are located in the offshore region. Analyzing the spatial distribution reveals a concentration of events in the southern region of the Lusitanian Basin, away from the PilotSTRATEGY injection site. The events listed in the current catalog have magnitudes (Ml) ranging from 0.5 to 3.0, with epicentre depths not exceeding 30 km.

The level of seismic activity around Lopín is relatively low, primarily concentrated in the mountain ranges surrounding the Ebro Basin. The maximum calculated magnitude by IGN is 4.1 for an event located 30 km to the south of the Lopín area. Additionally, two focal mechanisms have been calculated for an extended area. For the Lusitanian area, the number of events is higher, though the maximum magnitude is less at 3.0. For both areas, the level of activity is now well characterized, and does not pose a threat to the proposed underground storage of CO_2.

The PilotSTRATEGY project has received funding from the European Union's Horizon 2020 research and innovation programme under grant agreement No. 101022664

Contents

The PilotSTRATEGY project has received funding from the European Union's Horizon 2020 research and innovation programme under grant agreement No. 101022664

The PilotSTRATEGY project has received funding from the European Union's Horizon 2020 research and innovation programme under grant agreement No. 101022664

1. Introduction

This deliverable reports on the assessment and monitoring of local seismicity in the PilotSTRATEGY target areas of Lopin (Spain) and the Lusitanian basin, offshore from Figueira da Foz (Portugal). Pre-injection monitoring is an essential task for any CO_2 injection project, to establish a baseline of natural and any man-made seismicity (such as explosions associated with quarrying). If CO_2 injection were to induce a seismic event, then knowing the natural pattern and intensity of seismic activity would be essential.

2. The Lopín area, Spain

2.1 Introduction to the Lopin area

The aim of this section of the report is to describe the studies and results carried out to characterize the baseline seismicity of the area of interest in the Ebro Basin region. Firstly, the IGN catalogue has been analyzed in order to have a general overview of the seismicity in the area.

The second chapter of the report reviews the seismic catalog from Instituto Geográfico Nacional (IGN), within a rectangular zone centered in the Lopín site (SE of Zaragoza), delimited by the geographical coordinates: 1.2°W - 0.5°W and 41.4°N - 41.7°N. This chapter was completed in collaboration with the Instituto de Ciencias del Mar, part of the Spanish Research Council (CSIC) and ICREA.

The last chapter is focused on the installation, processing and results obtained from a dedicated monitoring seismic network deployed in Lopín between August 2023 and August 2024. Repsol awarded a contract to the company Everest Geophysics to carry out the installation and maintenance of the equipment. Instituto de Ciencais de Mar (CSIC) and ICREA, in collaboration with Everest Geophysics, were responsible for processing the acquired data.

2.2 Review of the seismicity in the Lopín area

The seismic catalogue from the Spanish Geographic National Institute (IGN) includes records of earthquakes dating back to 1371. The selected study area for this analysis is bounded by the coordinates: north 42.5, south 40, west -2.5, and east 1 (Figure 1). The earliest recorded event occurred in Ribagorça (Lérida) in 1373, with an estimated intensity of VIII-IX on the European Macroseismic Scale (EMS-98). The Ebro Basin, where Lopín is located, exhibits relatively low seismic activity. In contrast, seismicity is more pronounced in the Iberian Chain to the south, the Catalan Coastal Range to the east, and the Pyrenees to the north.

In 2003, all seismic stations in the IGN network were upgraded to broadband, providing real-time data with extensive coverage. Figure 2 illustrates the locations of seismic events from January 2003 to September 2024. It is evident that seismic activity near Lopín is minimal, with only 13 events recorded

The PilotSTRATEGY project has received funding from the European Union's Horizon 2020 research and innovation programme under grant agreement No. 101022664

by the network. During this period, over 1,400 events have been documented. However, 398 of these events have been assigned a depth of 0 km, indicating uncertainty in their precise locations.

Most of the seismic activity is concentrated in the upper crust, at depths shallower than 12 km (Figure 3). Higher magnitude events are primarily located in the Aragonian Branch of the Iberian Range (Figure 3), such as the event in Herrera de los Navarros on April 8, 2011 (magnitude 4.1, depth 10.9 km, intensity IV-V).

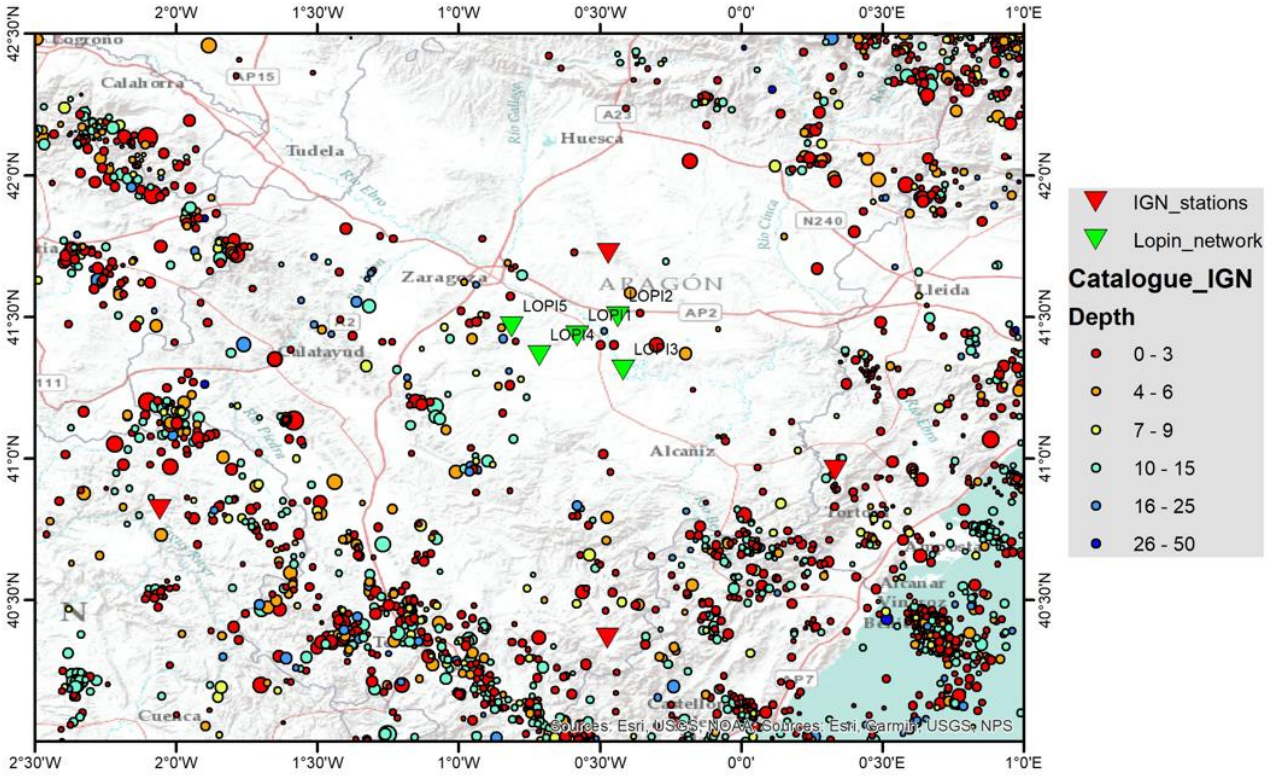

Figure 1. Earthquakes reported in the IGN catalogue from 1373 in the Lopín area. The size of the symbol depends on the magnitude and the results are color coded by depth (km).

The PilotSTRATEGY project has received funding from the European Union's Horizon 2020 research and innovation programme under grant agreement No. 101022664

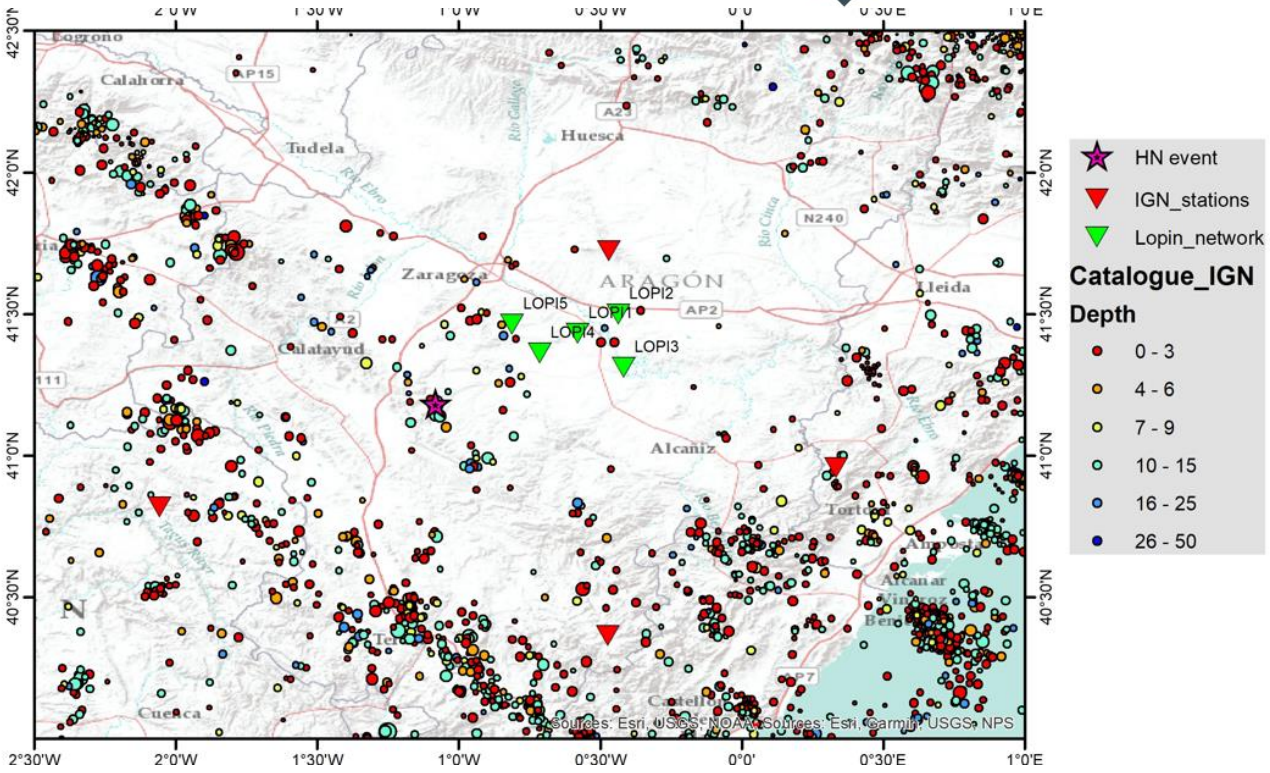

Figure 2. Earthquakes reported in the IGN catalogue from the year 2000 in the Lopín area. The size of the symbol depends on the magnitude and the results are color coded by depth (km). The star represents the Herrera de los Navarros event.

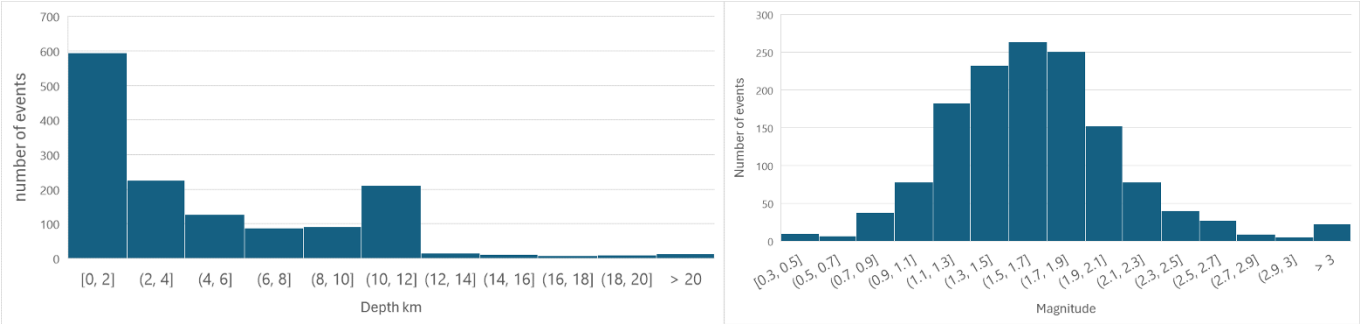

Figure 3. Depth (left) and magnitude (right) histograms of the IGN catalogue for the period 2003-2024.

2.3 Relocation of 2000 – 2022 events in the Lopín area

The main source for hypocenters and arrival times of earthquakes in the region of interest (the black box in Figure 4) is the bulletin of the Instituto Geográfico Nacional (IGN). In a strict sense we use the term seismic bulletin to describe a database consisting of earthquake source parameters (origin time, hypocenter, magnitude) and the phase arrival times used to determine the earthquake location. On the other hand, 'seismic catalog' is used to describe a database of only earthquake source parameters. In this report, unless indicated otherwise, we will use both terms interchangeably to refer to a seismic bulletin.

The PilotSTRATEGY project has received funding from the European Union's Horizon 2020 research and innovation programme under grant agreement No. 101022664

2.3.1 IGN catalog

The IGN catalog (hypocenters and phase arrival time data) was obtained from the IGN catalog web page: https://www.ign.es/web/ign/portal/sis-catalogo-terremotos last accessed in October 2022. Magnitudes and focal depths were obtained for all earthquakes within the rectangular box indicated above, for the period 2003-2021. The starting date of 2003 is chosen because it is when the new IGN broadband network was fully deployed, and complete waveform data are available. The search was ended in 2021 because it was the last complete year available at the time of the request (October 2022).

Hypocenter locations and phase arrival times were requested in order to (re)locate the seismicity. The result of this request were two files in IMS format, which is described in detail in this document: hsp://www.isc.ac.uk/standards/isf/download/ ims1_0.pdf

The file only contains 11 earthquakes.

It is also possible to request only hypocenter data from the IGN catalog web page. In this case we obtained a plain text file with one line per earthquake. In principle, the number of earthquakes and hypocentral parameters should be the same for both request types. However, the following discrepancies were found:

- The hypocenter-only file for Lopin contains 12 earthquakes, 1 more than the IMS file for this region.
- For some events the coordinates in the hypocenter-only and in the IMS file were slightly different.

The explanation for these discrepancies is the following (IGN, personal communication). Before 2015, a preliminary bulletin was obtained first, and then replaced by a final one after incorporating arrival times from other seismic networks. The discrepancies in coordinates for the same event occur when the update of the IMS file did not occur. Therefore, the hypocenter-only file contained the updated solution, but the IMS file still had the preliminary one. In addition, the missing events in the IMS file occurred because there was no preliminary entry for the event, but only the final one. When the update for these events did not occur correctly, the event was missing in the IMS file.

In our case the number of discrepancies is very small, only 1 missing event in the IMS file and it is an event of very small magnitude ($M < 2$).

For convenience, the files in IMS format have been converted to SEISAN's Nordic format, and all the subsequent processing will be done using the Nordic format (described in detail here: hsps://seis.geus.net/software/seisan/node243.html).

The IGN catalog spans a long time period during which changes in procedures (location code, magnitude scales) and reporting practices have taken place. The most relevant change for this project is the change in acquisition and location software that took place in mid-February 2016. Before 2016-02-15, the acquisition and location were performed using a proprietary software, that was then replaced with SeisComP3 (hsps://www.seiscomp.de/seiscomp3/). In addition to the change in location code, the following changes in reporting practice also occurred:

- S-wave arrival times before the change were commonly reported as Lg (due to a requirement of the location code). After the change the standard phase names S, Sg, and Sn were used instead.

The PilotSTRATEGY project has received funding from the European Union's Horizon 2020 research and innovation programme under grant agreement No. 101022664

- After the change, the IMS file contains information about the channel (E, N, Z) in which the phase arrival time was measured. Before that the channel used to pick the arrival time is unknown.
- Before the change all arrival times used to compute the hypocenter were listed, including those of other networks such as IPMA (Portugal), ICGC (Catalonia), IAG (Andalusia), OMP (France) and CNRST (Morocco). After the change only arrival times of stations of the IGN network were reported in the IMS files even when stations from other networks were used.

2.3.2 Events in the Lopín area

For this region only 12 events are listed in the IGN catalog (one of them on 2012-03-14 that did not have available arrival times in the IMS file). The data of the 11 events in the IMS file were converted to Nordic format (S-files), and then an additional S-file was created for the missing event with only hypocenter information. For this event, P and S wave arrival times were manually picked, so it could be relocated. Figure 4 shows the boundary of the Lopín region, and the epicenters of the events in 2003-2021 selected for relocation.

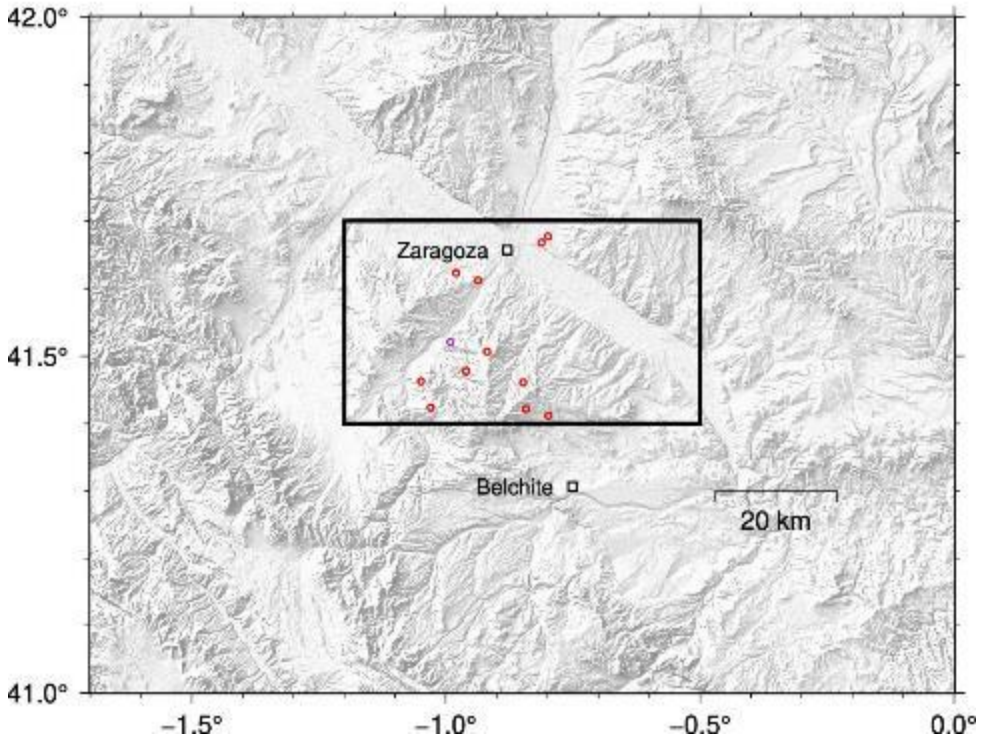

Figure 4. Location map of the Lopín area (black box) with the seismicity reported in the IGN catalog for the time period 2003-2021 (both included). Red circles are earthquakes with available phase data in the IGN bulletin, and purple circle is an event in 2012-03-14 10:03:37 UTC for which only a hypocentral location was available.

2.3.3 Velocity model

In order to locate earthquakes using arrival times, it is necessary to have a reference velocity model of P and S wave propagation, or a P velocity model with a constant v_P/v_S ratio. For quick routine location 1D velocity models are often used (models in which velocity only varies with depth), while more advanced studies use 3D models if available. Here we describe the 1D and 3D models that have been considered for earthquake location.

The PilotSTRATEGY project has received funding from the European Union's Horizon 2020 research and innovation programme under grant agreement No. 101022664

2.3.3.1 1D velocity model

Monitoring networks often use 1D velocity models to locate seismicity. This is because it is much faster to calculate travel times using 1D models, and because often a reliable 3D model is not available for the region of interest. The IGN uses a 1D model for its routine network processing. The model is representative of the central part of the Iberian Peninsula (Iberian Massif) and therefore it has relatively high velocities and lacks a sedimentary layer (Table 1).

Top of layer (km)	P-wave velocity (km/s)
0.0	6.1
11.0	6.4
24.0	6.9
31.0	8.0
half-space	8.0

Table 1. 1D model used by IGN for earthquake location.

2.3.3.2 3D velocity model

Two different 3D velocity models have been considered:

- *S-wave model of Palomeras et al. (2017)*

The first 3D model that we have considered is the S-wave velocity model of Palomeras et al. (2017), hereafter referred to as PM17. This model has been obtained from the inversion of surface wave dispersion data (Rayleigh wave phase velocities obtained from earthquakes and seismic ambient noise). The model extends in longitude from 10°W to 3.5°E, in latitude from 29°N to 44°N, and in depth from 0 to 250 km below sea level. The model is parameterized in a regular grid of 0.5° in latitude and longitude, with a vertical v_S profile of 1 km thick layers at each grid point. This is a smooth regional model that contains all the major features of the Iberian Peninsula and surrounding regions: high velocities in the Iberian Massif; low velocities in the major sedimentary basins; thick crust beneath the major orogens (Pyrenees, Betics) and thin crust beneath extended regions such as the Alboran Sea and the Valencia Trough (see Figure 5).

The purpose of using a low-resolution regional model is first to see the influence of large-scale structures in the earthquake location. This model could be used as background/starting model for higher-resolution local models in regions with good earthquake and station coverage.

The PM17 study only uses surface-wave dispersion data, which are sensitive only to S-wave velocity. From the S-wave model we have obtained a P-wave model by applying a constant v_P/v_S ratio of 1.80. This value has been obtained to match the uppermost mantle P-wave velocity to the global average value of 8.0 km/s. The actual value of the v_P/v_S ratio used to obtain the P model from the S model is only a scaling factor and it should not be used to draw any inferences about physical properties of the crust or mantle. The value of the ratio has also only a moderate influence in the earthquake locations.

To use the PM17 model for earthquake location with NonLinLoc (Lomax et al., 2000; http://alomax.free.fr/nlloc/) we first need to convert it from geographic (spherical) to cartesian (flat

The PilotSTRATEGY project has received funding from the European Union's Horizon 2020 research and innovation programme under grant agreement No. 101022664

Earth) coordinates. For this, two coordinate origins for the coordinate transformation (0.6°W, 41.4°N for Lopín area) have been chosen. Centered in this point the subregion of the PM17 model is extracted with an area of 400 x 400 km. Then, a 1 x 1 km grid is created centered in the coordinate origin and evaluated layer by layer the S-wave velocity at those grid points using bilinear interpolation. Since the vertical parameterization of the PM17 model is in 1 km layers, the resulting sub-model in cartesian coordinates is parameterized in 1 x 1 x 1 km cells. Figure 5 (lower panel) shows the interpolated model at 4km depth.

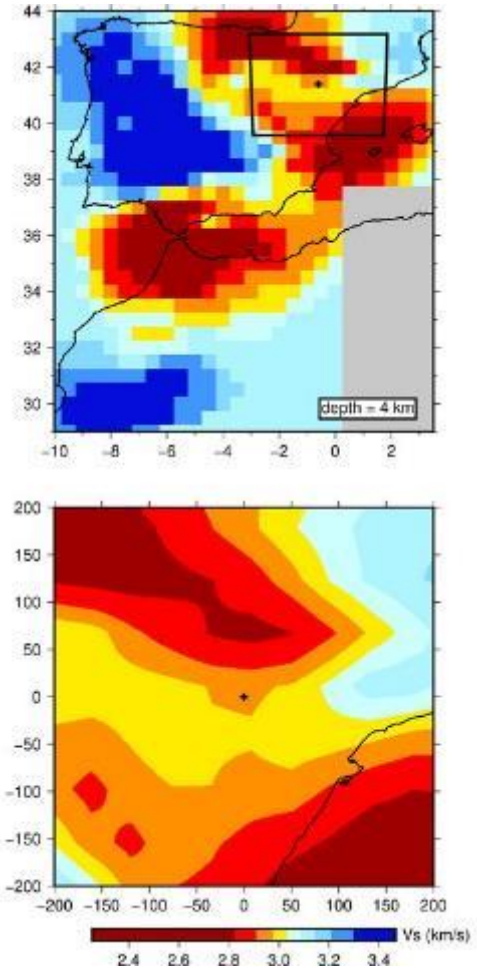

Figure 5. Horizontal layers of the PM17 v_s model at 4 km depth. The top panel shows the entire extension of the PM17 model in its uninterpolated grid spacing of 0.5 x 0.5 degrees. Here, the model has been interpolated linearly to a grid of 1 x 1 km. The black cross indicates the origin of the cartesian model and the black box the extent of the 3D model used for earthquake location with NonLinLoc (the axis of the upper figures are latitude – longitude; the axis from the lower figures are km relative to the centre point).

- *Velocity model from earthquake tomography*

P and S wave velocity models for the region using local earthquake tomography (LET) have been created. When a dense distribution of sources (earthquakes and/or explosions) and receivers (seismic stations) is available, LET models have higher resolution than models obtained with surface waves. However, in regions with sparse seismic networks and moderate seismicity the ray-path coverage provided by P and S wave arrival times is insufficient to obtain a good model of the study region. As a result, the obtained models contain large unsampled regions and are not suitable to be used in locating earthquakes.

The PilotSTRATEGY project has received funding from the European Union's Horizon 2020 research and innovation programme under grant agreement No. 101022664

For the Lopín region, the earthquakes and arrival times listed in the IGN catalog from 2000 to 2020 have been used. The model region consists of a rectangular box of 525 x 440 km (in the E- W and N-S direction respectively) centered on 42.7°N, 0.5°E. The top of the model is at 4 km above sea level (to include all the stations, even those at high elevations), and the bottom of the model is at 50 km below sea level. We have selected earthquakes in the IGN catalog inside the model region that were recorded with at least 8 P wave arrival times and 4 S wave arrival times at distances less than 350 km, and with a maximum azimuthal gap of 200°. This selection criteria resulted in a dataset of 229 stations, 577 earthquakes with 9,131 P arrival times and 5,882 S arrival times. The model has been parameterized in constant velocity cells of 15 x 15 x 4.5 km (in the X, Y, and Z coordinates respectively). The total number of cells in the model is 35 x 30 x 12.

The tomography method used to obtain these models is that of Benz et al. (1996) modified by Tryggvason et al. (2002) to include S waves. This method inverts simultaneously for P and S wave structure and for earthquake relocation. A horizontal slice of the resulting P wave model is shown in Figure 6. While the resolution and ray coverage of the model is good for the Pyrenees and surrounding regions, it is clearly inadequate for the Aquitanian and Ebro basins. In particular, the Lopín region (centered at 0.6°W, 41.4°N) is very poorly covered, with only limited coverage beneath the few existing seismic stations in the area.

Therefore, for the Ebro onshore region instead of using the 3D LET model for earthquake location we will use the PM17 model.

The PilotSTRATEGY project has received funding from the European Union's Horizon 2020 research and innovation programme under grant agreement No. 101022664

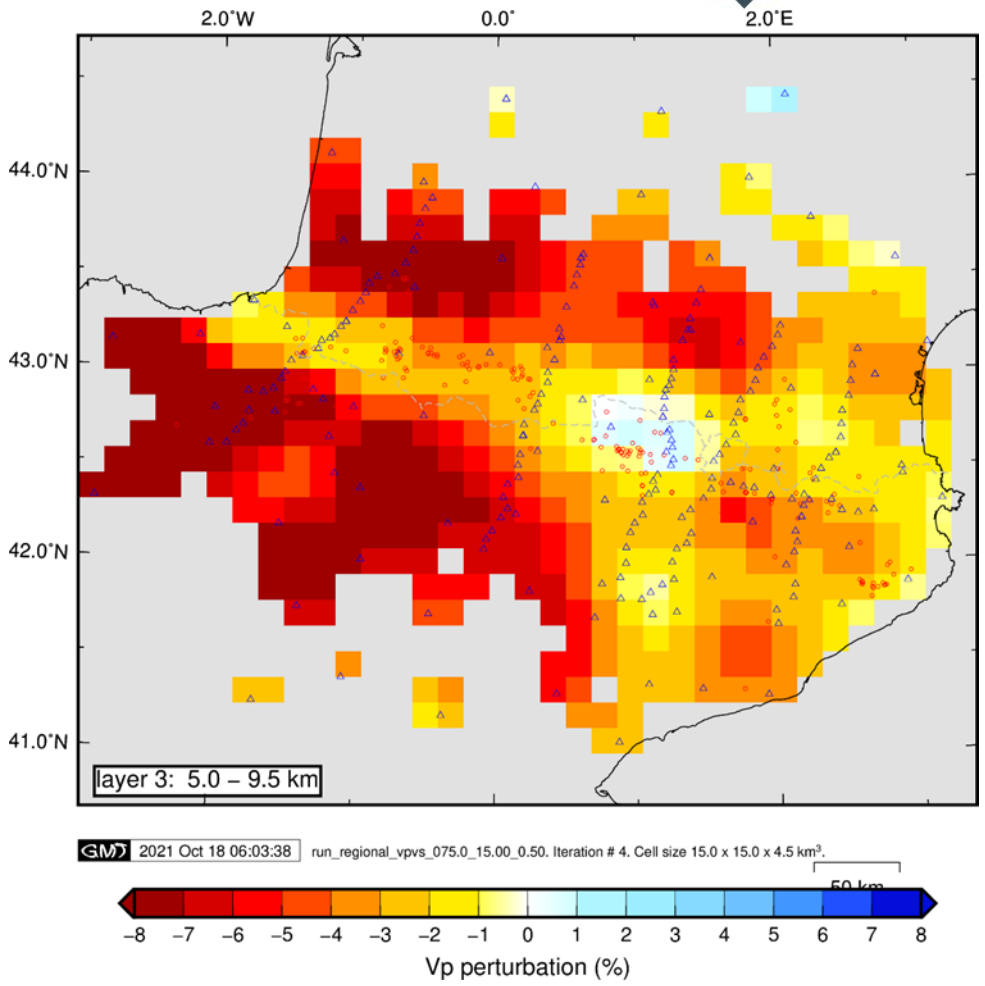

Figure 6. Horizontal slice of the P wave velocity model obtained for the extended Ebro onshore region (layer extends from 5 to 9.5 km below sea level). Red circles are relocated earthquakes within the layer, and blue triangles are seismic stations. Cells that are not illuminated by any ray path are shown in grey. Velocity perturbations are shown with respect to the starting model used in the tomographic inversion.

2.3.4 New phase arrival times using Deep Learning

To perform the picking of P and S waves we have considered the events in the seismic catalog for the Ebro onshore area between 2003 and 2021 obtained in section 2. Again, this period is considered because it is the time for which the IGN network was fully deployed with broadband instruments. The waveform data from the permanent network is supplemented by data from the PilotSTRATEGY temporary deployments.

Waveform data have been extracted for stations located at less than 300 km from the center of the region (41.4°N,0.6°W for Lopín area). This choice is motivated by two reasons: first the Deep Learning pickers that we have used are trained with earthquake data at less than 100 km, so they do not perform well for seismograms recorded at longer distances; and second the location method that we use is based on flat-Earth approximation so only epicentral distances smaller than approximately 300 km can be considered without suffering from distortion errors caused by the sphericity of the Earth. This choice does not affect the quality of the relocation because the most important constraints for local earthquake location are provided by the arrival times to the closest stations, while distant stations do not provide significant new formation.

The PilotSTRATEGY project has received funding from the European Union's Horizon 2020 research and innovation programme under grant agreement No. 101022664

For each earthquake we have extracted a data window with a length of 4 minutes (240 s) starting 30 s before the origin time.

For the Lopín region, we have extracted a total of 1,374 seismogram belonging to the following 9 seismic networks (Table 2):

#seismograms	Network code	Network name
16	2M	MISTERIOS
372	CA	ICGC permanent
36	EK	EUSKALSIS
494	ES	IGN permanent
99	IB	IberArray
6	LC	Canfranc
219	SC	SISCAN
6	WM	ROA-UCM
126	X7	PYROPE

Table 2 Seismic networks using in this project

For detailed information about network codes see https://www.fdsn.org/networks/.

To all these waveform data we have applied two modern pickers based on Deep Learning (deep neural networks):

- PhaseNet (Zhu and Beroza, 2019).
- EQTransformer (Mousavi et al., 2020).

We have carried out a detailed analysis of these two pickers (García et al., 2022) using earthquakes from different regions, including events of the 2013 CASTOR sequence. We found that the best performing picker is PhaseNet, with a higher sensitivity (also called true positive rate, defined as the proportion of true picks that are correctly identified) than EQTransformer. For the CASTOR dataset, the sensitivity of EQTransformer is 75%, while PhaseNet is close to 100%. The comparison is worse for datasets in the Canary Islands (El Hierro) and western Pyrenees, for which the sensitivity of EQTransformer is lower than 50%.

Therefore, for this final report we have only considered picks obtained with PhaseNet.

PhaseNet is a Python package that uses the TensorFlow libraries, and is publicly available on GitHub (https://github.com/AI4EPS/PhaseNet , last accessed October 25, 2022). Unlike other conventional pickers that have many parameters that need to be adjusted, PhaseNet (and other Deep Learning pickers) have only one relevant parameter: the probability threshold to accept a pick as valid (a value that ranges between 0 and 1). The value we have chosen for the probability is 0.3. This value is a good compromise between obtaining a high sensitivity, while keeping the number of false picks low (see García et al., 2022).

The output of PhaseNet is a csv (comma-separated values) file with arrival times, phase type (P or S) and the probability of the pick. A description of the different formats can be found here:

- PhaseNet new output: https://avillasenorh.github.io/DLPickersDoc/pickers/phasenet/#new- output

The PilotSTRATEGY project has received funding from the European Union's Horizon 2020 research and innovation programme under grant agreement No. 101022664

From visually inspecting automatic picks done by PhaseNet we have found that these are either correct (very close to an existing pick or to what an analyst would pick), or obvious false positives. Therefore, to eliminate false positives we have only kept the PhaseNet picks that fall within 2 seconds of the theoretical arrival time. We show a comparison of manual IGN and automatic PhaseNet picks for an event offshore Tarragona. In this case (station CAVN, epicentral distance = 120 km) the agreement is very good, with the PhaseNet P pick slightly later than the IGN pick, and the S wave picks almost identical.

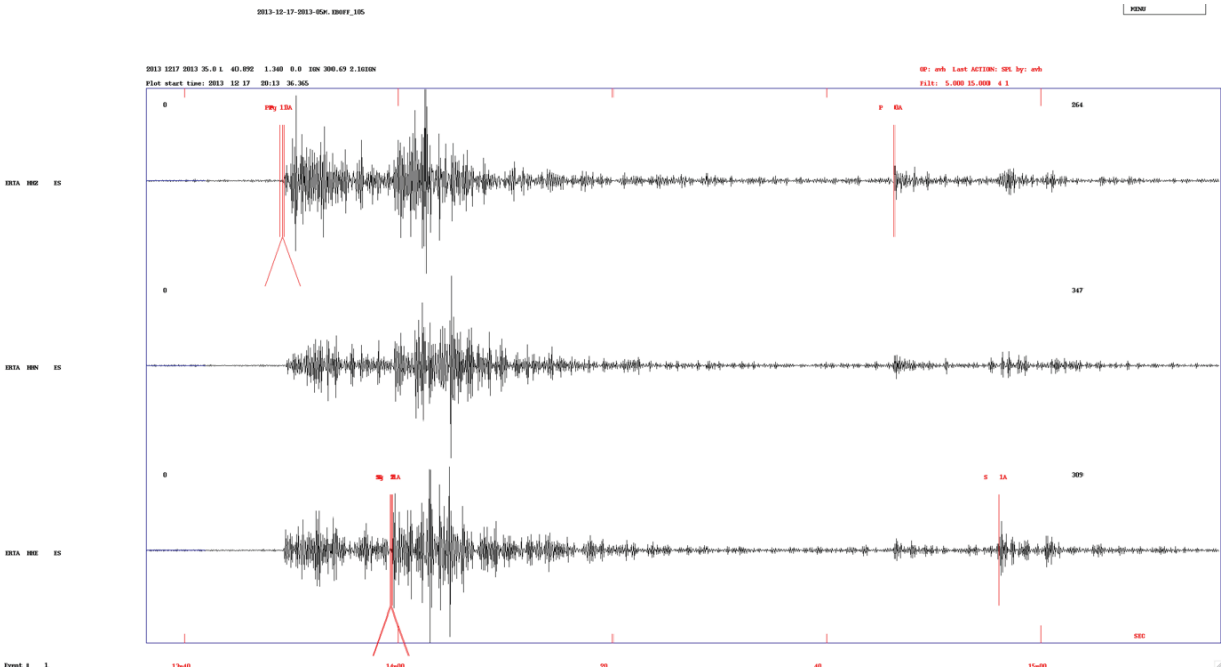

Figure 7 Comparison P and S picks obtained by the IGN and using PhaseNet for an event on 2013-12-17 20:13:15 UTC occurred 25 km SE of Tarragona (mbLg=2.1) recorded at station CAVN. Black lines are unfiltered seismograms (top: vertical component, center: north, bottom east). Phase picks are indicated by vertical red lines. The phases obtained with PhaseNet are labelled with an "A" for automatic.

Figure 8 shows another example of picks for this earthquake, this time for station ERTA (epicentral distance = 85 km). In this case we see that the P and S waves picks from IGN and PhaseNet are coincident. However, we can also see a smaller event following the main one for which PhaseNet has picked good P and S wave arrival times. This smaller event does not appear in the IGN nor ICGC catalogs.

The PilotSTRATEGY project has received funding from the European Union's Horizon 2020 research and innovation programme under grant agreement No. 101022664

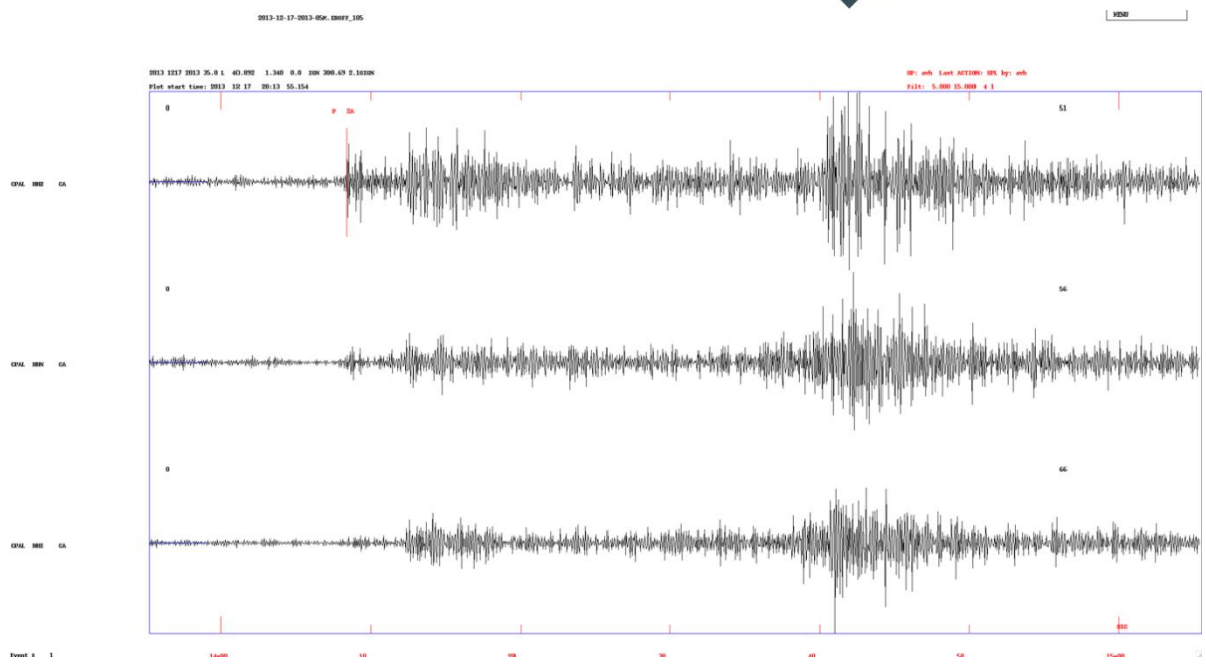

Figure 8 Comparison P and S picks obtained by the IGN and using PhaseNet for an event on 2013-12-17 20:13:15 UTC occurred 25 km SE of Tarragona (mbLg=2.1) recorded at station ERTA. Black lines are filtered seismograms between 5 and 15 Hz (top: vertical component, center: north, bottom east). Phase picks are indicated by vertical red lines. The phases obtained with PhaseNet are labelled with an "A" for automatic.

Finally, in Figure 9 an example for station CPAL is shown (epicentral distance = 218 km). The IGN and ICGC catalogs do not list arrival times for this station. However, PhaseNet has obtained P and S wave picks for this station. The P-wave arrival time coincides with a clear increase in amplitude in the vertical component and has a residual of only 0.18 s. However, the S-wave arrival time is clearly too early, located in the P-wave coda. This incorrect arrival time can be easily removed because it has a large residual of –20 s (the negative sign indicates an arrival earlier than the one predicted by the 1D reference velocity model). Therefore, it will not be used in the relocation and will not affect its quality.

In summary, although there are many exceptions and particular cases, we find that the arrival times obtained by PhaseNet are reliable, particularly for epicentral distances smaller than ~ 100 km. This allows us to verify the arrival times listed in the IGN and ICGC catalogs, and also obtain additional picks, such as the one shown in Figure 8.

The results of this processing are new S-files (text files in Nordic format with network hypocenter and phase arrival times) that contain all available phase arrival times: those from the IGN and ICGC catalogs, and the ones obtained with the DL picker PhaseNet. This combined and augmented dataset is the one that will be used in the next step to obtain improved earthquake locations.

The PilotSTRATEGY project has received funding from the European Union's Horizon 2020 research and innovation programme under grant agreement No. 101022664

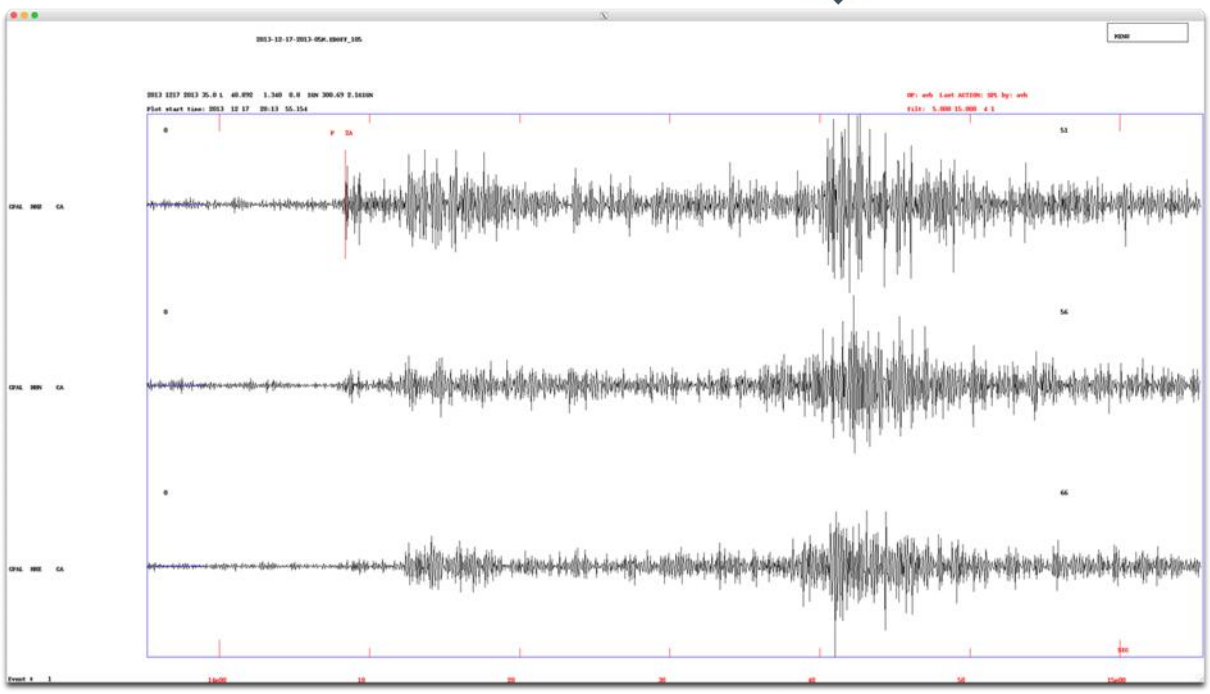

Figure 9. P and S picks obtained by PhaseNet for an event on 2013-12-17 20:13:15 UTC occurred 25 km SE of Tarragona (mbLg=2.1) recorded at station CPAL. Black lines are filtered seismograms between 5 and 15 Hz (top: vertical component, center: north, bottom east). Phase picks are indicated by vertical red lines. The phases obtained with PhaseNet are labelled with an "A" for automatic.

2.3.5 Earthquake relocation

We use the NonLinLoc software package (NLL) for relocating the earthquakes (Lomax et al., 2000; http://alomax.free.fr/nlloc/. It provides a probabilistic solution to the location problem by means of a non-linear earthquake location technique. The location algorithm is based on the formulation proposed by Tarantola and Vallete (1982). The travel-times between each station and all nodes of a 3D spatial grid are calculated by means of the Eikonal finite-difference algorithm of Podvin and Lecomte (1991). To compute the complete, probabilistic solution in terms of the Probability Density function (PDF) in 3D space for the hypocenter location, we use in this work the Equal Differential Time likelihood function. EDT performs better than the L2-RMS likelihood function in the presence of data outliers, which may be the case in this work. In this study, the maximum likelihood hypocenter and the PDF have been estimated using the accurate and reliable Oct-Tree Importance sampling algorithm. This location method can be used with either 1D or 3D velocity models.

Figure 10 shows the comparison between original (IGN) locations and the relocations obtained with NonLinLoc for the Ebro onshore region.

Due to the low seismicity of this region, it is difficult to find any significant pattern in the new locations. However, the relocated seismicity in the southern part of the Ebro onshore region seems to be more clustered than the original IGN locations.

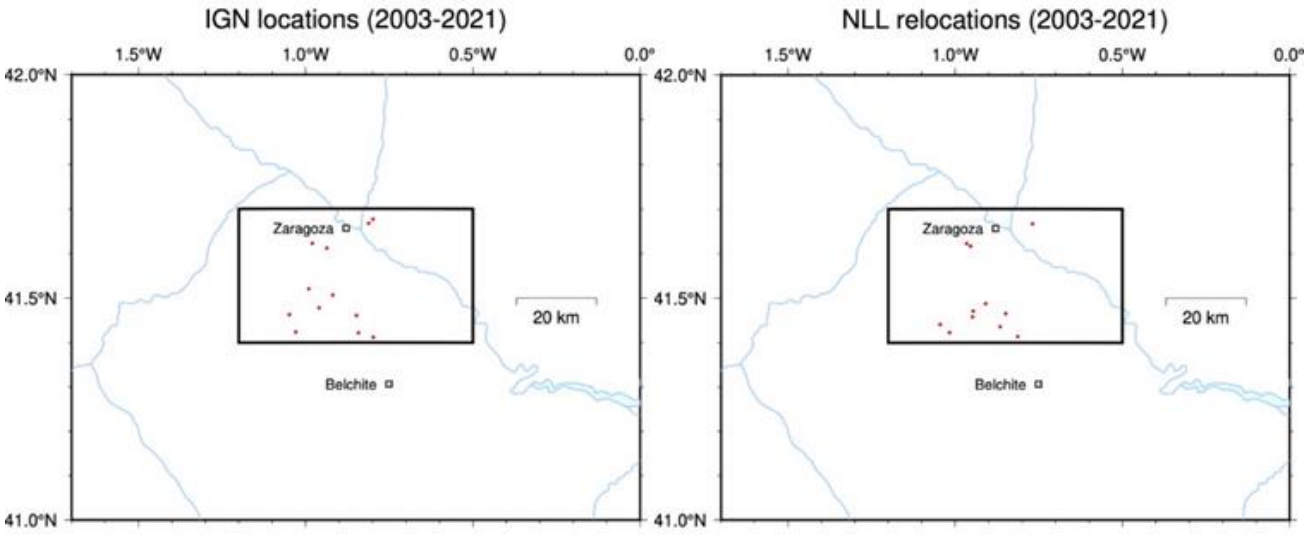

Figure 10 Original locations (red dots) in the IGN catalog for the earthquakes in the Ebro onshore region. Right: relocations obtained using NonLinLoc and the Palomeras et al. (2017) 3D model.

Figure 11 shows the mislocation (or relocation) vectors between the original IGN location and the new relocations with NonLinLoc. As illustrated by the rose diagram, there is no systematic direction for the relocation vectors. With respect to focal depth, in the IGN catalog about half of the events in the region had focal depths of 0 km, indicating unconstrained depth. However, the NonLinLoc relocations are systematically deeper, with an average depth of 12 km, and no earthquakes shallower than 6 km. The obtained focal depths are typical of continental crust and are the result of using a more realistic velocity model that takes into account the presence of slow sediments of the Ebro Basin in the region.

2.3.6 Focal mechanisms

Two complementary methods to obtain focal mechanisms of earthquakes in the Lopín area have been used.

The first method obtains the orientation of the nodal planes of the double-couple focal mechanisms (strike, dip, rake), focal depth (h), and moment magnitude (Mw) from the time-domain inversion of the vertical, radial and transverse components of the complete seismograms available for the earthquake. This is the preferred method to use, because of the sensitivity of waveforms to focal depth and to the source mechanism.

In addition to the time-domain waveform inversion method, we have also used a method based on the inversion of spectral amplitudes of Love and Rayleigh surface waves. This method has slightly lower sensitivity to focal depth but has the advantage that it is less influenced by the choice of the velocity model and, in some cases, can obtain mechanisms for lower magnitude earthquakes.

The PilotSTRATEGY project has received funding from the European Union's Horizon 2020 research and innovation programme under grant agreement No. 101022664

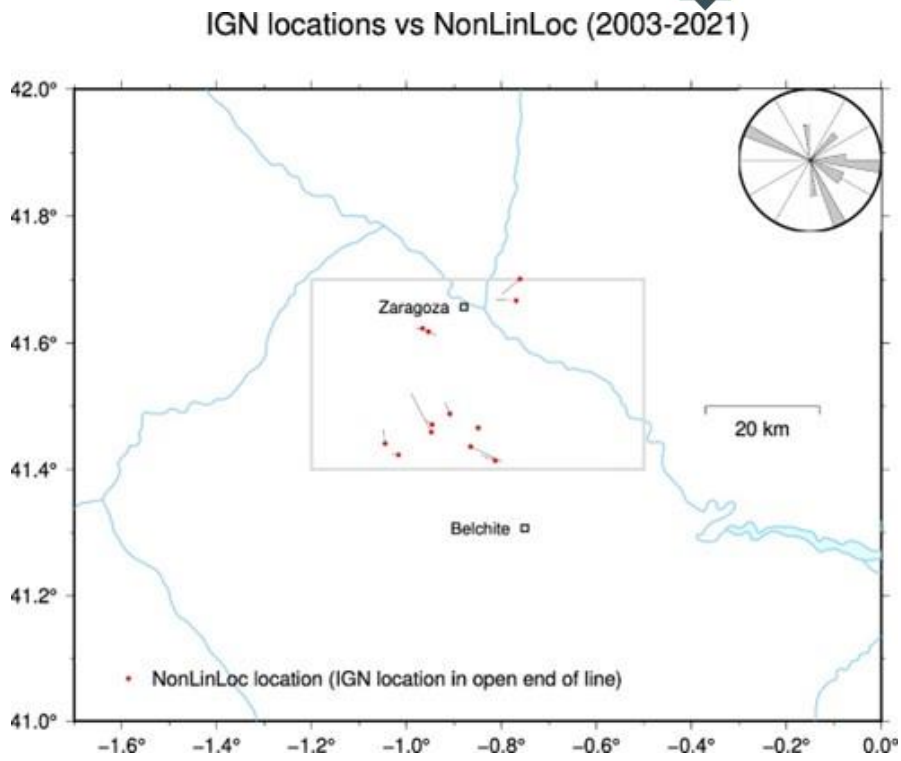

Figure 11. Mislocation vectors between the original and relocated epicenters in the Ebro onshore region. The NonLinLoc location is indicated by a red circle, and the IGN location is at the open end of the line. The rose diagram at the top right indicates the azimuthal distribution of the mislocation vectors (line from the NonLinLoc epicenter to the IGN one). In the rose diagram the azimuths are weighted by the length of the mislocation vector.

Both the above methods are described in detail in Herrmann et al. (2011). In both cases the inversion is performed by doing a grid search over depths (for this study region we varied depths from 1 to 25 km in steps of 1 km), and for each depth obtaining the best double-couple focal mechanism. In this grid search we compare the recorded seismograms in velocity with synthetic seismograms of the VALEN 1D model, specifically developed for this region (see Villaseñor et al., 2020 for further details on the method and model).

The methods selected to obtain focal mechanisms work well for events approximately greater than Mw 3.5. Depending on the number of recording stations, their geographical distribution, and the signal-to-noise ratio of the recorded seismograms, this threshold can be higher or lower. For older events, because of the smaller number of broadband stations in the IGN network it might not be possible to obtain a reliable mechanism for events with Mw > 3.5. Similarly, for recent years and for well-covered regions we can obtain good mechanisms for events with Mw < 3.5. It is also possible that some events are listed in the IGN catalog with overestimated magnitudes (due to, for example, poor constraints in focal depth). Some of these events may have a larger reported magnitude, but after processing it might become clear that this magnitude was overestimated, and no focal mechanism can be obtained.

In order to take into account these effects, we have used for our processing all the earthquakes in the IGN catalog with M ≥ 3.0 (see Figure 12 for location). We have not been able to obtain a mechanism for some of the smaller events, but in this way, we avoid missing events with potentially underestimated magnitudes or with particularly good seismogram recordings.

The PilotSTRATEGY project has received funding from the European Union's Horizon 2020 research and innovation programme under grant agreement No. 101022664

There were no earthquakes with M ≥ 3.0 inside the two initial study regions (Ebro onshore and Ebro offshore, the former was selected as the final storage site as part of the PilotSTRATEGY project). However, after extending the Ebro offshore region, 3 events with magnitudes between 3 and 3.5 fall inside this area. However, these events were too small to produce seismograms with good signal-to-noise ratio. Therefore, in order to obtain some mechanisms that can provide information of the regional stress regime, we have considered a larger rectangular region between 40.1°N and 42.1°N in latitude, and between 1.75°W and 2.0°E in longitude that encompasses both onshore and offshore regions (Fig 12).

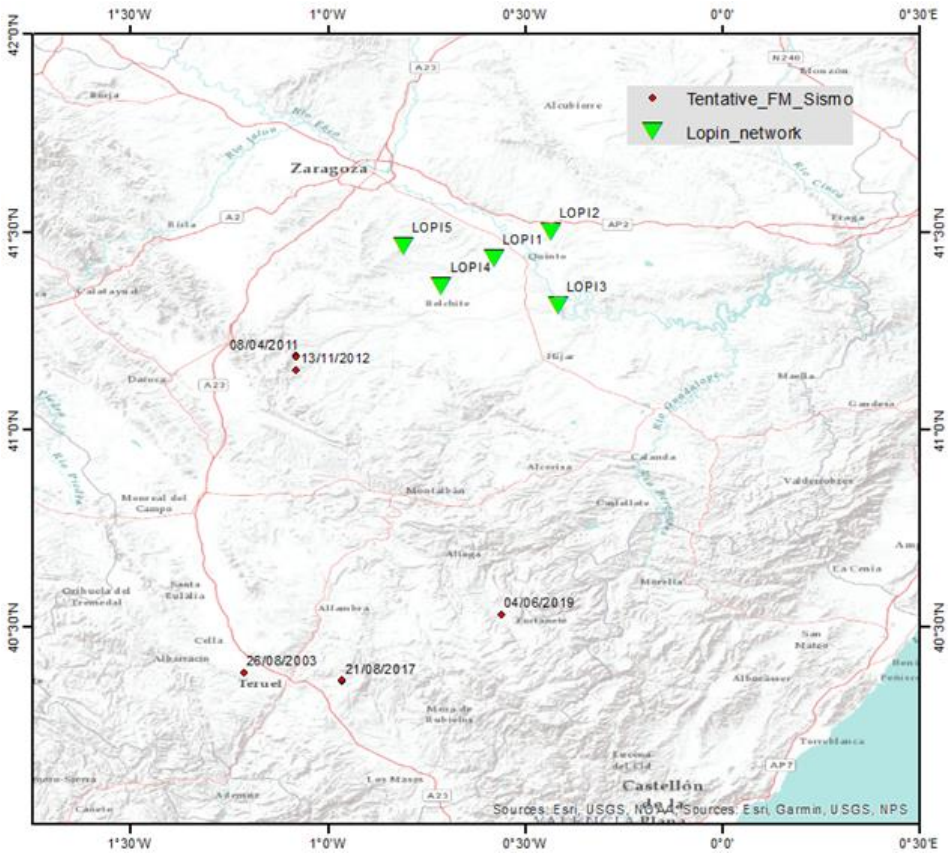

Figure 12. Events which occurred between 2003-2021 in the extended Lopín region with reported magnitudes ≥ 3.0 (red dots). The date (year and month) of each event is plotted for reference. Note that the search area was extended to 2°E but the eastern section has no events and is not shown for clarity.

Given these selection criteria (inside the rectangular box and with M ≥ 3.0) we have obtained a total of 5 events in the IGN catalog between 2003 and 2021 (Table 3).

Date	Time	Latitude	Longitude	Depth	Mag
2003-08-26	03:15:42	40.3830	-1.2146	10.6	3.5
2011-04-08	15:07:13	41.1839	-1.0821	10.9	4.1*
2012-11-13	19:18:25	41.1475	-1.0804	11.0	3.2
2017-08-21	03:10:13	40.3625	-0.9641	12.0	3.3*
2019-06-04	20:58:02	40.5287	-0.5617	0.0	3.3

Table 3. IGN events located in Lopín area between 2003 and 2021. The events for which there is a focal mechanism calculated by the IGN (see https://www.ign.es/web/ign/portal/tensor-momento-sismico/-/tensor-momento-sismico/getExplotacion) are indicated with an asterisk.

The PilotSTRATEGY project has received funding from the European Union's Horizon 2020 research and innovation programme under grant agreement No. 101022664

For each event we have first converted the 3-component raw seismograms in digital counts to velocity. Then we have rotated the velocity seismograms to obtain the vertical (no rotation needed), radial and transverse components. We have performed a visual quality control and selected those with clear signal-to-noise ratio and other quality indicators (e.g., elliptically polarized Rayleigh waves, Love waves arriving before Rayleigh waves).

Then for each earthquake a grid search is carried out over the depth range 1-25 km in steps of 1 km. For each depth an additional grid search over the strike, slip, and rake angles is done in order to find the double couple mechanism that best fits the selected waveform data. Figure 13 shows the results of the depth grid search in an example. The plot shows a broad maximum between 6-12 km depth with a maximum value of fit of 0.64 corresponding to a depth of 9 km. The sharpness or broadness of the maximum gives an indication of the quality of the depth constraint, and the value of the best fit indicates the quality of the solution. Values of fit above 0.5 indicate generally a reliable solution (perfect fit cannot be achieved because of noise in the data and 3D propagation effects that are not accounted for with our 1D model).

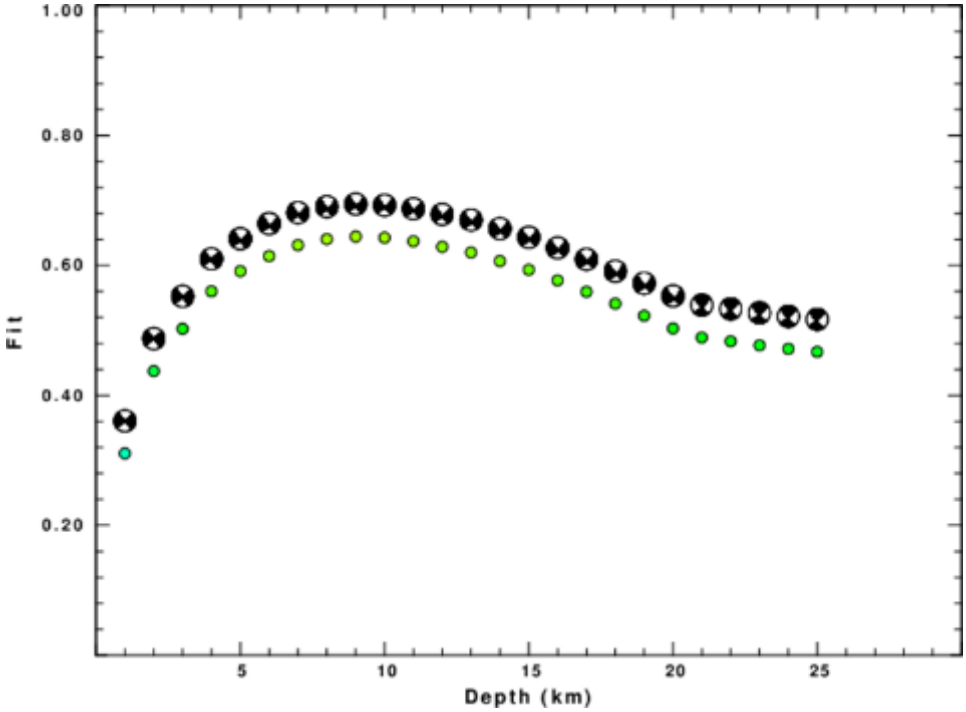

Figure 13. Results of the depth grid search for an example event. The green circle indicates the goodness of fit (0=no fit, 1=perfect fit) of the best mechanism for each depth. Above the green circle the 'beach ball' is the best focal mechanism solution obtained for each depth where black is extension and white is compression.

Figure 14 shows the comparison between the observed velocity seismograms and the synthetic seismograms for the obtained solution corresponding to the same event shown before.

The plots shown in Figure 13 and Figure 14 (results of the grid search in depth for best double-couple focal mechanism, and comparison between observed and synthetic seismograms) have been obtained for all the events with reliable solutions and are in the REG/GRD folder inside each event directory.

The PilotSTRATEGY project has received funding from the European Union's Horizon 2020 research and innovation programme under grant agreement No. 101022664

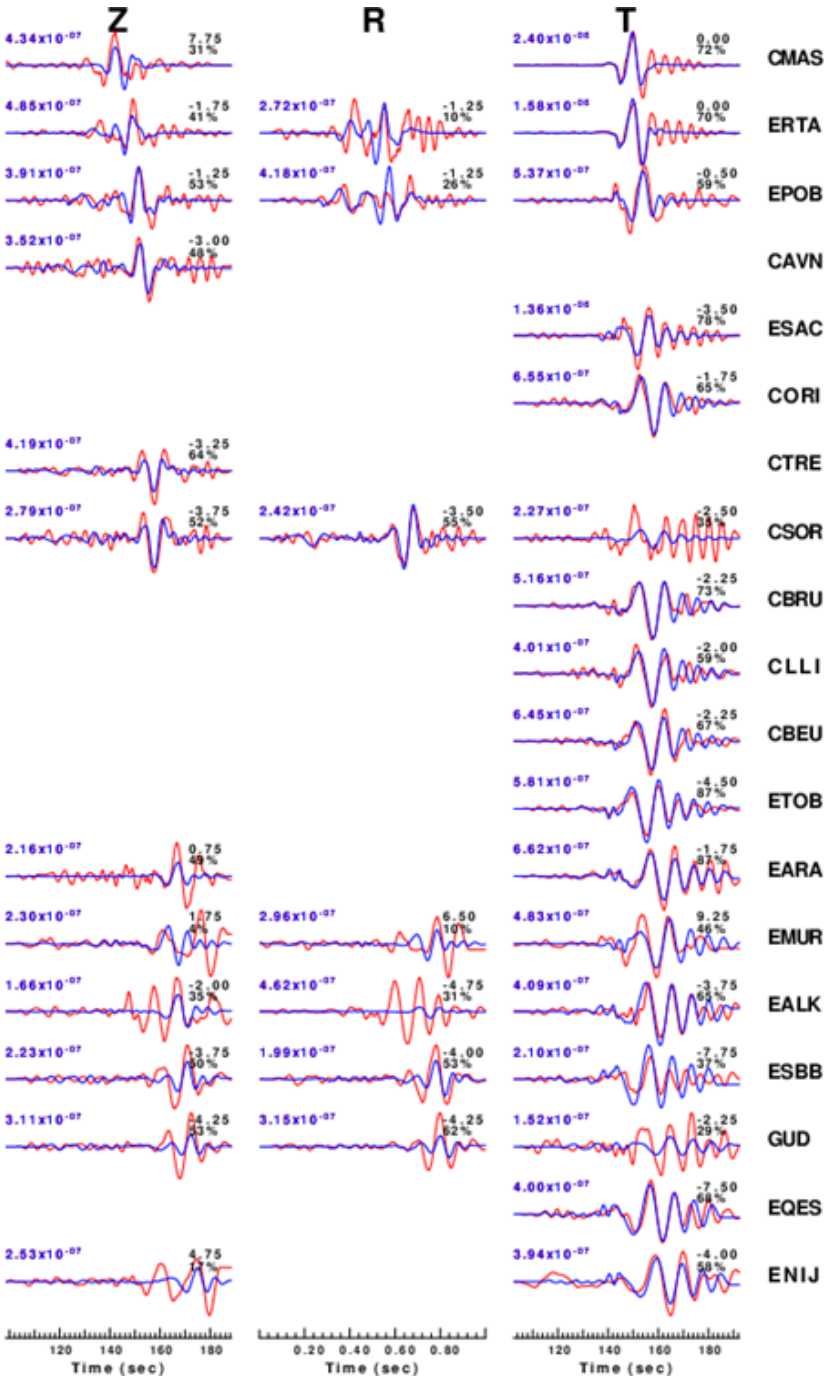

Figure 14. Comparison between the observed seismograms (red lines) and synthetic seismograms (blue lines) for solution obtained for the event. Left column = vertical component, center column = radial component, right column = transverse component. Each line of the seismograms corresponds to a seismic station, with its station code indicated to the right. The bottom *scales are time in seconds.*

The PilotSTRATEGY project has received funding from the European Union's Horizon 2020 research and innovation programme under grant agreement No. 101022664

For the 5 earthquakes listed in the IGN catalog as having M ≥ 3.0, the focal mechanism events using the time-domain waveform inversion can only be obtained for 2 events (Figure 15). The remaining events did not have enough waveforms with good signal-to-noise ratio to obtain reliable solutions. For the same events, the inversion of surface-wave spectral amplitudes has been applied. When the quality of the focal mechanism solution is good, the mechanisms obtained using both methods are very similar. However, for poorly constrained events the surface-wave spectral amplitude method is less reliable. Therefore, in the following table only the solution obtained with the time-domain waveform inversion are listed. The surface-wave solution is also provided in the deliverable included in this report, but it should never be preferred over the one obtained from time-domain inversion.

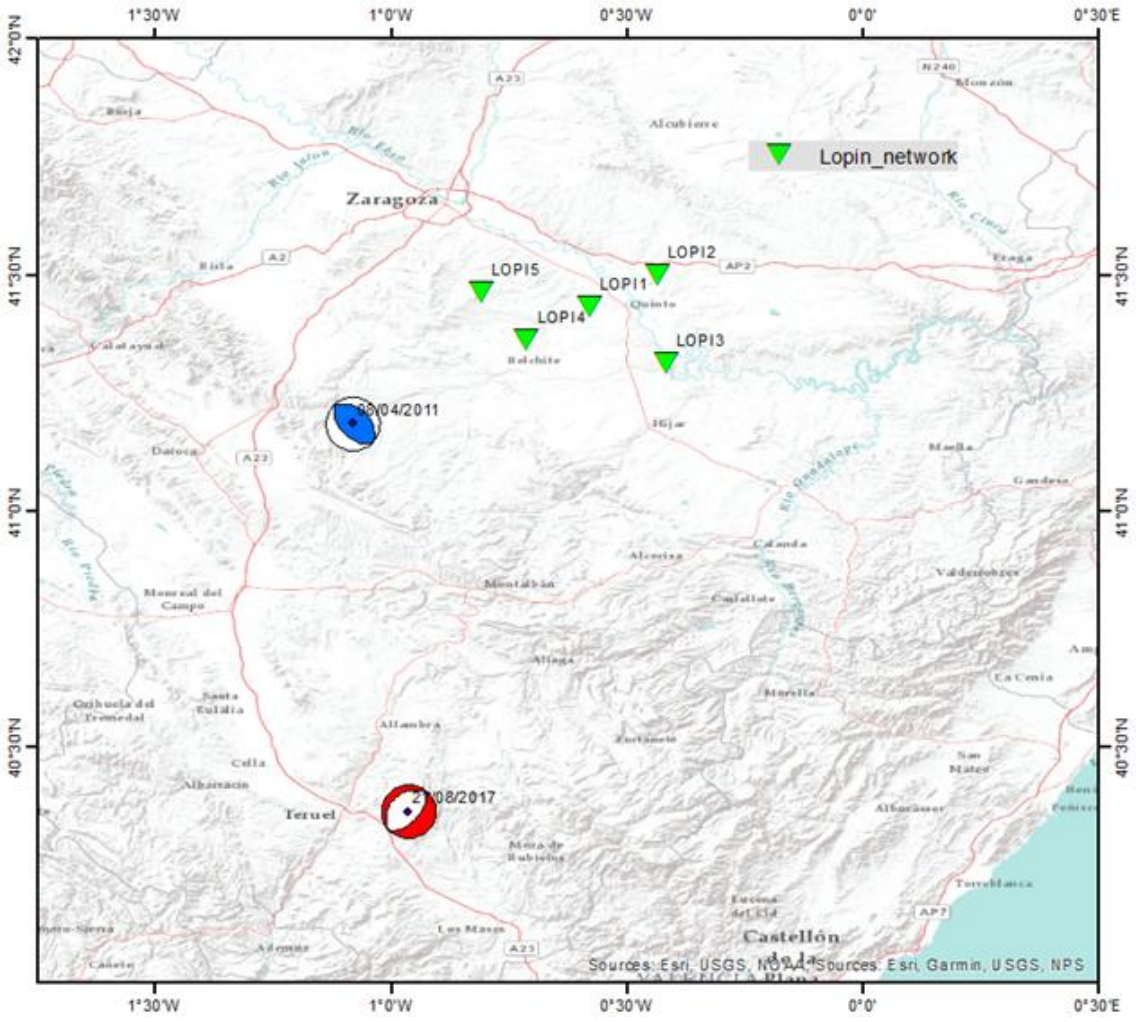

Figure 15. Events occurred between 2003-2021 in the extended Lopín region with reported magnitudes ≥ 3.0. Lower hemisphere projection (see *Table 4*). Red focal mechanism is extensional, Blue focal mechanism is compressive.

The PilotSTRATEGY project has received funding from the European Union's Horizon 2020 research and innovation programme under grant agreement No. 101022664

Date	Time	Lat	Long	Depth(*)		Mw		St	Dp	Rk	Fit
2011-04-08	15:07:13.00	41.1840	-1.0820	8	(10.9)	3.8	(4.1)	310	40	85	0.3568
2017-08-21	03:10:13.70	40.3620	-0.9640	12	(11.9)	3.1	(3.6)	230	30	-85	0.4623

Table 4. Focal parameters of the events for which mechanisms have been calculated.

The meaning of the columns in this table is the following:

- Date: year, month and day in ISO 8601 format
- Origin time of the earthquake (UTC): hour, minute and seconds in ISO 8601 format
- Latitude in degrees (positive in northern hemisphere)
- Longitude in degrees (positive in eastern hemisphere)
- Depth obtained from the time-domain waveform inversion in km. *Between parenthesis is the original depth reported in the IGN catalog
- Moment magnitude obtained from the time-domain waveform inversion. **Between parenthesis is the original magnitude (mbLg) reported in the IGN catalog
- Strike, dip and rake of the focal mechanism in degrees
- Data fit. A value of one indicates a perfect fit, and a low value (close to 0) indicates a poor fit. We have considered reliable solutions with a data fit greater than 0.35 and with a good visual similarity between data and synthetics.

The PilotSTRATEGY project has received funding from the European Union's Horizon 2020 research and innovation programme under grant agreement No. 101022664

2.3.7 Regional stress

Because of the low magnitude of the seismic activity in the study regions, only focal mechanism from outside of the Lopín area have been obtained. Therefore, earthquakes in a larger area have been analyzed. (Figure 15 as above and Figure 16).

The orientation of SHmax (the direction of maximum horizontal compressional stress in the rock) is consistent with the mean orientation obtained in the World Stress Map (Heidbach et al., 2016; Figure 17). However, the stress regime suggested by De Vicente et al. (2008) and Olaiz et al. (2009) is mainly extensional, associated with NW-SE faults with quaternary activity in the Iberia Chain. In the Ebro Basin, only poor-quality data from geological indicators, borehole breakouts and drilling induced fractures are available (Heidbach et al., 2016; Figure 17), but might suggest local stress perturbations.

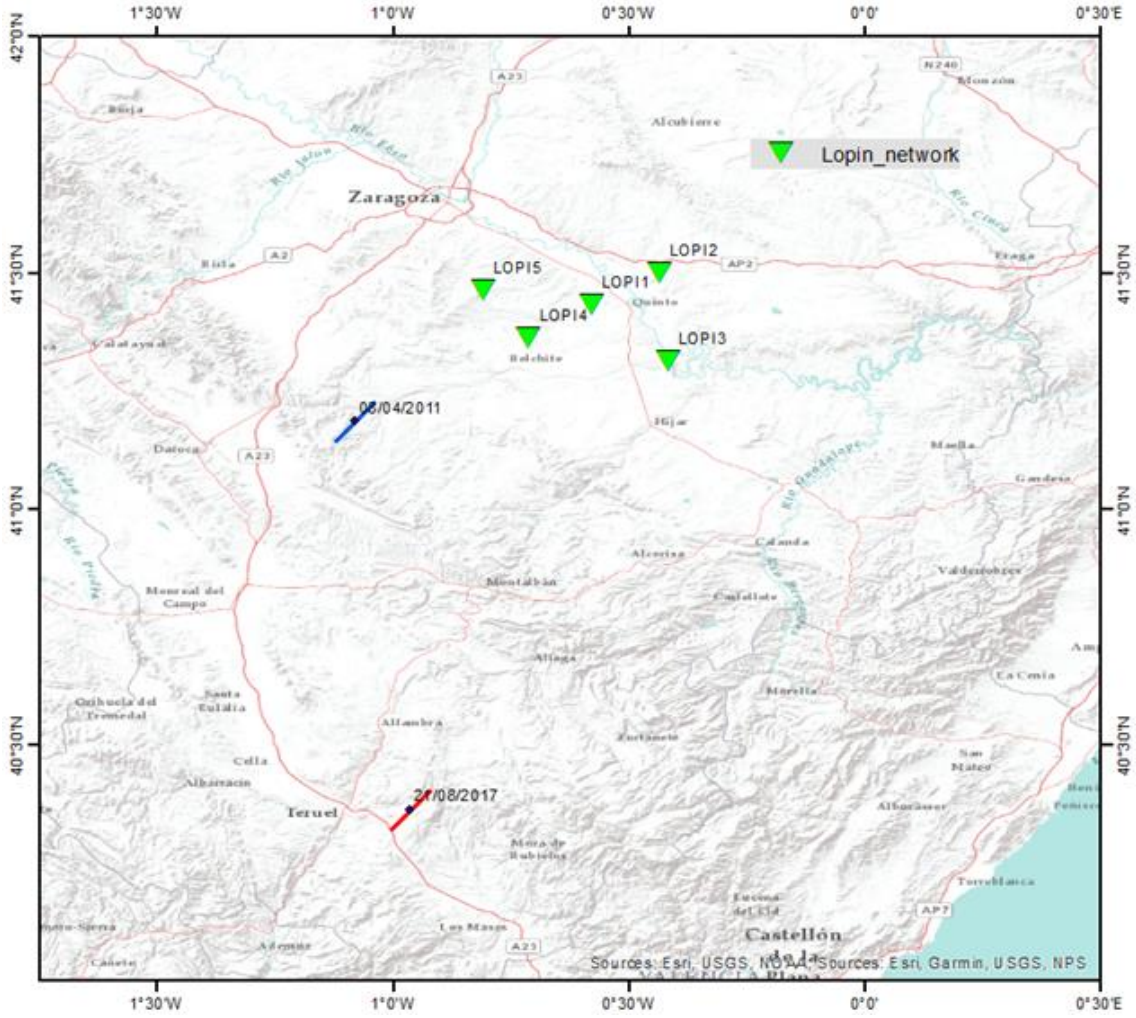

Figure 16. Orientation of the S_{HMAX} (the direction of maximum horizontal compressional stress in the rock) obtained from the focal mechanism in the Lopín area. Red S_{HMAX} line for extensional focal mechanism, Blue Red S_{HMAX} line for compressive focal mechanism.

The PilotSTRATEGY project has received funding from the European Union's Horizon 2020 research and innovation programme under grant agreement No. 101022664

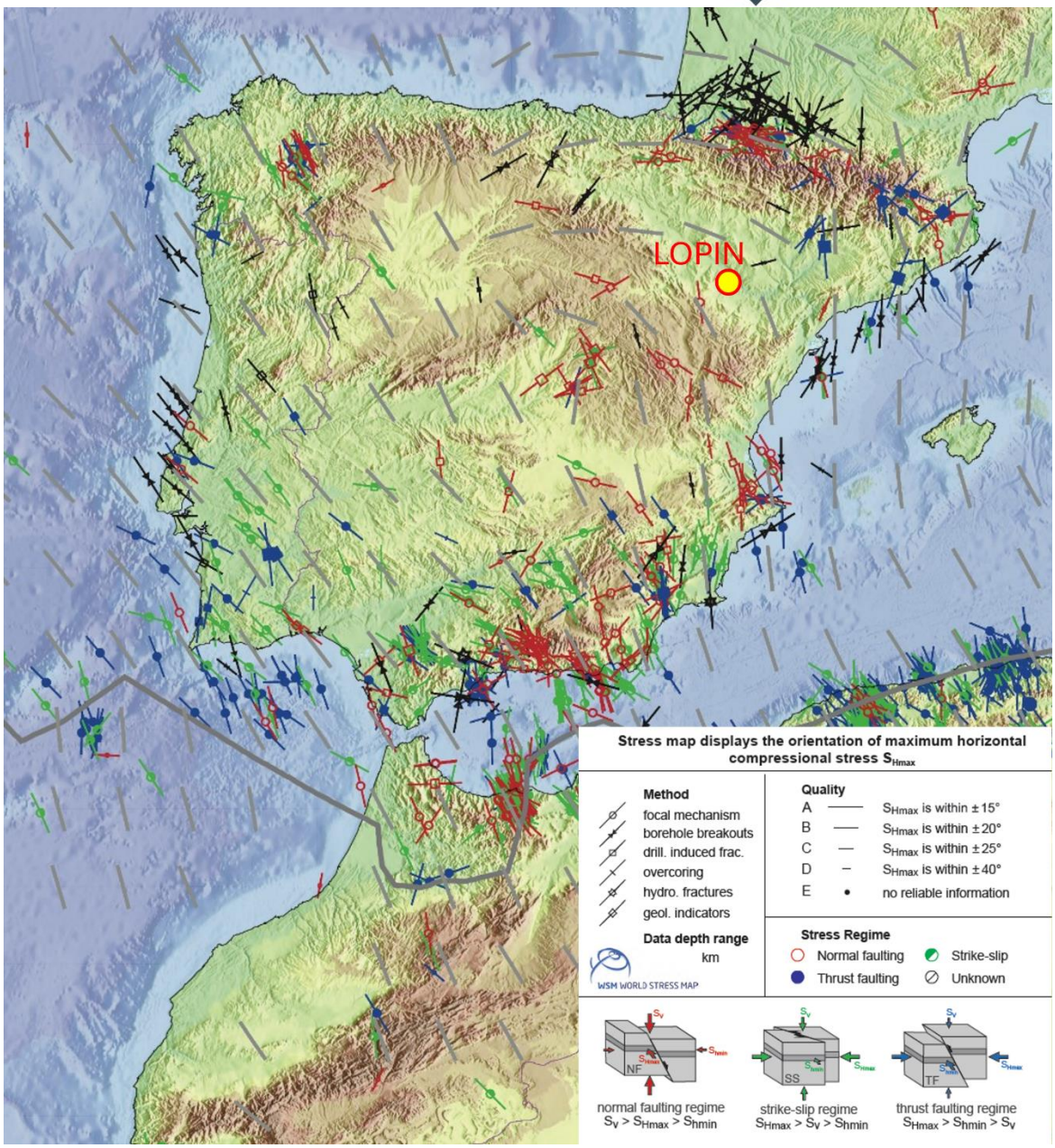

Figure 17. Stress measurements and mean SHmax orientations in the Iberina Peninsula from the current update of the World Stress Map (Heidbach et al., 2016). Grey bars are the mean SHmax orientations on a 1◦ grid estimated with a 250 km search radius and weighted by data quality and distance to the grid point. For other symbols see the legend in Heidbach et al. (2016).

The PilotSTRATEGY project has received funding from the European Union's Horizon 2020 research and innovation programme under grant agreement No. 101022664

2.4 Monitoring network

The aim of this section is to show the results of the micro-seismicity in the Lopin area (Figure 18), using the data from dedicated short period seismic stations deployed and maintenance by Everest Geophysics for the PilotSTRATEGY project. The seismic network was centred in 41.4°N by 0.6°E. There were five stations, with an offset between 12-20 km and maximum aperture of 35 km.

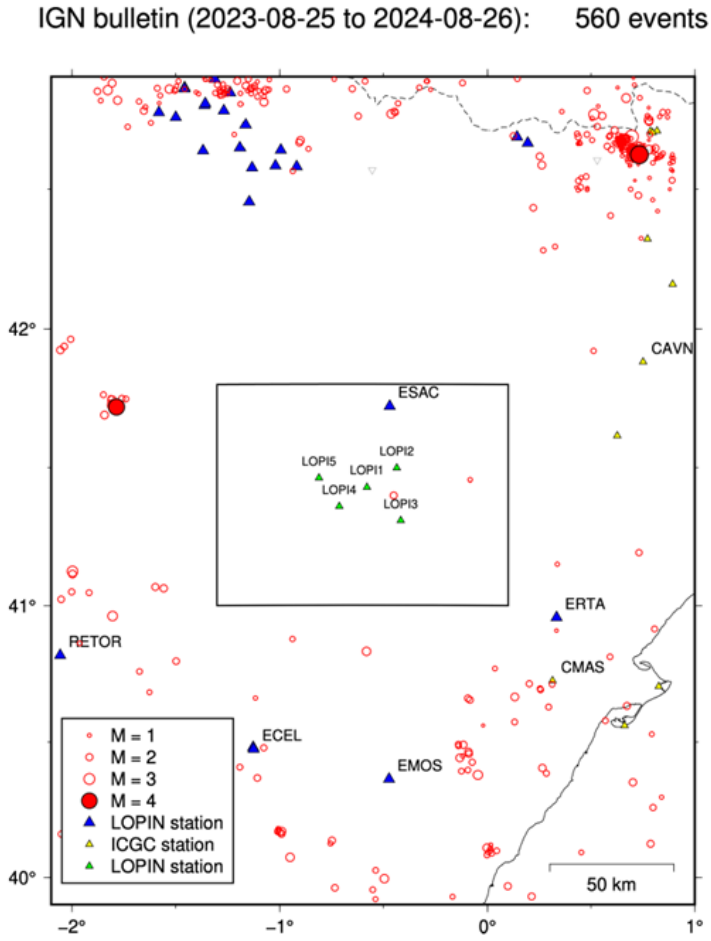

Figure 18. The Lopin seismic network installed for PilotSTRATEGY (green triangles), IGN stations (blue triangles) and ICGC (yellow triangles). Red circles events from IGN bulletin (from 2023-08-25 to 2024-08-26)

The PilotSTRATEGY project has received funding from the European Union's Horizon 2020 research and innovation programme under grant agreement No. 101022664

2.4.1 LOPIN network

Table 5 summarises the locations of the temporary stations.

Code	Network	Latitude (°N)	Longitude (°E)	Elevation (m)
LOPI1	LO	41.430512	-0.579092	234.9
LOPI2	LO	41.498801	-0.434963	310.3
LOPI3	LO	41.310222	-0.415981	203.2
LOPI4	LO	41.361176	-0.712392	321.7
LOPI5	LO	41.462636	-0.810329	491.1

Table 5.locations of the Lopin seismic stations installed for PilotSTRATEGY

2.4.1.1 Description of sites

To ensure minimal human-induced seismic interference with the stations, locations have been chosen in rural areas with minimal access, as far away as possible from sources of artificial vibrations such as roads, wind farms, train lines, etc., which could generate noise in the measurements. The final locations for the installation of the seismic stations were in the following municipalities:

- LOPI1: Municipality of Quinto, on a rural plot under private ownership. The station was installed on the edge of a field that was to lie fallow during the year-long study.
- LOPI2: Municipality of Pina de Ebro, on a rural plot under collective private ownership. The station was installed on top of a small hill at the back of a rarely used small building, sufficiently far from it.
- LOPI3: Municipality of Sástago, on a rural plot owned by the Town Hall. The station was installed at the back of an abandoned water tank.
- LOPI4: Municipality of Codo, on a rural plot under private ownership. The station was installed on the edge of a field that had been left uncultivated for an indefinite period.
- LOPI5: Municipality of Mediana de Aragón, on a rural plot under private ownership. The station was installed on the edge of a field that was difficult to access and had been left uncultivated for an indefinite period.

The installation of the seismic stations was carried out in the following phases:

PHASE 1. Preparation of the land at the chosen locations: the land where the seismic sensor and datalogger were to be placed was excavated manually to minimize environmental impact and to a depth sufficient to avoid interference (Figure 19). The base of the excavation for the sensor placement was left as level and compact as possible (Figure 20).

The PilotSTRATEGY project has received funding from the European Union's Horizon 2020 research and innovation programme under grant agreement No. 101022664

Figure 19. Site excavation example

Figure 20. Complete site excavation

PHASE 2. Construction of a solid concrete base (Figure 21) for the seismic sensor and placement of a protective box (PVC tank) lined with rock wool (Figure 22) to thermally insulate the sensor and protect it from animals or other potential damage. A prefabricated concrete slab was embedded in the still fresh base concrete as support for the seismic sensor (Figure 23). The junction of the PVC tank base with the concrete bed was sealed with a special Sika silicone to prevent water infiltration in case of rain.

The PilotSTRATEGY project has received funding from the European Union's Horizon 2020 research and innovation programme under grant agreement No. 101022664

Figure 21. Concrete base construction

Figure 22. PVC tank, concrete slab and rock wool to thermal isolation

PHASE 3. Installation of the seismic sensor and the datalogger: the seismic sensor was placed inside the protective box on the prefabricated concrete slab, oriented North-South and properly leveled (Figure 24). The datalogger was installed next to the sensor, buried and protected from the weather by its own transport case and a plastic tarpaulin to shield the case from dirt and possible rainwater accumulation (Figure 25). The wiring of both components was placed in corrugated tubes to protect them from the weather and fauna (Figure 26).

The PilotSTRATEGY project has received funding from the European Union's Horizon 2020 research and innovation programme under grant agreement No. 101022664

Figure 23. Levelling of the base

Figure 24. Seismic sensor, leveled and north oriented

Figure 25. Datalogger placement in LOPI3

The PilotSTRATEGY project has received funding from the European Union's Horizon 2020 research and innovation programme under grant agreement No. 101022664

Figure 26.Datalogger installation in LOPI5. Notice the corrugated tube for the connection between sensor and datalogger.

PHASE 4. Communication and data transmission system: for data transmission from the seismic stations LOPI1, LOPI2, LOPI3, and LOPI4, antennas already incorporated within the datalogger case were used (Figure 27 and Figure 28). For the LOPI5 station an external omnidirectional antenna was installed (Figure 29 and Figure 30) due to the low coverage of the GSM (Global System for Mobile communication) at the site. Each of the stations has an integrated GPS for time synchronization of the data (Figure 28).

PHASE 5. Solar power supply system: the seismic stations were equipped with a 12V, 120Ah deep cycle battery (Figure 31), which was powered by a solar panel anchored to the ground. The wiring of the power system was placed inside semi-buried corrugated tubes to prevent damage from weather or animals (Figure 32).

Stations are connected to a server in real time through a SIM-card. Additionally, stations are visited for maintenance and data collection bi-monthly.

Figure 27. Antenna installed in LOPI1, LOPI2, LOPI3 and LOPI4 stations.

The PilotSTRATEGY project has received funding from the European Union's Horizon 2020 research and innovation programme under grant agreement No. 101022664

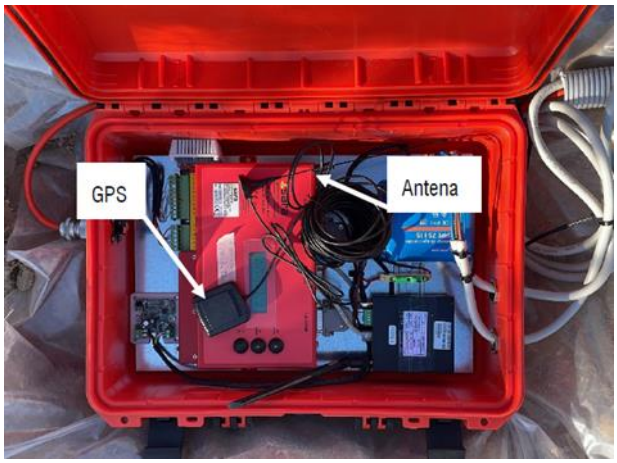

Figure 28.Datalogger, GPS and antenna

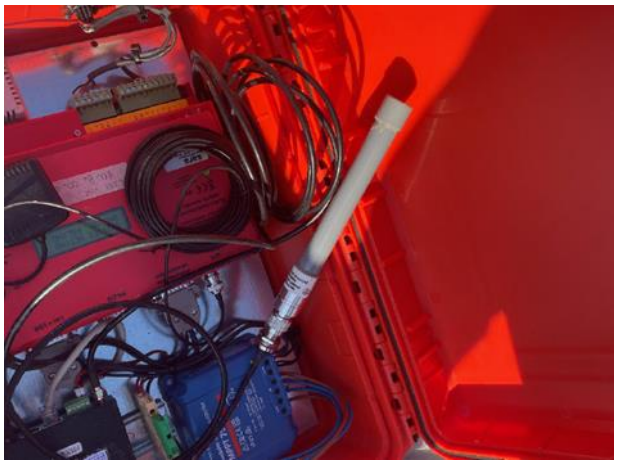

Figure 29. Directional Omni antenna for external use installed in LOPI5

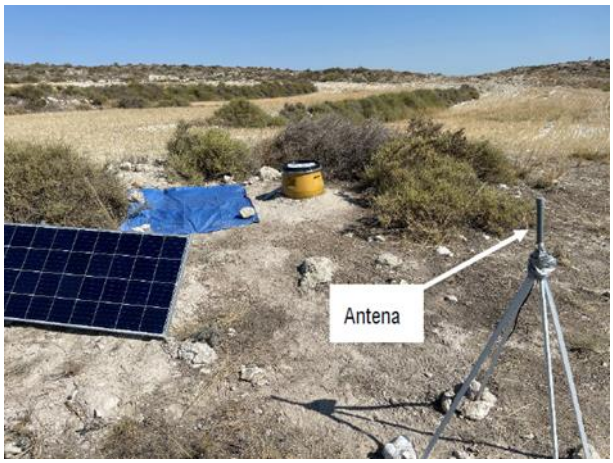

Figure 30. Directional Omni antenna in LOPI5

The PilotSTRATEGY project has received funding from the European Union's Horizon 2020 research and innovation programme under grant agreement No. 101022664

Figure 31. Deep cycle battery during the current study

Figure 32. Panel solar installation in LOPI3

2.4.2 Equipment description

For this project the selected datalogger (SL06) and seismic sensor (SS10) manufactured by SARA (Figure 33 and Figure 34). The equipment were selected due to their compactness and weight (Table 6).

Station	Datalogger	Datalogger Serial Number	Seismic Sensor	Seismic Sensor Serial Number
LOPI1	SL06	6385	SS10	6182
LOPI2	SL06	6386	SS10	6186
LOPI3	SL06	6387	SS10	6185
LOPI4	SL06	6388	SS10	6183
LOPI5	SL06	6389	SS10	6187

Table 6 Type of sensor, datalogger and serial number

- Type of seismic sensor: Short Period (1,0 Hz)
- Datalogger: 128 MB storage. Sampling 100psp
- Power: deep cycle battery and solar panel
- Communication: Internet connection (3G/UMTS/4G/LTE) with directional Onmi antenna GPS for timing synchronization.

The PilotSTRATEGY project has received funding from the European Union's Horizon 2020 research and innovation programme under grant agreement No. 101022664

sara electronic instruments

SS10/05/02/01 Velocitymeters

standard compact

The SSXX velocitymeters series are electrodynamic triaxial sensors equipped with a precision electronic circuitry which make them homogeneous and linearized, in order to obtain a flat band between the nominal resonance: 1.0, 0.5, 0.2 or 0.1Hz frequency to the upper limiting frequency of 50Hz*.

This kind of sensors represent the best alternative to mechanical 1Hz sensors and broad band sensors, for their compactness, lower cost and weight. The sensor elements can be also embedded in our SR and SL instruments.

Simplicity
The SSXX sensors are compact, reliable and ease of use. You don't need to check the damping resistors, orienting or applying mass locking devices. All these operation are automatically made by the electronic inside.

Flexibility
The high sensitivity allow the use also with third party digitizers/recorders. Modularity of the system allow to have monoaxial, biaxial or the standard triaxial setup in order to reduce costs and weight, where is needed. Upgrades are always possible also customization of the bandpass also after the purchase. (within some limits and sending the instruments at our labs)

Precision
The SSXX series sensors use the best electrodynamic transducer available in the market with high stability and robustness. All is assembled in a machined solid block of aluminum treated again corrosion as all our other instruments. Each unit is provided by a transfer function in poles and zeroes according to the international seismological standards for an easy ground motion restitution.

Low noise
The SSXX noise floors are measured using three channel crossed power spectral density and directly compared with the global Peterson's noise model.

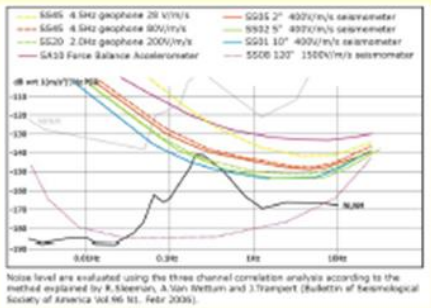

Applications
These sensors finds one main application in the noise surveys (as Nakamura method) and microseismic and seismic monitoring; they can also be used for artificial vibration monitor (explosion, machining, etc..), structures health monitoring like dams, high raise buildings, etc.
The sensor has a low power consumption (ultra low power consumption versions available upon request), making it suitable also for remote installations with limited power sources like in volcanoes monitoring, or temporary seismic networks for aftershocks studies.

Several solutions are available for the sensor anchoring from floor or wall mounting to temporary deployment on soft soil or shallow subsoil; feel free to ask us for explanation on the available solutions.

SSXX technical feature summary

Model		10	05	02	01
Eigenperiod	s	1 (+/- 2%)	2 (+/-2%)	5 (+/-3%)	10 (+/-10%)
Useable bandwidth*	Hz	0.2--50/100	0.2--50/100	0.03--50/100	0.03--50/100
Damping	h	0.69 - 0.71	0.69 - 0.71	0.69 - 0.71	0.69 - 0.71
Sensitivity§	V/m/s	400 +/- 2%	400 +/- 2%	400 +/- 2%	400 +/- 2%
Output impedance	ohm	100	100	100	100
Tilt tolerance	°	+ / - 4	+ / - 4	+ / - 2	+ / - 1.5
Weight (3d std version)	g	2200	2200	3200	3200
Weight (3d compact)	g	1650	1650	--	--

Dimensions:	standard box 180x170x90mm for SS10 and SS05 compact box is available 145x115x78mm
Connectors:	MIL-C 10-pin Lennartz compatible
Output:	true differential output
Protection grade:	IP68 (higher upon request)
Power supply:	9-18Vdc (9-36V upon request, power consumption changes)
Power consumption:	< 50 mA @ 12V = 0.6W 3D version
Ultra low power versions:	< 13 mA @ 12V = 0.16W 3D version
Battery:	For standard size unit, internal battery operated version available
Regulation Compliance:	CE

* Band pass for this sensor series shall be interpreted in terms of useable standard bandwidth after ground motion restitution for averaged worldwide background noise for the standard versions listed above. Some others attenuation happens inside and near outside the declared bandpass which have no practical effect. ***Other bandwidths can be customised at order;*** ultra low power units have no output filter, bandwidth depends on type of sensors, ask to us for details.

§ It is possible to have sensor with higher or lower sensitivity to match your recording system, ask us for more information.

SARA Electronic Instruments s.r.l. reserves the right to apply in any moment modifications and changes to the features and prices of all products without any prior notice.

SARA electronic instruments s.r.l. – 06129 – Perugia – Via Armando Mercuri, 4 – ITALY
Phone: +39 075 5051014 – Fax: +39 075 5006315 - www.sara.pg.it - info@sara.pg.it
Reg. Trib. Perugia N-5718 – C.C.I.A.A. 109864 - C.F. e P.iva 00380320549 - N.Reg.RAEE: IT08020000001128

Figure 33. Technical specifications of SS10 from SARA Geophysics.

The PilotSTRATEGY project has received funding from the European Union's Horizon 2020 research and innovation programme under grant agreement No. 101022664

sara electronic instruments

SL06 SEISMOGRAPH

Linux

The SL06 seismograph is a high performance recorder based on Linux o.s. capable to record the seismic signal at high resolution in standard USB flash pen drives.

It provides several Internet services like SeedLink, FTP client & server to transmit data flow toward the most popular central station recording software like SeiscomP, Earthworm, Seislog, etc..; this is possible thanks to the *SEISMONUX software*, capable to make the instrument VERY easy to use and giving great operability and flexibility in operation.

SL06
This seismograph is a dedicated recorder designed to work for espcially for earthquakes monitoring. It is compact, reliable and flexible, thanks to its recording software, Linux based, SEISMONUX.
Three or six analogue channels with sampling rates from 1 to 600 samples per seconds allow a variety of applications.

Connectivity
The Linux o.s. offer several native protocols and we added also more protocols, among them: TCP, UDP, HTTP, FTP, SSH, Telnet. Remote command of smart relays with MODBUS protocol is integrated. The unit can be accessed by console port as terminal emulator both by Ethernet and RS232; this allow fully operativity with any data carrier PSTN, GSM, GPRS, SAT, WAN, LAN, etc. VPN guarantee to reach the instrument even behind firewalls and NAT filters.

Energy
The low power consumption allow the SL06 to be used in remote installation and powered with small accumulators and solar panels.

Synchronization
As all our instruments SL06 is equipped with an embedded GPS receiver to synchronize the data flow with the UTC time worldwide used time in seismology. Additionally an NTP client can be used to synchronize devices which cannot receive a GPS signal.

Modularity
In our design we always follow a modular approach allowing the instruments to be easily repaired and upgraded. This safeguard your investment and the environement from waste of equipment increasing the duration of the product.

Development
Our softwares are always updated on a free base allowing improvements of functionalities. Development is constantly done in contact with our clients as geophysicists, civil engineers and seismologists.
Among our clients we can list: INGV, OGS, ENEA., C.N.R. (Italia) and many others worldwide.

Applications
SL06 is excellent for mobile networks, small local networks, single stations, structure health monitoring. It can accept signals from any velocity or accelerometric sensor and even from Broad Band sensor like our SS08. (SL06BB is recomended for Broad-Band sensors). The three channel version can have embedded sensors named VELBOX and ACEBOX commercial version for the seismograph unit and for the accelerograph unit respectively.

The A/D Converter gives its maximum performances with electrodynamic sensors (geophones). In this setup it can resolve low amplitude of background seismic noise providing performance at same and sometime higher level than much more expensive instruments.

If used in a indoor high seismic risk application, the robust housing milled from a solid block of aluminum, can resist to high loads in case of building collapse and then protect the data memory

With a series of trigger algorythms it can work in network with other SL06 instruments in order to avoid false triggers or don't miss any small signal. A numbers of automation are available inside and allow the automatic send to a data server of all the recorded files to be analised with modules of SEISMOWIN software suite like the DESK (for seismology) or ESCAP module (for engineering). SL06 can be also used for Nakamura (HVSR) surveys.

Thanks to the WEB based management system you can control the SL06 in a very simple and easy manner.

Customization on the unit are possible, on both hardware and software side.

Some technical features

Power :	9-36Vdc, power consumpion less than 2.5W (3 channel with geophones)
Number of channel:	3 or 6 channels 24 bit (ΣΔ) 144dB
Sensitivity:	119nV/count / 238 nV/count (jumper selectable)
Sampling rates:	10,20,50,100,200,250,300,400,480,500,600 Hz
Real Time Clock:	GPS disciplined clock +/- 10ppm -20/+50°C (+/- 40µs to the respect of UTC)
GPS Antenna:	external with coaxial cable of 10 meters and BNC connector
Mass Memory:	USB pen-drives, with EXT2 file system up to 8 Terabytes
Data Format:	GSEcm6, GSEint, SAC, SAF, SEED, miniSEED, SEG2
Data Links:	Ethernet 10-100 and RS232
Triggering:	multimode STA/LTA, amplitude, IP voting and scheduled
Housing:	machined aluminum solid block IP67, wall mounting possible 205x170x107 mm
Operating temperat.:	-20/+70°C option
Sensor connector*:	MIL-C 10, MIL-C 18, or MIL-C-26 (for Broad Band sensors)

** From 2010 our 10 poles connector follows the Lennartz standard, it is then directly compatible with.*

SARA Electronic Instruments s.r.l. reserve the right to modify features and prices at any time and without any prior notice.

SARA electronic instruments s.r.l. – 6129 – Perugia – Via A.Mercuri, 4 – ITALY
Tel. +39 075 5051014 – Fax +39 075 5006315 - www.sara.pg.it - info@sara.pg.it
Reg. Trib. Perugia N-5718 – C.C.I.A.A. 109864 - C.F. e P.iva 00380320549 - N.Reg.RAEE: IT08020000001128

Figure 34. Technical specifications of SL06 from SARA Geophysics.

The PilotSTRATEGY project has received funding from the European Union's Horizon 2020 research and innovation programme under grant agreement No. 101022664

2.4.3 Instrumental response

The instrumental response of the network seismographs has been provided by the manufacturer in the RESP format (http://ds.iris.edu/ds/nodes/dmc/data/formats/resp/). The response is identical for the five stations in the network and the three components of each station. Figure 35 shows the shape of the instrumental response in velocity for amplitude and phase.

It can be observed that the response is flat between approximately 1-40 Hz and rapidly decays for lower frequencies. This is consistent with the fact that the sensors used have a natural frequency of 1 Hz. Having a correct instrumental response allows the use of waveform data from the LOPIN network for analyses such as magnitude estimation or focal mechanisms by waveform inversion.

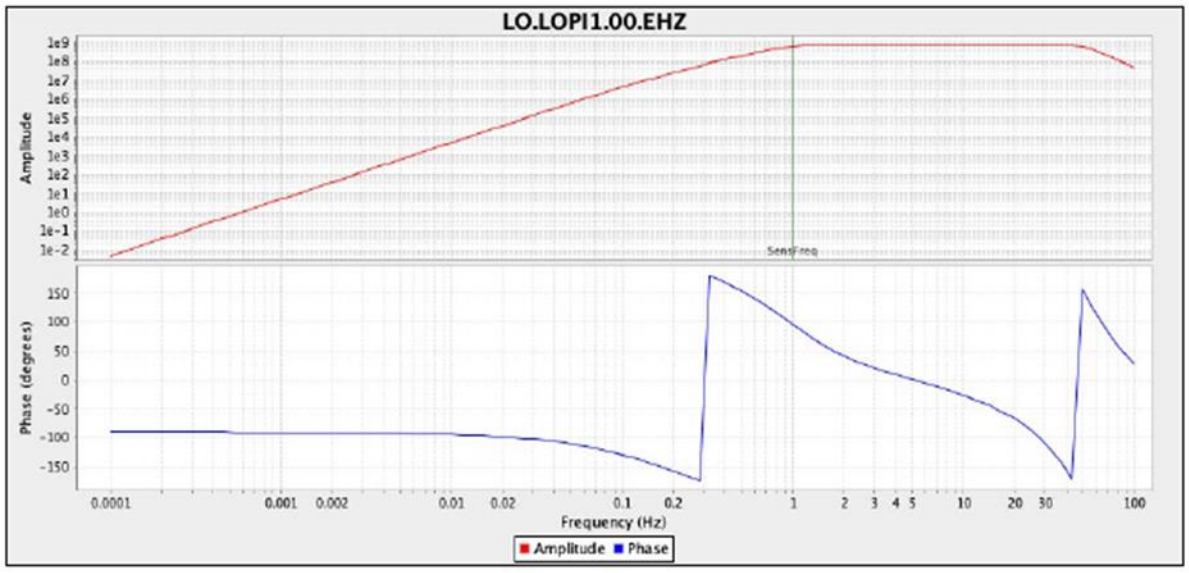

Figure 35 Instrumental response in velocity from LOPIN temporary network stations. Red line (upper) shows amplitude and blue line (lower) represents phase.

2.4.4 Waveform data

In this section the waveform data used in this report are described.

2.4.4.1 Data from Lopin short period network

The waveform data from these stations have been received in miniSEED format and organized in SeisComp or SDS directory structure (short for 'SeisComP directory structure'). The directory structure follows the scheme YYYY/NN/STA/CHN.Q, where YYYY is the year, NN is the network code (in this case 'LO'), STA is the station code (LOPI1 to LOPI5), CHN is the channel (EHE, EHN, EHZ for the three components of motion), and Q is a quality indicator which in our case will always be D (data). The directory tree structure would be (Figure 36):

The PilotSTRATEGY project has received funding from the European Union's Horizon 2020 research and innovation programme under grant agreement No. 101022664

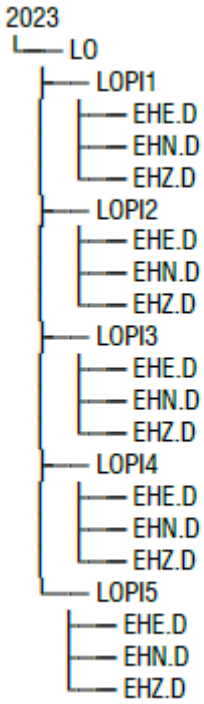

Figure 36. Example of folders structure

Within each directory, there are 1-day files for each station and component. The files may contain gaps (missing data) and overlaps (duplicate data). The file names follow the scheme NN.STA.LL.CHN.Q.YYYY.JJJ where NN is the network code (LO), STA is the station code (LOPI1 to LOPI5), LL is the instrument number at this location (there is only one instrument with code 00), CHN is the channel name (EHE, EHN, EHZ), Q is the quality indicator (D), YYYY is the year, and JJJ is the day of the year (000 to 365 or 366).

The completeness of the data contained in the SDS structure has been analyzed, and almost all stations and components are at least 99.5% complete. Station LOPI1 shows a large number of gaps in August 2024, but these are of very short duration At the end of September and the beginning of October 2023 and in March 2024, there are some gaps affecting all stations and components (Figure 37), but overall, the network performance is very good.

The PilotSTRATEGY project has received funding from the European Union's Horizon 2020 research and innovation programme under grant agreement No. 101022664

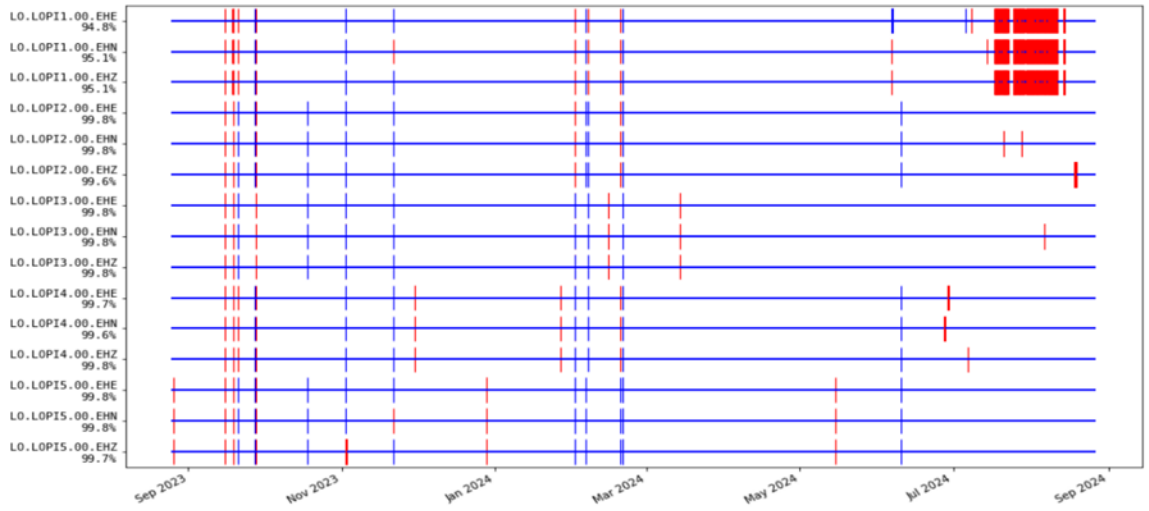

Figure 37. Data availability for each component of the 5 Lopin short period stations. Station name and channel are represented in Y axis. Horizontal blue line shows the continuity of the data while vertical redlines indicate data gaps.

2.4.4.2 Additional stations from permanent networks

In addition to the LOPIN network, waveform from broadband permanent stations, deployed by other institutions, have been included in the project. Accelerometers are not included due to their limited sensitivity to low magnitude earthquakes. Coordinates are in Table 7:

Name	Network (Code)	Latitude (°N)	Longitude (°E)	Elevation (m)	Location
ECEL	IGN (ES)	40.473962	-1.125770	1160.0	Celadas (Teruel)
ESAC	IGN (ES)	41.721900	-0.469300	815.0	Farlete (Zaragoza)
ERTA	IGN (ES)	40.956700	0.333500	547.0	Horta de Sant Joan (Tarragona)
EMOS	IGN (ES)	40.363900	-0.472100	1694.0	Mosqueruela (Teruel)
RETOR	IGN (ES)	40.818524	-2.056649	1023.0	Torete (Guadalajara)
CMAS	ICGC (CA)	40.725680	0.313875	530.0	Mas de Barberans (Tarragona)
CAVN	ICGC (CA)	41.881578	0.750608	634.0	Les Avellanes (Lleida)

Table 7. Coordinates of the permanent broadband stations.

Original waveform data were obtained in miniSEED format and has been organized in the same directory structure (SDS). Overall, the stations have recorded more than 99% of the data. Only EMOS have gaps, but these are short periods of time that should not affect the processing (Figure 38).

The PilotSTRATEGY project has received funding from the European Union's Horizon 2020 research and innovation programme under grant agreement No. 101022664

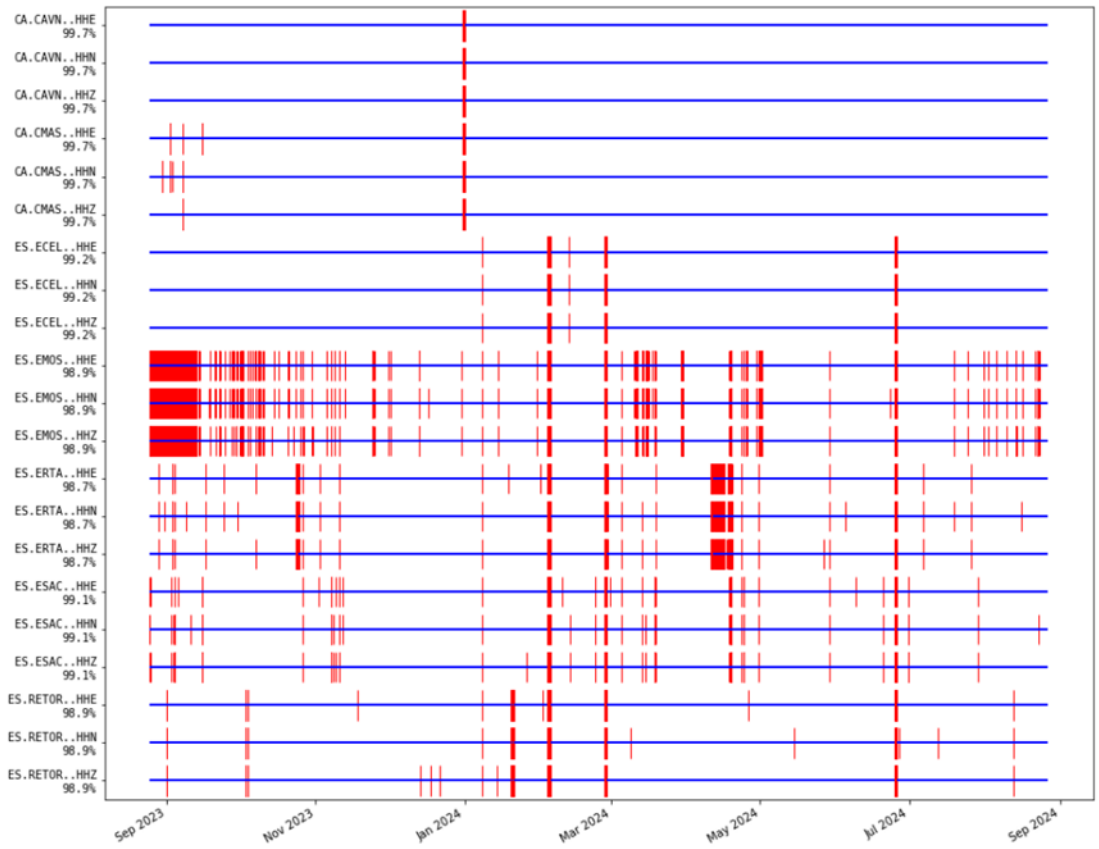

Figure 38. Availability of the data for broadband stations. Station name and channel are represented in Y axis. Horizontal blue lines show the continuity of the data while vertical red lines indicate data gaps.

2.4.5 Ambient seismic noise analysis

The noise level of the continuous recording from the five stations of the LOPIN network was analyzed for the period from 2023-08-25 to 2024-06-30 (311 days). This was done using the PQLX software (Boaz and McNamara, 2008). The principles of this analysis and its application are described in McNamara and Buland (2004) and McNamara et al. (2009).

The analysis consists of calculating the power spectral density (PSD) of the continuous recording of the 3 components of each station in one-hour segments. From these individual PSDs, the probability density function (PDF) can be calculated. The PDF provides, for each frequency (or period), the probability of finding a given value of the spectral amplitude. Therefore, the median or mode of the PDF provides the average noise level of each station and component as a function of frequency. These PDFs are particularly useful for characterizing the performance of the stations and allow for the detection of operational problems, such as incorrect response files, malfunctioning of any of the components, or very high noise levels in general or for a specific frequency range.

Figure 39 and Figure 40 show the PDFs corresponding to the three components of the five stations that make up the LOPIN network. It can be observed that the noise level of all of them is within the limits set by the new low-noise model (NLNM) and the new high-noise model (NHNM) determined by Peterson (1993). This means that they are satisfactory locations and therefore have sufficient detection capability for local earthquakes. The noise level increases significantly for periods longer

The PilotSTRATEGY project has received funding from the European Union's Horizon 2020 research and innovation programme under grant agreement No. 101022664

than 10 s (lower frequencies of 0.1 Hz) because we are using instruments with a natural period of 1 Hz and therefore the geophone has no sensitivity for those periods.

Therefore, the shape of the PDFs in Figure 39 and Figure 40 shows correct behavior of all components of the 5 stations without any notable anomalies.

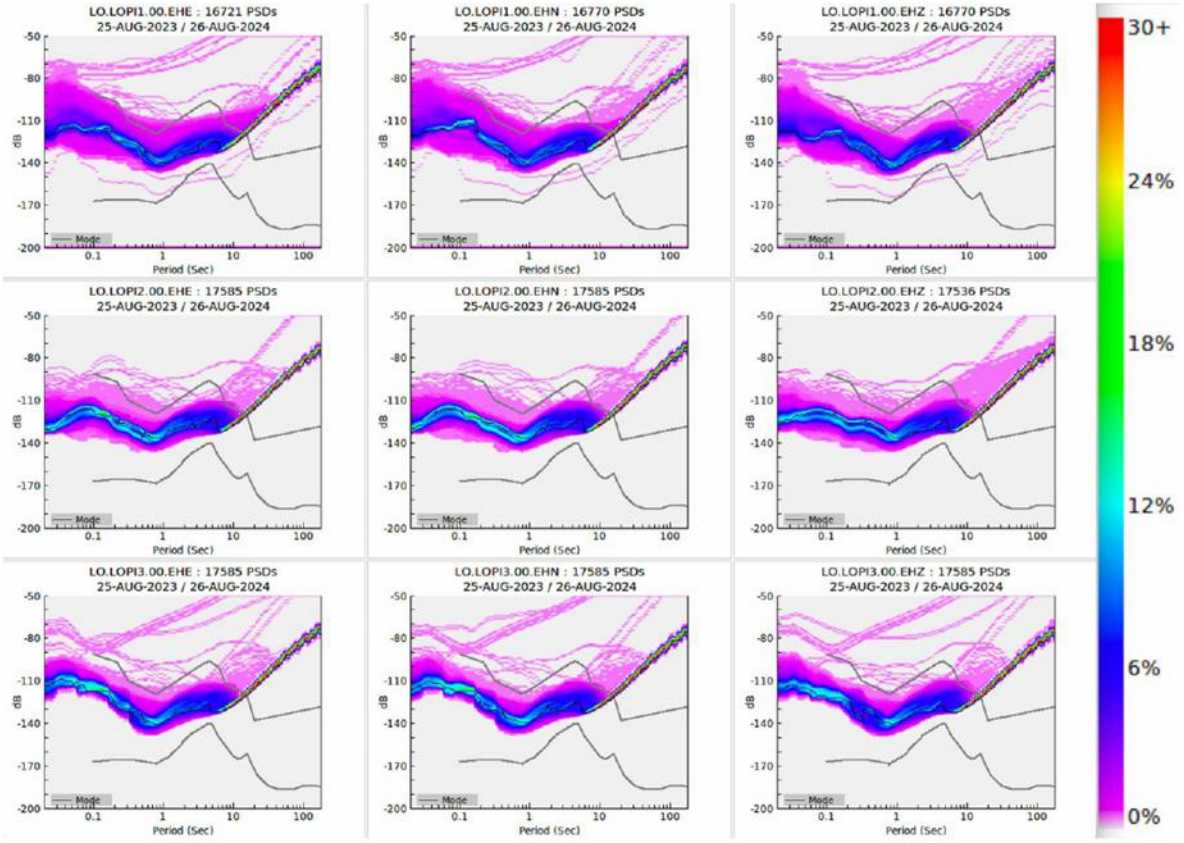

Figure 39 PDFs for the 3 components (EHE, EHN, EHZ) of the stations LOPI1 (top), LOPI2 (middle), and LOPI3 (bottom). The station name, component, and analyzed time period are indicated above each graph. Units are dB relative to a reference acceleration of 1 m/s2.The upper gray line indicates the New High-Noise Model (NHNM) and the lower gray line indicates the New Low-Noise Model (NLNM). The black line corresponds to the mode of the PDF for each period. Cool colors correspond to low (unlikely) values of the PDF, and warmer colors to high values

The PilotSTRATEGY project has received funding from the European Union's Horizon 2020 research and innovation programme under grant agreement No. 101022664

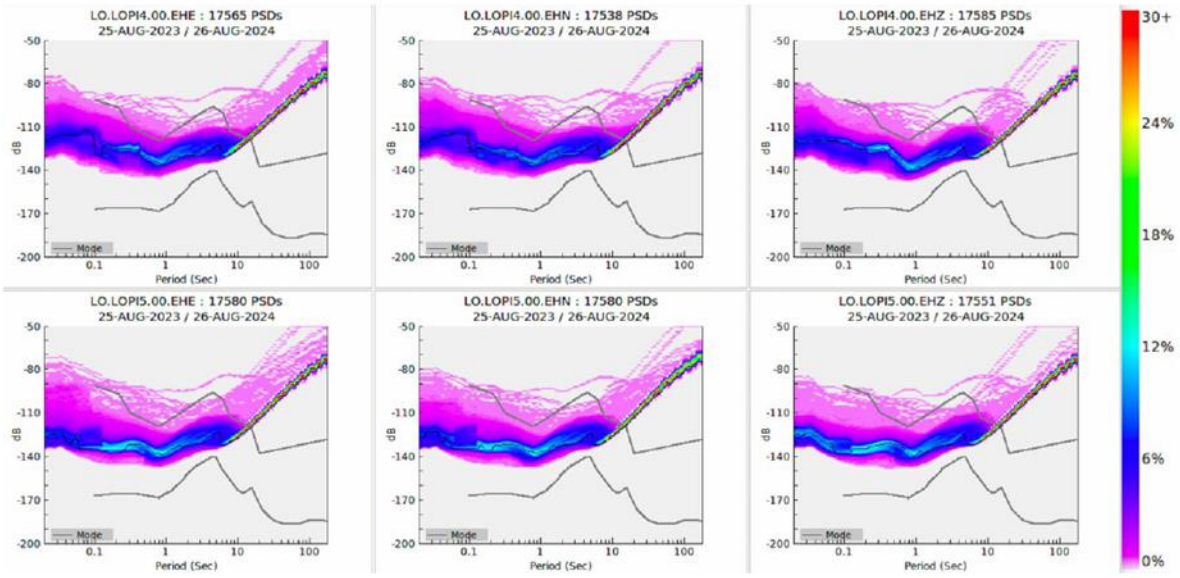

Figure 40. PDFs for the 3 components (EHE, EHN, EHZ) of the stations LOPI4 (top) and LOPI5 (bottom). The station name, component, and analyzed time period are indicated above each graph. Units are dB relative to a reference acceleration of 1 m/s2.The upper gray line indicates the New High-Noise Model (NHNM) and the lower gray line indicates the New Low-Noise Model (NLNM). The black line corresponds to the mode of the PDF for each period. Cool colors correspond to low (unlikely) values of the PDF, and warmer colors to high values.

The use of the PQLX software allows for interactive analysis of regions of the PDFs to clarify their origin, such as investigating the existence of noise level variations between day and night or seasonal changes. The PDFs shown in Figure 39 and Figure 40 do not show notable indications of day-night variations except for the LOPI2 station. For this station, it is observed that in the range of 0.1 to 1 s (1-10 Hz) there are two separate branches with high probability (Figure 39, central panels). Figure 41 shows the results of selecting the PSDs corresponding to the branch with the highest amplitude in dB, which presumably corresponds to daytime noise. In Figure 41 (bottom right), it is observed that the time segments with the highest amplitude of the continuous record (ambient noise) correspond to the hours between 6 and 18 UTC. Additionally, these high amplitudes are not observed every day but in groups of 5 that coincide with the weekdays. This observation indicates that it is anthropogenic noise related to industrial activities or traffic. As indicated, these variations are only observed at the LOPI2 station and are small amplitude differences, so they do not affect the station's detection capability.

The PilotSTRATEGY project has received funding from the European Union's Horizon 2020 research and innovation programme under grant agreement No. 101022664

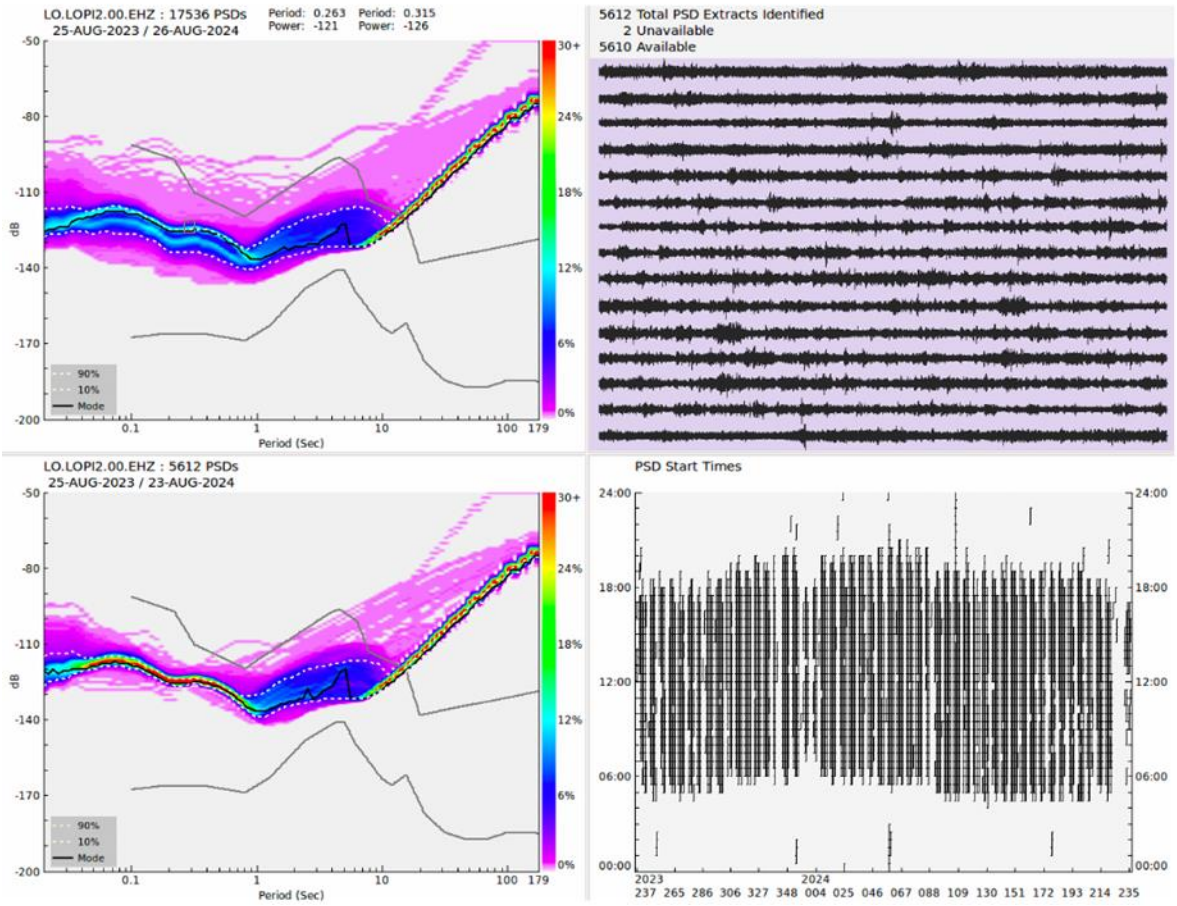

Figure 41. Analysis of day-night variations in ambient noise at the LOPI2 station in its vertical component (EHZ). (Top-left) PDF of the entire analyzed time period. A small rectangular box centered at 0.2 s and -120 dB indicates the upper branch of high-frequency noise analyzed. (Bottom-left) PDF of the 1-hour PSDs selected in the rectangular box. (Top-right) Waveforms corresponding to the selected PSDs. (Bottom-right) Time segments (black vertical lines) corresponding to the selected PSDs.

Another signal that can be observed in the PDFs is the presence of amplitudes above the NHNM (New High Noise model) around the frequency of 1.25 Hz (0.8 s). This energy is more visible at the LOPI4 station. In Figure 29, the PSDs corresponding to this energy have been selected, and it is observed that they mainly correspond to signals that appear to be explosions (Figure 29, top-right). The occurrence time of these signals is around 11 UTC (12 noon local time), which is precisely the time window when controlled explosions in quarries are usually carried out.

The PilotSTRATEGY project has received funding from the European Union's Horizon 2020 research and innovation programme under grant agreement No. 101022664

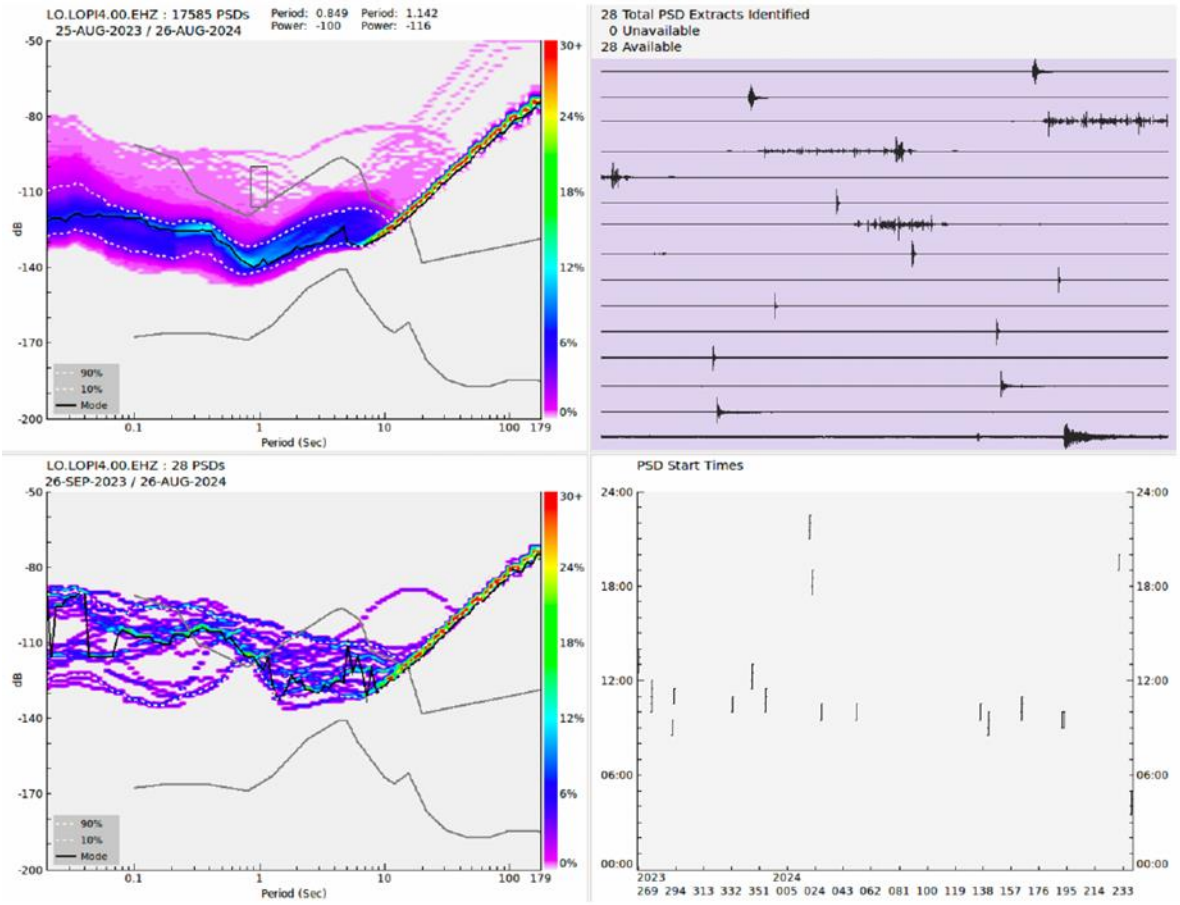

Figure 42. Analysis of the short-period (~ 2.5 Hz) high-amplitude signals observed in the vertical component (EHZ) of the LOPI4 station. (Top-left) PDF of the entire analyzed time period. A small rectangular box centered at 0.8 s and -100 dB indicates the area with high amplitudes at high frequencies analyzed. (Bottom-left) PDF of the 1-hour PSDs selected in the rectangular box. (Top-right) Waveforms corresponding to the selected PSDs. (Bottom-right) Time segments (black vertical lines) corresponding to the selected PSDs.

In summary, the spectral analysis of the continuous recording of the three components of the five stations that make up the LOPIN network allows us to establish that:

- The response files provided by the manufacturer are correct.
- No operational anomalies of the instruments were observed during the study period.
- The noise level of all stations is within the NHNM and NLNM limits, so the station locations are satisfactory and appropriate for detecting local seismicity.
- No variations in ambient noise levels due to anthropogenic activities were observed, except for one station (LOPI2), where these variations are of small amplitude and do not affect its detection capability.
- A relatively frequent energy centered at 1.25 Hz (0.8 s) can be observed, which probably corresponds to controlled explosions in nearby quarries.

The PilotSTRATEGY project has received funding from the European Union's Horizon 2020 research and innovation programme under grant agreement No. 101022664

2.4.6 Processing

The processing of waveform data to obtain earthquake locations consists of the following phases: picking the arrival times of P and S waves; automatic association of arrival times compatible with a seismic event; manual review of automatically associated events; location using a 1D velocity model with the Hypocenter code (included in the SEISAN processing package); and finally, relocation using a 3D velocity model with the NonLinLoc code.

2.4.6.1 Phase picking

Picking of P and S wave arrival times from the continuous records of the stations indicated in the previous section have been completed using the Deep Learning-based picker PhaseNet (Zhu and Beroza, 2019).

The analysis with PhaseNet is performed by jointly processing all miniSEED files from all stations for one day and analyzing each hour separately. This way, a single CSV (comma-separated values) file is obtained that contains all arrival times, phase type (P or S), and the pick probability for a day and hour, which are subsequently combined to obtain all picks for a day.

2.4.6.2 Associator and preliminary location

The files with arrival times for a complete day may contain arrival times of seismic events, but the vast majority of the picks are false positives. To determine which arrival times are compatible with a seismic event, a program called an associator is used. This program reads all the arrival times and determines (based on temporal and spatial proximity) which arrival times may belong to a seismic event, and generates a preliminary, generally very approximate, location. In this report, we have used the REAL associator (Zhang et al., 2019), which is appropriate for small-aperture local networks.

The parameters used to decide if a group of picks is compatible with a seismic event are: at least 3 P-wave arrival times and at least 2 S-wave arrival times (therefore, at least 5 arrival times per event). Since these parameters are very restrictive (at least 4 arrival times are needed to locate an earthquake), it is possible that several of these events are not seismic events but false associations. Therefore, it is necessary to visually check these events to eliminate false associations.

2.4.6.3 Integration of seismic bulletins from permanent networks

To compare the results obtained by our analysis of the LOPIN seismic network data with other permanent networks in the area, the seismic bulletins (containing locations and associated arrival times) corresponding to the time of operation of the network have been obtained. Specifically, the IGN seismic catalogue has been obtained for the study period of this report (25-08-2023 to 26-08-2024) within the rectangular zone 39.9°N-42.9°N and 2.1°W-0.9°E (https://www.ign.es/web/ign/portal/sis-catalogo-terremotos; accessed on 25 July 2024). This area has been chosen to be much larger than the study area in order to include the largest number of earthquakes potentially detected by the LOPIN network. During this time, the IGN recorded about a dozen earthquakes within 100 km of the network center, but only two inside the target/study region: 2024-03-05 at 01:39:55.80 UTC, mbLg=2.0, and 2024-08-21 at 10:05:59.20 UTC, mbLg=1.2 (Fig. 12)

The PilotSTRATEGY project has received funding from the European Union's Horizon 2020 research and innovation programme under grant agreement No. 101022664

2.4.6.4 *Visual analysis of detected events*

The output generated by REAL is converted to Nordic classic format (https://seisan.info/v13/node259.html) and the manual review has been completed in SEISAN (https://seisan.info/v13/seisan.html).

The manual analysis consisted of reviewing all available waveforms for each of the events associated by REAL. A first visual analysis allows eliminating false events (the results of spurious associations) and distinguishing between tectonic earthquakes and explosions, due to the differences in their waveforms. In a second visualization, the automatic arrival times obtained by PhaseNet are modified if necessary, and arrival times not selected by PhaseNet are added in cases where they are clearly visible.

Figure 43 shows the seismograms of 2 small tectonic earthquakes recorded at the nearest station (LOPI1). The records are typical of very close local earthquakes, with a distance between P and S arrival of about 1 second. Since the hypocenters of the earthquakes are quite close, the waveforms are similar, although not identical, indicating that they are different earthquakes and not repetitions of the same type of event.

These seismograms are also significantly different from those corresponding to explosions. Figure 44 shows the 3 components of the movement of an explosion at the LOPI1 station. It can be seen how the frequency content is very different, with very high frequencies in the arrival of P waves, and very low frequencies for S waves, with very well-developed surface waves. Likewise, the duration of the record is much longer (25 seconds for the explosion compared to just 5 seconds for the earthquake), which may indicate that the explosion is not a point source but distributed over a time and/or spatial interval.

Since the objective of the project is to study natural seismicity, the detected explosions, once identified, have been processed with less precision than the local earthquakes. Therefore, their epicenters correlate well with the location of known quarries in the area, but no attempt has been made to obtain accurate focal depths. This is not only outside the scope of the project, but also has the difficulty that many of the P-wave first arrivals are very emergent (because of the characteristics of the explosive source), and their picking uncertainty is large. Therefore, the focal depths shown for example in Table 8 are merely the output of the location program and should not be interpreted.

The PilotSTRATEGY project has received funding from the European Union's Horizon 2020 research and innovation programme under grant agreement No. 101022664

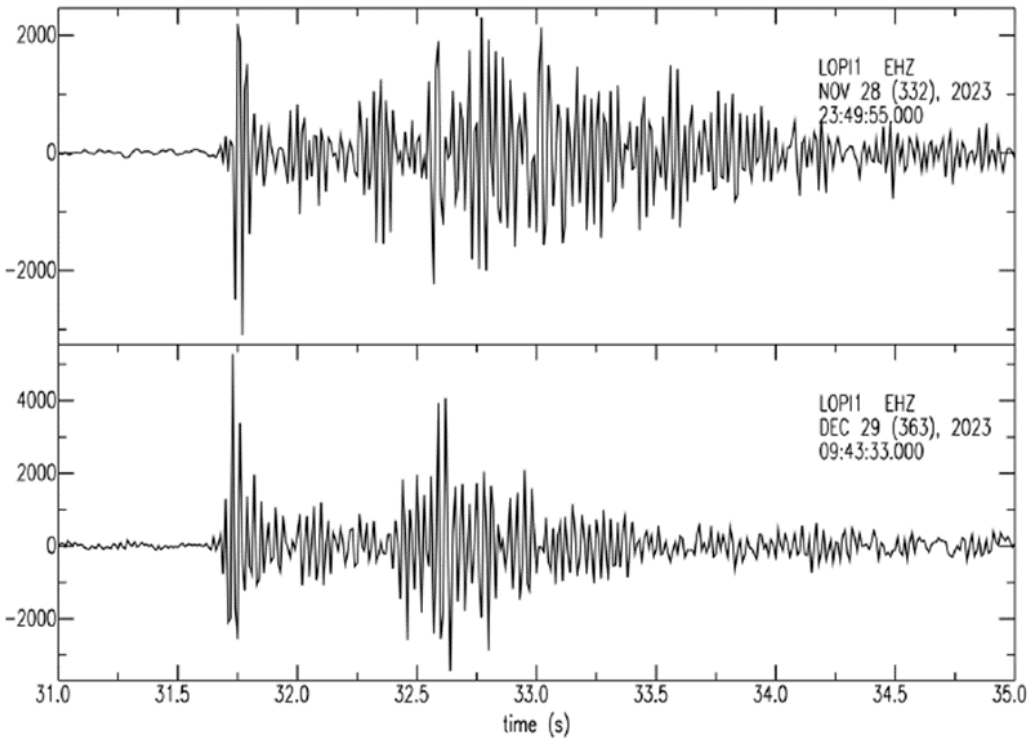

Figure 43. Seismograms of two tectonic earthquakes located within the LOPIN network. The date and time of the events is indicated in the upper right part of each seismogram.

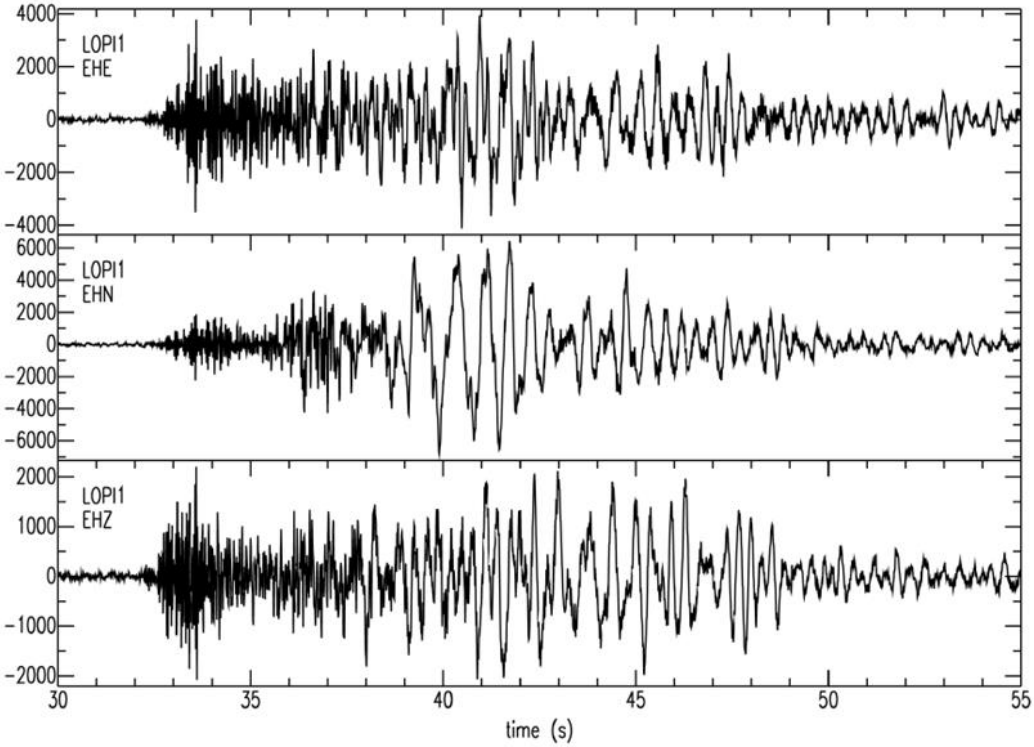

Figure 44. Seismograms of the explosion that occurred on 2023-09-06 at 10:03:50 UTC recorded in the 3 components of LOPI1 station. The name of the station and component is indicated at the top left of each seismogram.

The PilotSTRATEGY project has received funding from the European Union's Horizon 2020 research and innovation programme under grant agreement No. 101022664

2.4.6.5 Event location using SEISSAN and a 1D model

Finally, using the corrected and arrival times, the earthquakes and explosions are relocated using the Hypocenter code included in SEISAN and the 1D velocity model of the IGN (Table 8. IGN 1D Velocity Model

).

Depth of the top of the layer (km)	Velocity P (km/s)
0.0	6.1
11.0	6.4
24.0	6.9
31.0	8.0
Half space	8.0

Table 8. IGN 1D Velocity Model

The result of the manual analysis is the detection and localization inside the study region of 5 local earthquakes (4 of them within the network) and 58 explosions (probably in quarries near the LOPIN network). Table 9 shows the focal parameters of the earthquakes detected in the study area using the IGN 1D model and the Hypocenter localization program. Similarly, APPENDIX I shows the focal parameters corresponding to the recorded explosions.

Date	Time	Latitude (°N)	Longitude (°E)	Depth (km)	M_L
2023-11-28	23:50:25.60	41.3870	-0.596	5.0	0.3
2023-12-29	09:44:03.60	41.4210	-0.567	5.0	-0.3
2024-03-05	01:39:55.30	41.3920	-0.489	5.0	1.3
2024-07-14	08:36:35.50	41.4330	-0.570	4.7	-0.7
2024-08-21	10:05:59.20	41.4520	-0.084	6.6	0.5

Table 9 Earthquakes detected by LOPIN network using 1D velocity model in Hypocenter software

Figure 45 shows a map of the LOPIN area with the epicenters of the earthquakes and explosions located within this zone. The three tectonic earthquakes that occurred within the LOPIN network are located near the central station of the network (LOPI1), and Hypocenter determines a depth of 5 km for all of them. For the other events identified as explosions, the depth is set to 0 km.

The PilotSTRATEGY project has received funding from the European Union's Horizon 2020 research and innovation programme under grant agreement No. 101022664

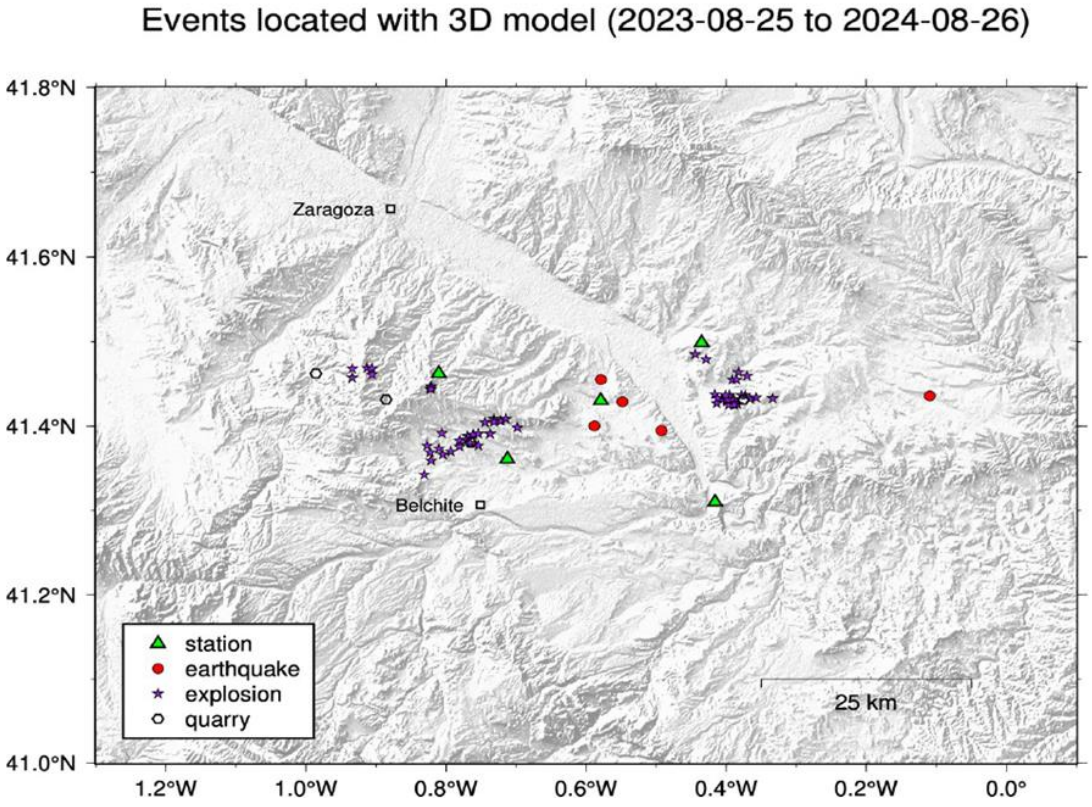

Figure 45. Map of the LOPIN area with the epicenters of earthquakes and explosions located in this study using the Hypocenter program and the 1D model of the IGN. The position of the quarries has been obtained from the images of Google Earth.

2.4.6.6 Relocation of seismic events using NonLinLoc and a 3D velocity model

The seismic event locations described in the previous section can be improved using a 3D velocity model specific to the region and implementing a non-linear location method, which generates reliable estimates of the uncertainty of the location.

The 1D model of the IGN is representative of the cratonic stable area of the Iberian Peninsula and therefore contains relatively high speeds even for the uppermost layer (see Table 8. IGN 1D Velocity Model

). Therefore, it is not an appropriate model to use in our study area that is in the foreland sediment basin of the Pyrenees. However, the PM17 model (Palomeras et al., 2017) includes areas of relatively lower speeds associated with sediment basin and therefore it is more appropriate for this experiment.

The software used for relocation is NonLinLoc (Lomax et al., 2000; http://alomax.free.fr/nlloc/). Further details are in Section 2.3.5 of this document.

In Table 10, the focal parameters of earthquakes that occurred in the study area using the 3D PM17 model and the NonLinLoc localization program are indicated. Similarly, APPENDIX II**Erreur ! Source du renvoi introuvable.** indicates the focal parameters corresponding to the recorded explosions.

The PilotSTRATEGY project has received funding from the European Union's Horizon 2020 research and innovation programme under grant agreement No. 101022664

Date	Time	Latitude (°N)	Longitude (°E)	Depth (km)	ML
2023-11-28	23:50:26.76	41.4000	-0.588	8.5	0.3
2023-12-29	09:44:03.19	41.4550	-0.579	4.9	-0.3
2024-03-05	01:39:54.52	41.3950	-0.492	7.8	1.3
2024-07-14	08:36:34.88	41.4290	-0.548	5.1	-0.7
2024-08-21	10:05:58.48	41.4360	-0.109	10.1	0.5

Table 10. Earthquakes detected by LOPIN network using 3D velocity model in NonLinLoc

Figure 46 shows the epicenters of earthquakes and explosions located with NonLinLoc and the 3D PM17 model. The locations are similar to those obtained with Hypocenter and the IGN 1D model. However, the new locations show greater clustering, especially the explosions presumably associated with the easternmost quarry (41.4°N, 0.4°W). Likewise, the explosions that occurred in the western part of the network show less dispersion, although in this case it is more difficult to associate the explosions with a specific quarry.

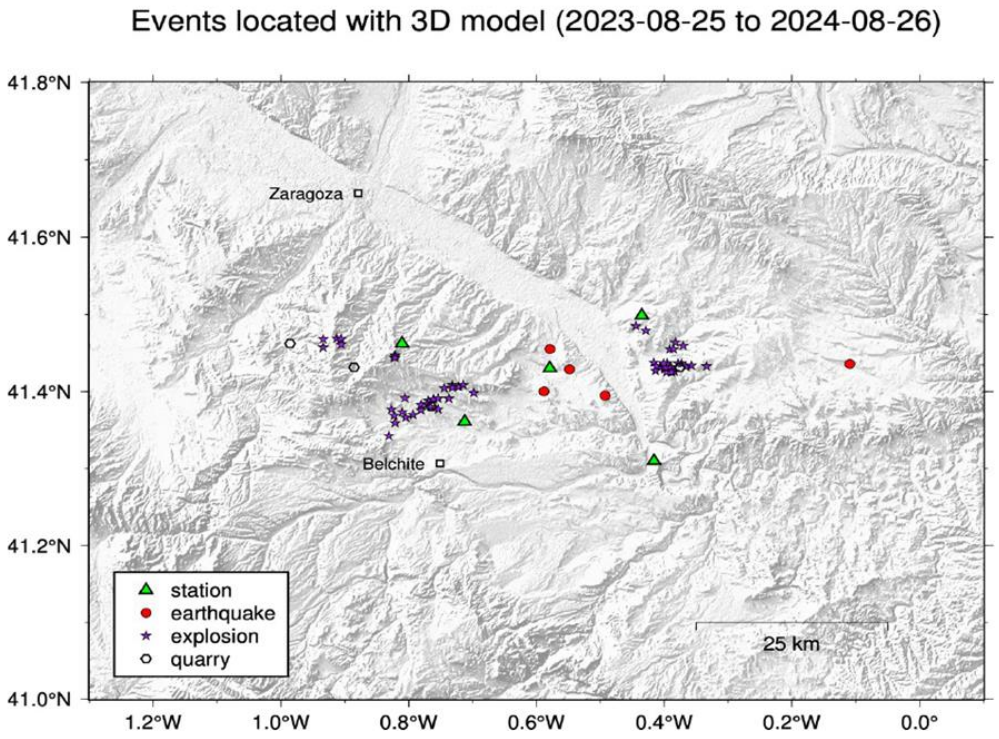

Figure 46. Map of the LOPIN area with the epicenters of earthquakes and explosions located in this study using the NonLinLoc program and the 3D PM17 model. The positions of the quarries were obtained from Google Earth images.

As for the recorded earthquakes, the difference in epicenter between the 1D and 3D locations is small, as they are within the network. The differences in depth are somewhat more significant. Using the IGN 1D model, the depths of the three events are 5 km, while those obtained with the 3D model range between ~5 and 10 km. This is a direct consequence of the 3D model being slower than the 1D model, resulting in greater depths. From the calculated depths, it is deduced the earthquakes do not occur in the sediments of the Ebro basin but in the crystalline basement.

The PilotSTRATEGY project has received funding from the European Union's Horizon 2020 research and innovation programme under grant agreement No. 101022664

Figure 47 compares the location obtained by the IGN and by this study for the only two events that occurred inside the study region during the operation of the PilotSTRATEGY temporary network that are listed in the IGN catalog: one inside the LOPIN network (2024-03-05 at 01:39:55.80 UTC, mbLg=2.0) and one outside the network to the east (2024-08-21 at 10:05:59.20 UTC, mbLg=1.2). The differences between the IGN epicenters and the ones obtained with a 3D model and NonLinLoc are small (less than 4 km). In both cases the 3D location is towards the west, that is towards the center of the network. However, the difference in depth is slightly more significant. For the event that occurred inside the network (2024-03-05) the IGN reports a depth of 0 km (which really means that depth was not determined), while the depth obtained in this study is 7.8 km. This difference is mainly due to the speed model used. The 1D model of the IGN is too fast for this area, resulting in shallower depths. Using a specific 3D model for the study area allows for more realistic depths. The same effect is observed with the earthquake that occurred outside the network (2024-08-21). The IGN lists a depth of 3.7 km, while the depth obtained using NonLinLoc and the 3D model is significantly deeper (10.1 km). In this case, since the earthquake is outside the network neither depth estimate is well constrained, and the effect of using a 3D model is less clear. Table 11 is a comparison of the focal parameters of the two events discussed here.

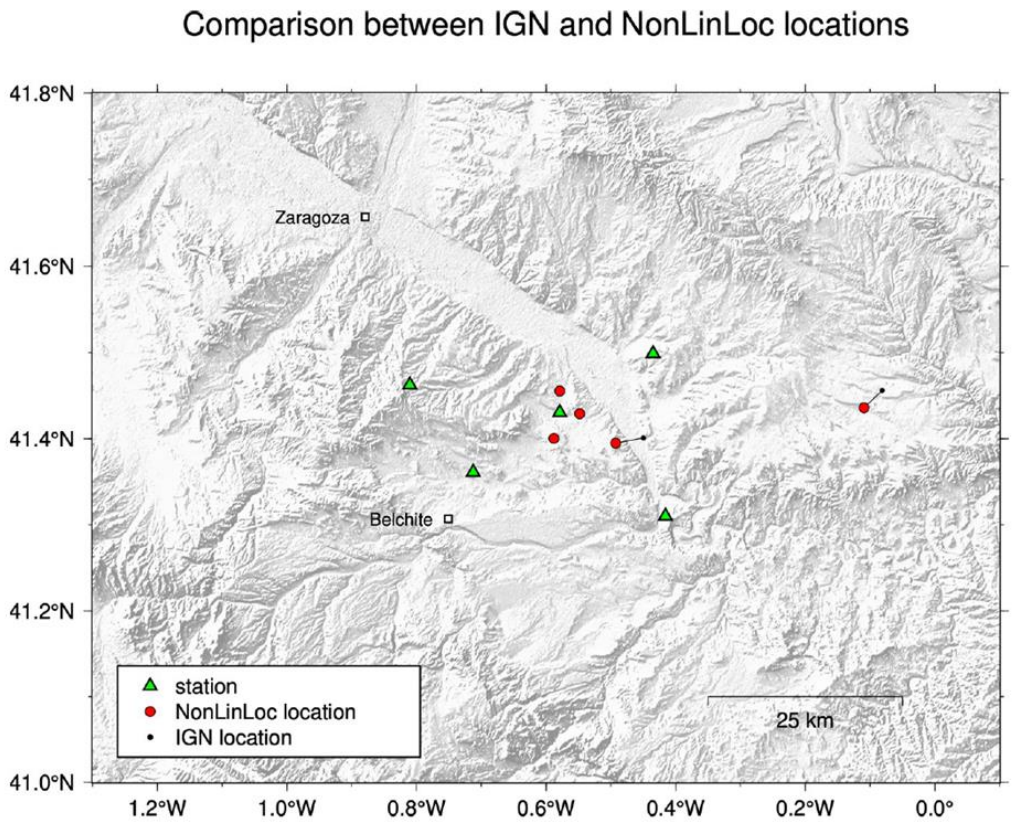

Figure 47. Map of the LOPIN area with the epicenters of earthquakes and explosions located in this study using the NonLinLoc program and the 3D PM17 model (red circles) and their comparison with the location obtained by the IGN for the earthquake on 2024-03-05 at 01:39:55.80 UTC (black circle).

The PilotSTRATEGY project has received funding from the European Union's Horizon 2020 research and innovation programme under grant agreement No. 101022664

Source (+)	Date	Time	Latitude (°N)	Longitude (°E)	Depth (km)
Event 1					
IGN	2024-03-05	01:39:55.80	41.401	-0.450	0.0
HYP	2024-03-05	01:39:55.30	41.392	-0.489	5.0
NLL	2024-03-05	01:39:54.52	41.395	-0.492	7.8
Event 2					
IGN	2024-08-21	10:05:59.20	41.456	-0.081	3.7
HYP	2024-08-21	10:05:59.20	41.452	-0.084	6.6
NLL	2024-08-21	10:05:58.48	41.436	-0.109	10.1

*Table 11 Comparison of the focal parameters for the events listed by the IGN catalog in the study region. *IGN=IGN location; HYP=location obtained with Hypocenter and a 1D model; NLL=location obtained with NonLinLoc and a 3D model*

2.5 Discussion and Summary

The main results are the generation of a new seismic catalog by combining existing catalogs, obtaining additional arrival times (when available) and using 3D velocity models with a non-linear location method. New focal mechanisms have been obtained for the largest earthquakes in the extended study region.

The region has a low level of natural seismicity. Inside the rectangular region indicated in Figure 4, only 15 events have been located since 1900. The earliest event listed occurred in 1993. The event with the largest magnitude (2.6) occurred on 1996-04-11. The seismicity is scarce throughout the region with no clear alignment of events on lineaments.

Focal depths for these events in the IGN catalog range from 5 to 20 km. However, 6 of the 15 events have a listed focal depth of 0 km which means that the available phase arrival time data were insufficient to determine a reliable depth due to the low number of picks and/or a bad azimuthal distribution. This situation is clearly explained by the distribution of seismic stations in the region. There is no permanent or temporary station within the Lopín region, and the closest station is the IGN station ESAC (San Caprasio, Zaragoza). The next closest permanent stations are more than 150 km away, and there is a significant azimuthal gap to the west (see the IGN map)

This situation could have been improved by the use of temporary stations of the IberArray network and other deployments. However, during the main period of these deployments (2007-2014) only 1 earthquake occurred in the study region, the event on 2012-03-14 for which the IGN bulletin reported no phase data. For this event, manually picking of P and S wave arrival times have been completed, at stations from the permanent and temporary networks. For the other events no additional arrival times from temporary networks could be obtained.

The use of a 3D model (PM17) and a non-linear location method (NonLinLoc) has had a positive effect on the earthquake locations in this region. Most important it has increased the value of the focal depth, and therefore eliminated all the events with surface focus (depth = 0

The PilotSTRATEGY project has received funding from the European Union's Horizon 2020 research and innovation programme under grant agreement No. 101022664

km). The average focal depth is 12 km, with an average increase in focal depth of 5.6 km. This result is expected since the 1D model used for earthquake location by the IGN is too fast for this region, and faster models result in shallower focal depths. The use of the PM17 model, with a clear expression of the Ebro basin as low velocities results in deeper focal depths (compensated by earlier origin times of 0.6 s on average). The lateral variations of the 3D model do not have a systematic effect on the new epicenters. This is probably because the azimuthal coverage of seismic stations in this region is reasonably good, and the lateral velocity variations are not very pronounced.

As a result of the seismic network deployment and analysis, the conclusions are:

- The seismicity level of this region is very low, and the configuration of the permanent networks in the region (IGN) is not favorable to the detection of small earthquakes. Therefore, to characterize the seismicity of this area it is necessary the deployment of a local seismic network and to operate it during a time period long enough to record a significant number of seismic events.
- The 1D model used by the IGN for earthquake location in the region is not appropriate (too fast) and results in very shallow focal depths. The use of a velocity model (1D or 3D) that takes into account the shallow low velocities associated with the Ebro basin sediments results in more reasonable focal depths of 12 km in average, typical of earthquakes in continental crust.
- The use of a 3D model did not result in large nor systematic shifts in epicenter. This is because the azimuthal coverage of the stations of the permanent network is relatively homogeneous (although the spatial station coverage is sparse and lacks nearby stations). Therefore, for this region the use of an appropriate 1D model would be enough for earthquake location.
- The most common seismic events in the area are explosions of mining activity in nearby quarries. The records of these explosions are easily distinguishable from tectonic events in the stations of the LOPIN temporary network.
- The study area is the foreland basin to the Pyrenees Mountain Range characterized by a thick sediment infill and with no faults mapped in the surface. The obtained earthquake depths support that they do not occur in the basin sediment infill. The seismic events occurred in unmapped structures in the basement of the basin.
- The SARA sensors and dataloggers have demonstrated excellent performance, maintaining nearly continuous real-time connectivity.

The PilotSTRATEGY project has received funding from the European Union's Horizon 2020 research and innovation programme under grant agreement No. 101022664

3. Lusitanian basin area

3.1 Introduction to the Lusitanian basin

Although the focus of this part of the PilotSTRATEGY project is on the offshore part of the Lusitanian Basin (BL), the data analysis was conducted for the entire basin area. Seismic alignments in the offshore region can only be observed if onshore seismicity is also considered in the analysis.

The first part of this section shows the analysis of seismic activity based on the data gathered in what has come to be known as the "National Seismic Catalogue." The analysis focused primarily on the period from 2000 to 2023, when the national seismic network reached its current configuration, which is characterized by a higher station density and uniformity in terms of detection capability than previously. This study was conducted in collaboration with the Institute for Sea and Atmosphere (IPMA), which provided the seismicity data for the region.

The second part is focused on the installation and monitoring of a bespoke, temporary, seismic network deployed for the PilotSTRATEGY project between January 2023 and December 2023.

The third part, which was the most demanding and time-consuming task, involved the presentation of the results of event detection and their location. This was made possible by the waveform data from the temporary network of seismic stations installed as part of the PilotSTRATEGY project, as well as the waveform data and bulletins provided by IPMA (Instituto Português do Mar e da Atmosfera, the Portuguese Institute for Sea and Atmosphere).

3.2 Review of the seismicity in the Lusitanian basin

The Portuguese National Seismic Catalogue, which, as previously mentioned, gathers contributions from various sources, includes both historical data (the oldest event reported dates to 309 AD) and instrumental data. It highlights maximum intensities, particularly in the Algarve and Lisbon regions (Figure 48). The largest magnitude events originate from the southwest margin of the Iberian Peninsula. However, due to the significant distance between the epicentres and the study area, these events typically do not result in high intensities or accelerations on the mainland (with the exceptions of the 1755 and 1969 earthquakes and other major historical events (Borges et al., 2001; Pereira et al., 2014; Ferrão et al., 2016; Carrilho et al., 2021).

The PilotSTRATEGY project has received funding from the European Union's Horizon 2020 research and innovation programme under grant agreement No. 101022664

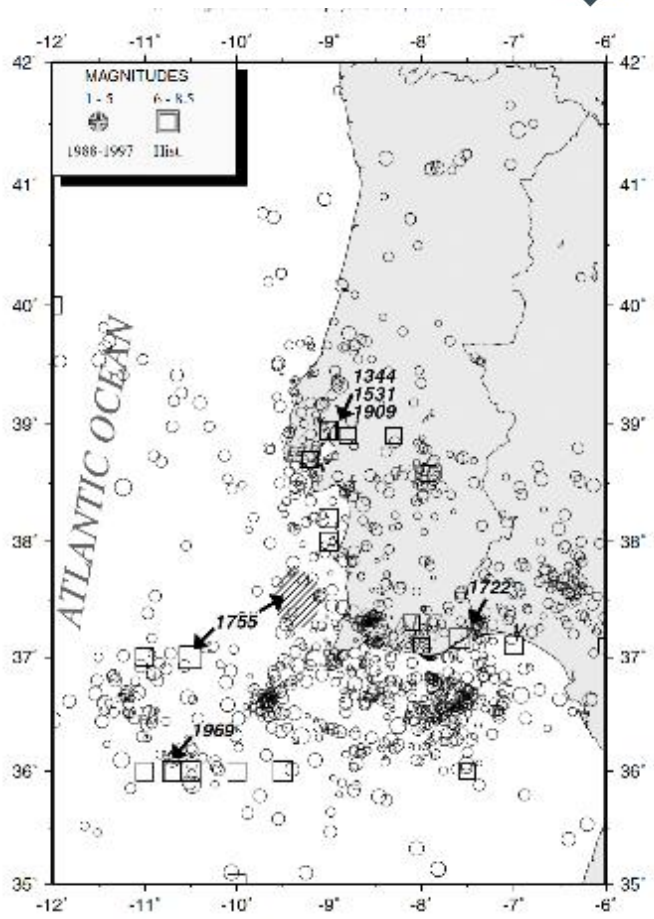

Figure 48. Instrumental seismicity (1988 - 1997) and most important historical earthquakes since 134 (Borges et al., 2001).

Events occurring in the Lower Tagus Valley (L.T.V.) region which lies to the north-east of Lisbon, while of smaller magnitude than those from the southwest margin, significantly contribute to the seismic hazard in the Lisbon and Tagus Valley areas. This is due to their closer proximity, and effects caused by the basin's structure, which dates from Cenozoic and is made up of poorly consolidated sediments. The study area, although close to the Lower Tagus Valley region and of Mesozoic composition, presents a moderate seismic hazard within the national context of Portugal.

Eurocode 8 (EC8) is a European standard that sets criteria for the design and construction of earthquake-resistant structures. In Portugal, it is adopted as the reference code to ensure the safety of buildings and infrastructure in seismic zones. According to this code, a maximum acceleration of 1.1 m/s² is expected for the Lusitanian Basin region (Figure 49).

The PilotSTRATEGY project has received funding from the European Union's Horizon 2020 research and innovation programme under grant agreement No. 101022664

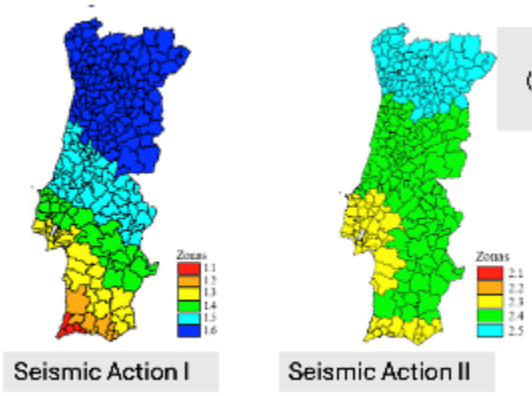

Seismic Action I. (far-field scenario)	a_{gr}(m/s^2)	Seismic Action II Near-field scenario	a_{gr}(m/s^2)
1.1	2,5	2.1	2,5
1.2	2,0	2.2	2,0
1.3	1,5	2.3	1,7
1.4	1,0	2.4	1,1
1.5	0,6	2.5	0,8
1.6	0,35	-	-

Figure 49. Seismic zoning in Mainland Portugal considered in Eurocode 8 (NP EN 1998-1) and the National Annex (2009). Source: https://spessismica.pt/eurocodigo-8/

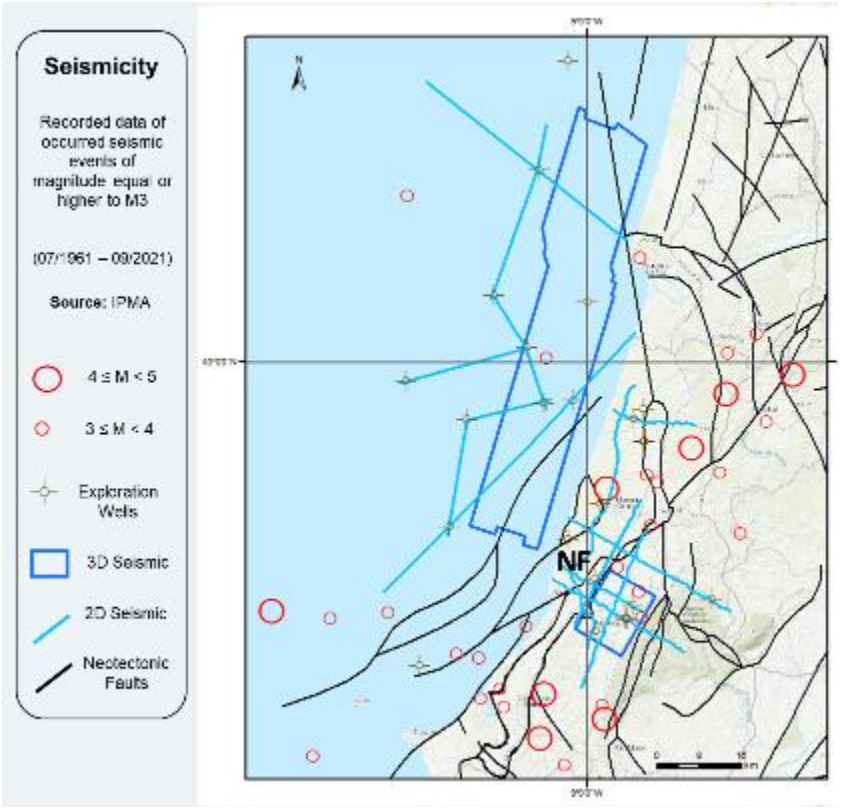

Figure 50. Seismicity for the period between 1961 and 2021 for magnitude M≥ 3 for the Lusitanian Basin and the main neotectonic faults for the region. The Nazaré fault (NF) is highlighted. The areas marked in blue represent the target zones of the project

Analyzing the seismicity of moderate magnitude (M ≥ 3, Figure 50), this is primarily concentrated in the southern part of the Basin. This seismicity may be related to a major tectonic feature in the region, specifically the Nazaré fault (NF) and its associated fault system. To the north of this area, seismicity in this magnitude range is practically nonexistent. The seismicity in the offshore area of the Lusitanian Basin is also dispersed, of lower magnitude, and apparently not related to the oceanic extension of any mapped fault.

The PilotSTRATEGY project has received funding from the European Union's Horizon 2020 research and innovation programme under grant agreement No. 101022664

Since 2000, all seismic stations of the IPMA network have been upgraded to broadband, providing real-time data with extensive and homogeneous coverage of Portugal mainland. This is the reason why we chose this period for the analysis of seismicity and micro-seismicity.

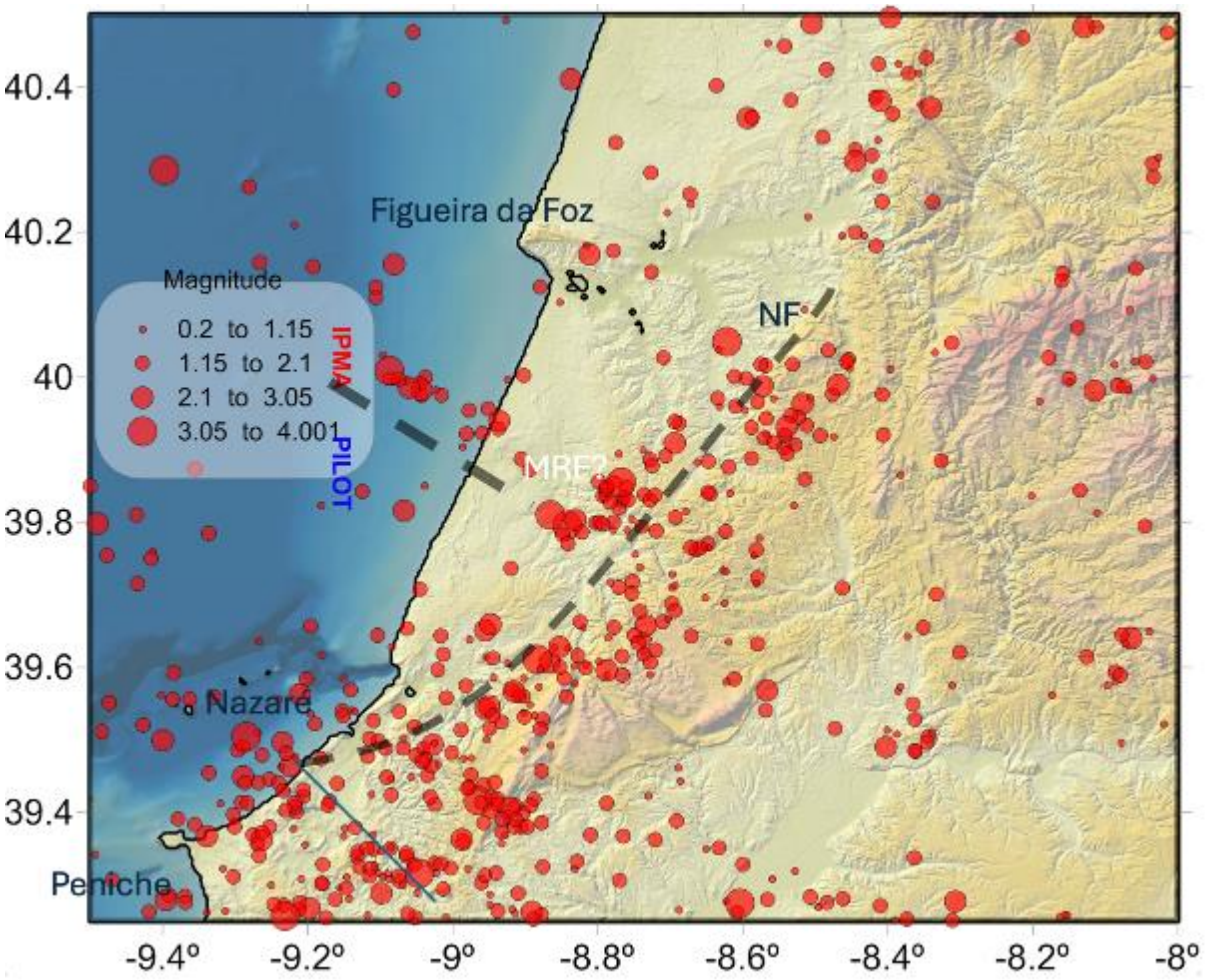

Figure 51. Seismicity for the period between 2000 and 2022 for all magnitude. (MRF - Possible Monte Real Fault (not mapped) and Nazaré Fault (NF).

The analyzed data were collected from seismic bulletins published by IPMA (https://www.ipma.pt/pt/geofisica/sismicidade/). The data were converted to NORDIC format (SEISAN) to facilitate easier manipulation and statistical analysis. The data were then filtered for a geographical area between latitudes 39.25º N and 40.5º N and longitudes 10.5° W and 8.0° W.

Looking at the seismicity between 2000 and 2022 we are considering the entire range of magnitudes of earthquakes (Figure 51). In addition to the previously mentioned alignment associated with the Nazaré fault (although with significant spatial dispersion), it is also important to note a second alignment of low-magnitude events: this alignment originates onshore and extends into the offshore area in an approximately NW-SE direction (possibly along the MRF- Monte Real Fault). Nonetheless, it is important to consider the actual existence of this alignment with caution, as the IPMA seismic

The PilotSTRATEGY project has received funding from the European Union's Horizon 2020 research and innovation programme under grant agreement No. 101022664

network's ability to accurately locate events in this magnitude range is limited, particularly due to low azimuthal coverage.

The selected events for this period and geographical area predominantly have magnitudes between 1 and 4 Mb (body wave magnitude) and are shallow, with hypocentre depths not exceeding 30 km.

3.3 Monitoring network

The aim of this section is to show the temporary seismic network deployed for the PilotSTRATEGY project, and the results of recording the microseismicitiy in the central and north sector of the Lusitanian Basin.

Two seismic networks were planned with the aim of monitoring seismic activity in the Lusitanian Basin, in both the onshore and offshore: areas one in the Alcobaça area for onshore monitoring, and another focused on offshore monitoring, consisting of two small-aperture arrays: one centered in Porto de Mós and the other in Figueira da Foz (Serra da Boa Viagem).

3.3.1 Installation and operation

- Site Selection: The ideal location was chosen in a rural area, far from sources of artificial vibration such as roads, industries, and railways. The selected terrain is stable and minimally impacted by human activities, reducing seismic noise.
- Digging and Ground Preparation: A small pit is dug into the ground to house the seismic sensor. The depth varies but is typically sufficient to mitigate the effects of temperature.
- Seismometer Installation: The seismometer was carefully positioned at the bottom of the pit, aligned according to precise coordinates (North-South and East-West). The instrument is then covered with materials, such as fine sand to ensure stability and reduce external interference.
- Power Supply: The station is powered by a set of batteries, specifically sized to ensure continuous operation for two months without the need for maintenance. The batteries are protected from weather and vandalism.
- Data Logger: A data logger is connected to the seismometer.
- Testing: After installation, the system is tested and calibrated to ensure it is functioning correctly and capturing seismic data accurately.
- Maintenance and Monitoring: Every two months, a technical team visits the station to check the equipment, replace the batteries, and ensure all components are in good working condition.

The PilotSTRATEGY project has received funding from the European Union's Horizon 2020 research and innovation programme under grant agreement No. 101022664

Figure 52. Example of installation

3.3.2 Onshore Array

Due to delays in the equipment acquisition process, the decision was made to initiate monitoring in the onshore area using portable broadband stations (Guralp - 6TD) that belong to the University of Évora. This data acquisition took place during the year 2022.

The stations of the onshore network were installed in areas where the soil is quite consolidated, including schists and limestone outcrops. The stations were fully buried to minimize visual impact and to prevent vandalism. They consist of Guralp 6TD instruments with a 30-second period, which have an internal digitizer and are connected to batteries to ensure approximately two months of autonomy. In Table 12, the names of the stations and their geographical coordinates can be found, Figure 53. Geographical location of the Onshore (OS) network.s hows the locations on a map.

Code	Network	Latitude (°N)	Longitude (°E)	Elevation (m)
PMOS	OS	39.59678	-8.83719	174
BAR01	OS	39.57566	-9.02500	286
COZ01	OS	39.58835	-9.02509	096
PIS01	OS	39.67146	-8.94356	094
PSBE	PM	9.514167	-8.79550	497
VIM01	OS	39.47219	-9.01076	170
EAL01	OS	39.50815	-8.91337	193

Table 12. Coordinates of onshore seismic stations (OS).

The PilotSTRATEGY project has received funding from the European Union's Horizon 2020 research and innovation programme under grant agreement No. 101022664

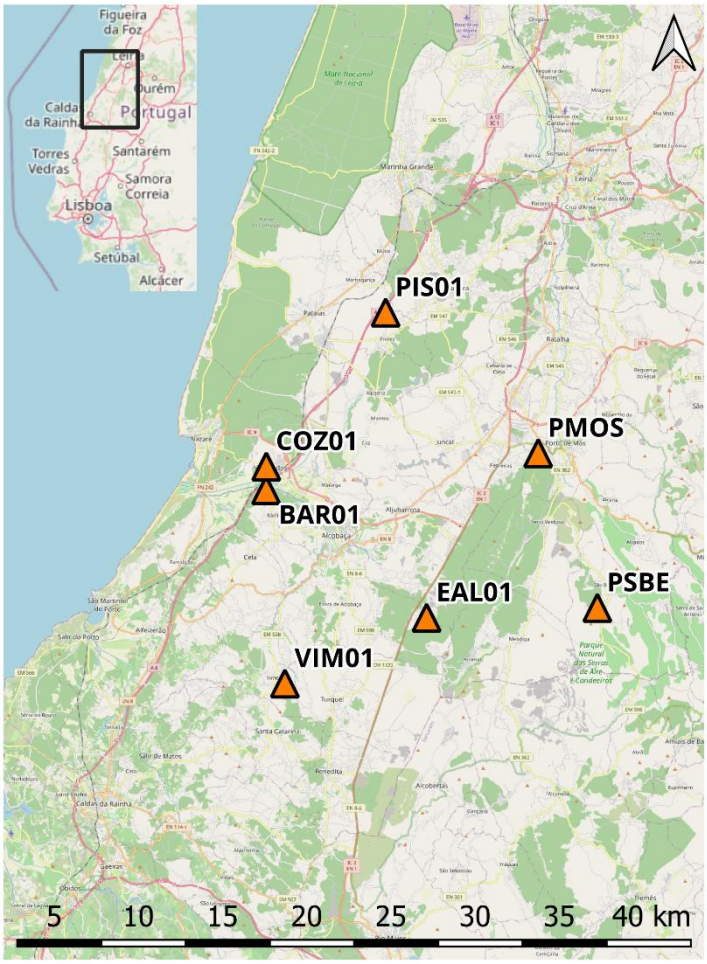

Figure 53. Geographical location of the Onshore (OS) network.

3.3.3 Offshore Array

The second deployment took place during the year 2023. During this period, two small-aperture arrays were installed, primarily aimed at monitoring the offshore area. These arrays consisted of 7 short-period autonomous stations (2 Hz). To minimize human-induced seismic interference at the stations, sites were selected in open areas positioned as far as possible from sources of artificial noise. We chose to power the stations with batteries to prevent theft or vandalism. These batteries were selected to ensure a data collection and power replacement frequency of every two months see Tables 15 and 16; Figures 54 and 55.

3.3.3.1 Porto de Mós Array (PS)

Code	Network	Latitude (°N)	Longitude (°E)	Elevation (m)
PS01	PS	40.19587	-8.83781	350
PS02	PS	39.5926	-8.83779	354
PS03	PS	39.5908	-8.83938	360
PS04	OS	39.5968	-8.83723	298
PS05	PS	39.5945	-8.83307	316

The PilotSTRATEGY project has received funding from the European Union's Horizon 2020 research and innovation programme under grant agreement No. 101022664

PS06	PS	39.5912	-8.83307	260
PS07	PS	39.5949	-8.83863	326

Table 15. Coordinates of offshore seismic stations – Porto Mós (PS).

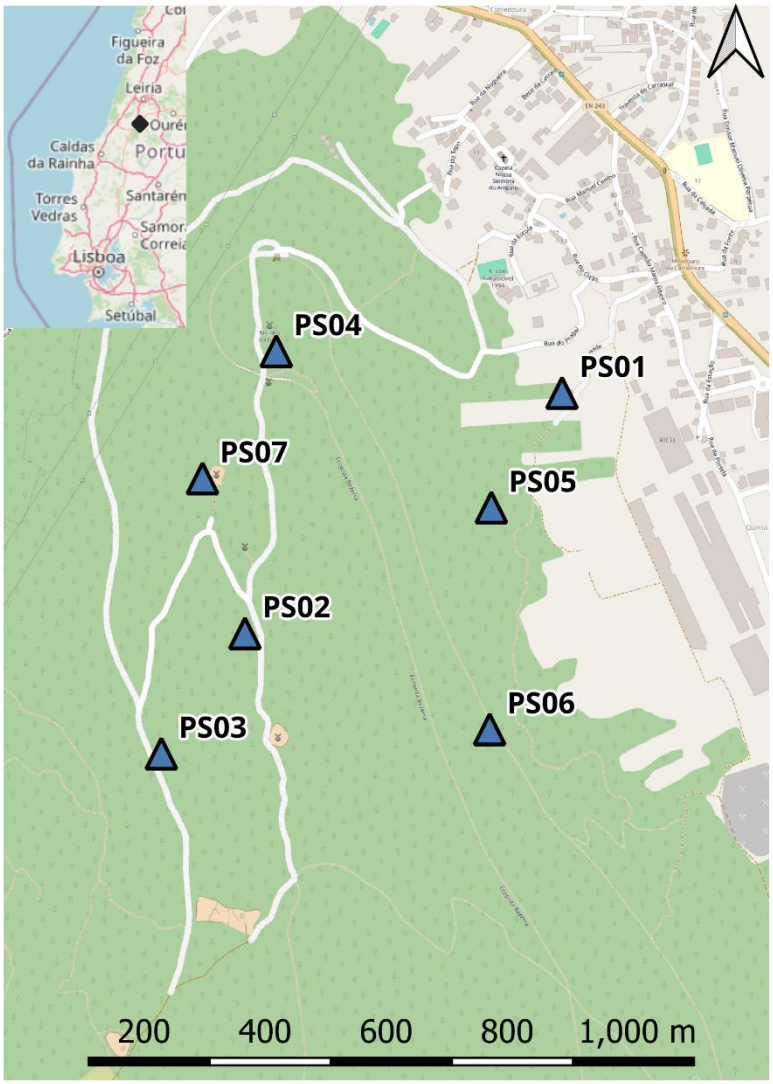

Figure 54. Geographical location of the Porto de Mos Array (PS). Coordinates in km; origin station PM01.

3.3.3.2 Figueira da Foz Array (FF)

Code	Network	Latitude (°N)	Longitude (°E)	Elevation (m)
FF01	OS	40.19587	-8.88438	237
FF02	OS	40.19647	-8.88777	216
FF03	OS	40.19472	-8.88461	252
FF04	OS	39.67146	-8.94356	094
FF05	PM	40.19996	-8.88378	247
FF06	OS	40.19428	-8.88871	234
FF07	OS	40.20204	-8.88073	251

The PilotSTRATEGY project has received funding from the European Union's Horizon 2020 research and innovation programme under grant agreement No. 101022664

Table 16. Coordinates of offshore seismic stations – Figueira da Foz (FF).

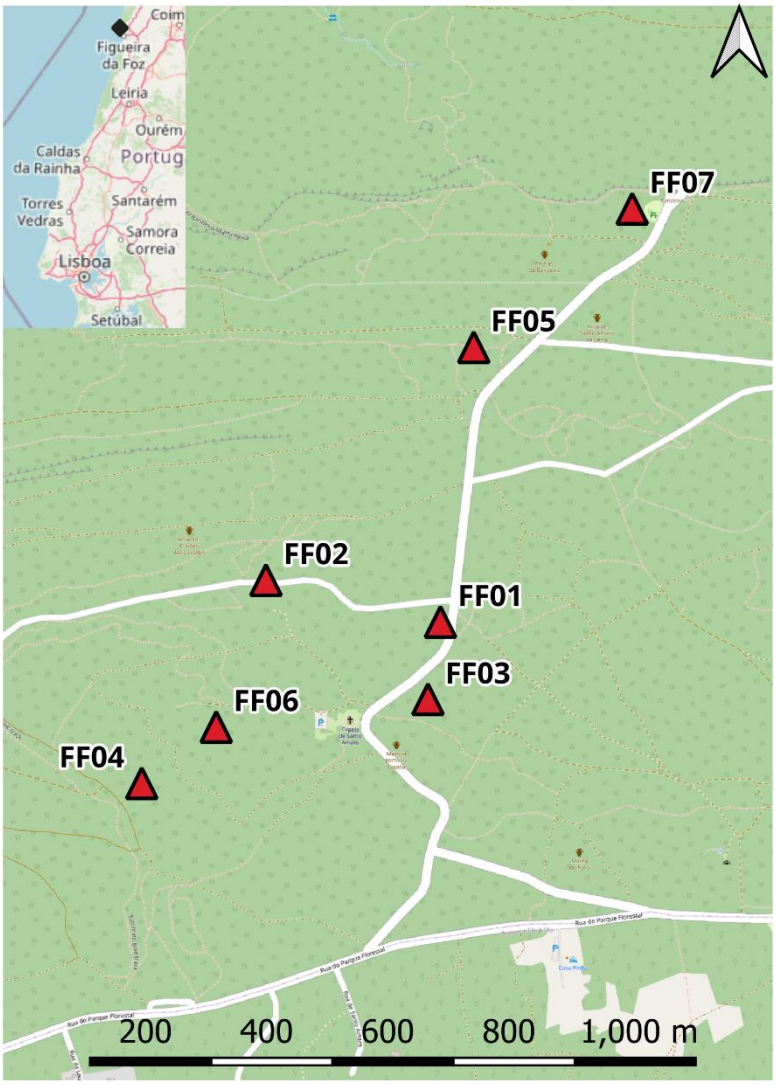

Figure 55. Geographical location of the Figueira da Foz Array (FF). Coordinates in km; origin station FF01.

3.3.4 Instruments

Guralp – CMG-6TD (broadband)

ST-2-3D :

2Hz Short Period Instrument
Data Cube Digitizer

The PilotSTRATEGY project has received funding from the European Union's Horizon 2020 research and innovation programme under grant agreement No. 101022664

Figure 56. Broad band (left) and Short Period (right) instruments.

The instrumental response of the network seismographs has been provided by the manufacturers (Figure 6)

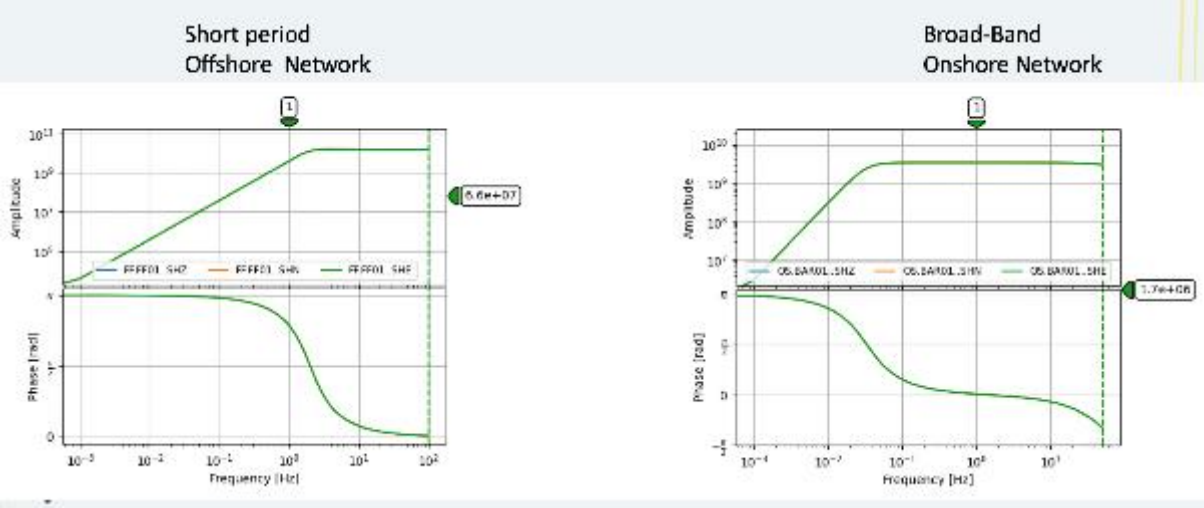

Figure 57. Frequency and Phase responses for the Broad Guralp 6TD instrument (30s) and DIGOS and short period Instrument (2 Hz).

3.3.5 Waveform data

3.3.5.1 Data structure

The waveform data from the stations have been received in original formats and converted to miniSEED format and organized in SeisComp or SDS directory structure (short for 'SeisComP directory structure'). The directory structure follows the scheme YYYY/NN/STA/CHN.Q, where YYYY is the year, NN is the network code (in this case 'LO'), STA is the station code (FF01 …), CHN is the channel (SHE, SHN, SHZ for the three components of motion), and Q is a quality indicator which in our case will always be D (data). The directory tree structure would be (Figure 58):

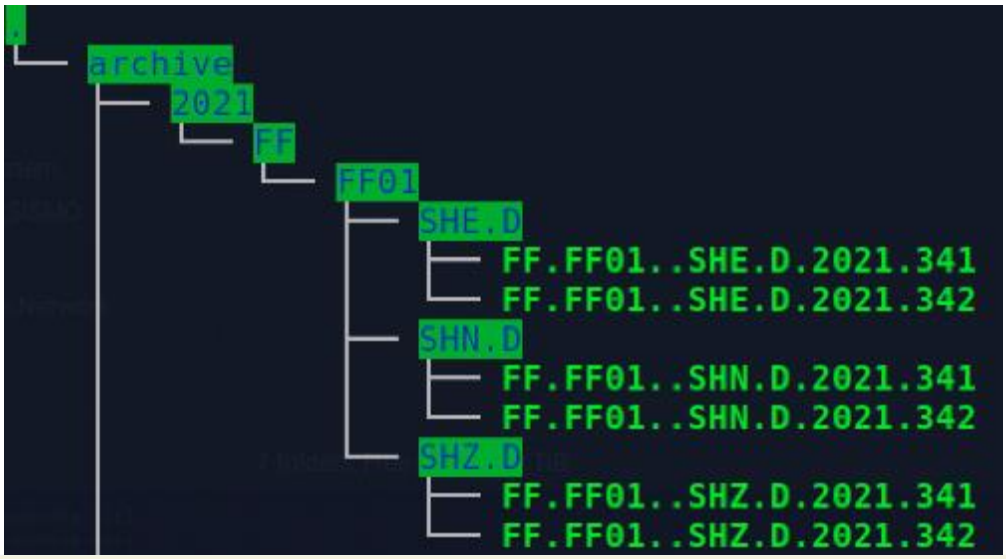

The PilotSTRATEGY project has received funding from the European Union's Horizon 2020 research and innovation programme under grant agreement No. 101022664

Figure 58. Database structure - similar to SEISCOMP structure.

The file names follow the scheme NN.STA.LL.CHN.Q.YYYY.JJJ where NN is the network code (OS/FF/PS), STA is the station code (ex. FF01 to FF07), LL is the instrument number at this location (there is only one instrument with code 00), CHN is the channel name (EHE, EHN, EHZ), Q is the quality indicator (D), YYYY is the year, and JJJ is the day of the year (000 to 365 or 366). In Figure 58, an example is shown.

3.3.5.2 Continuity of the data

Within each directory, there are 1-day files for each station and component. The files may contain gaps (missing data) and overlaps (Figure 59). It is noted that there were long periods without recordings due to equipment malfunctions, unexpected battery depletion, or failure to detect the GPS.

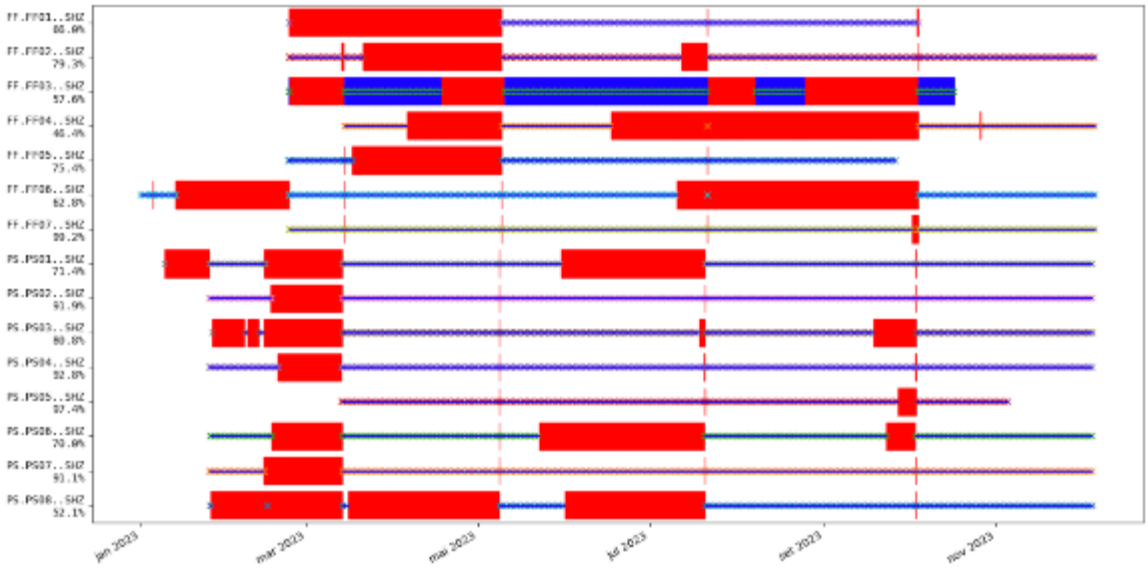

Figure 59. Data availability for vertical components of the offshore stations. Station name and channel are represented on the Y axis. The horizontal blue line shows the continuity of the data while vertical redlines indicate data gaps. It is noted that there were long periods without recordings due to equipment malfunctions, unexpected battery depletion, or failure to detect the GPS.

3.3.6 Ambient seismic noise analysis

The noise levels of continuous recordings from the offshore network during 2023 were analyzed using PQLX software (Boaz and McNamara, 2008), following the methods outlined in McNamara and Buland (2004) and McNamara et al. (2009).

The analysis are based on calculating the power spectral density (PSD) segments of continuous data and after calculating the probability density function (PDF), which indicates the quality of the data for each frequency.

Figure 60 show the PDFs for the offshore network. The PDF values for long periods (e.g. > 1s) become less relevant, as the instrument's response significantly decreases beyond this period. It can be observed that the noise level of all of them is within the limits set by the new low-noise model (NLNM) and the new high-noise model (NHNM) determined by Peterson (1993). As with most stations/components, the PDF level is significantly below the NHNM level, indicating good performance capabilities for local earthquakes.

The PilotSTRATEGY project has received funding from the European Union's Horizon 2020 research and innovation programme under grant agreement No. 101022664

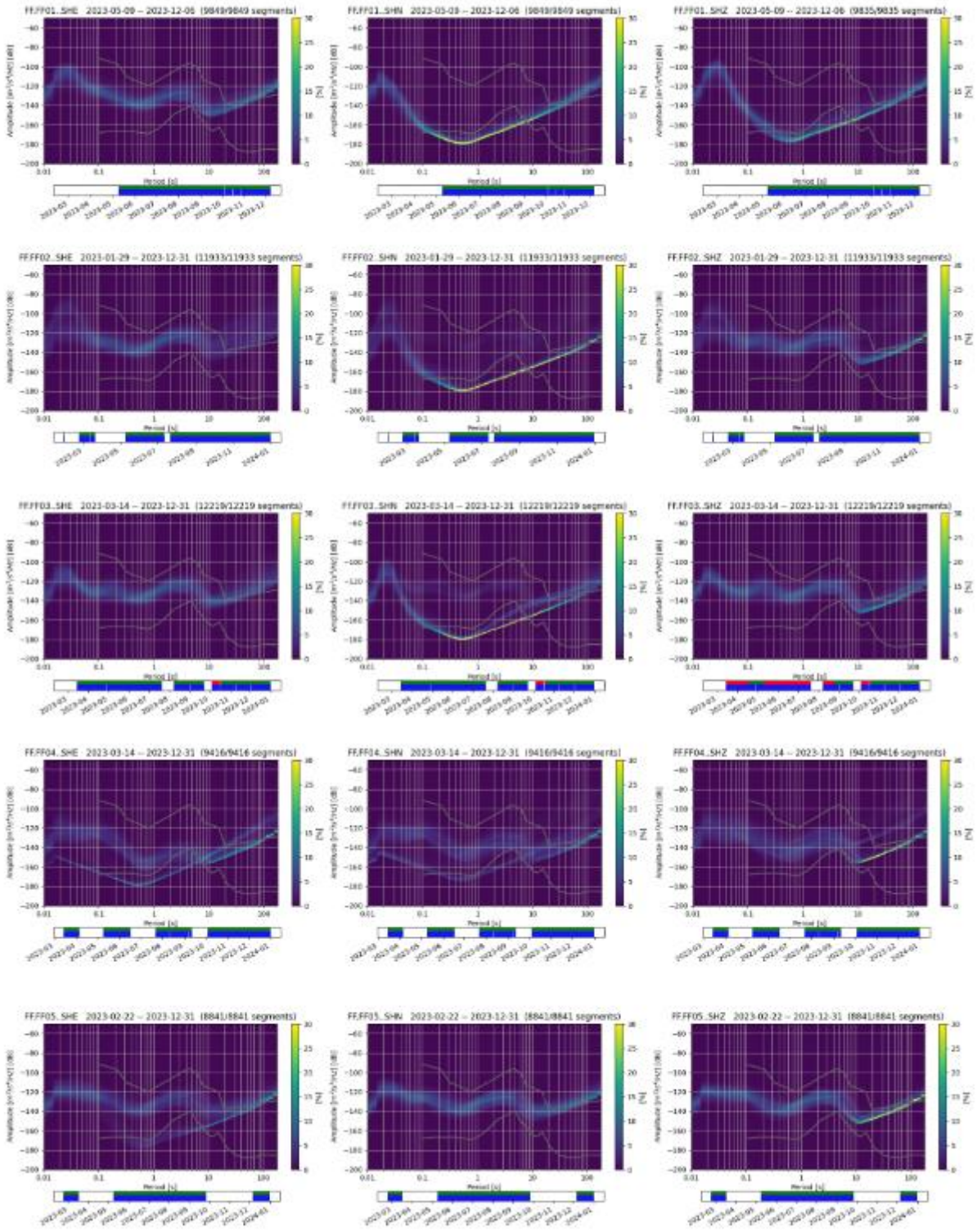

The PilotSTRATEGY project has received funding from the European Union's Horizon 2020 research and innovation programme under grant agreement No. 101022664

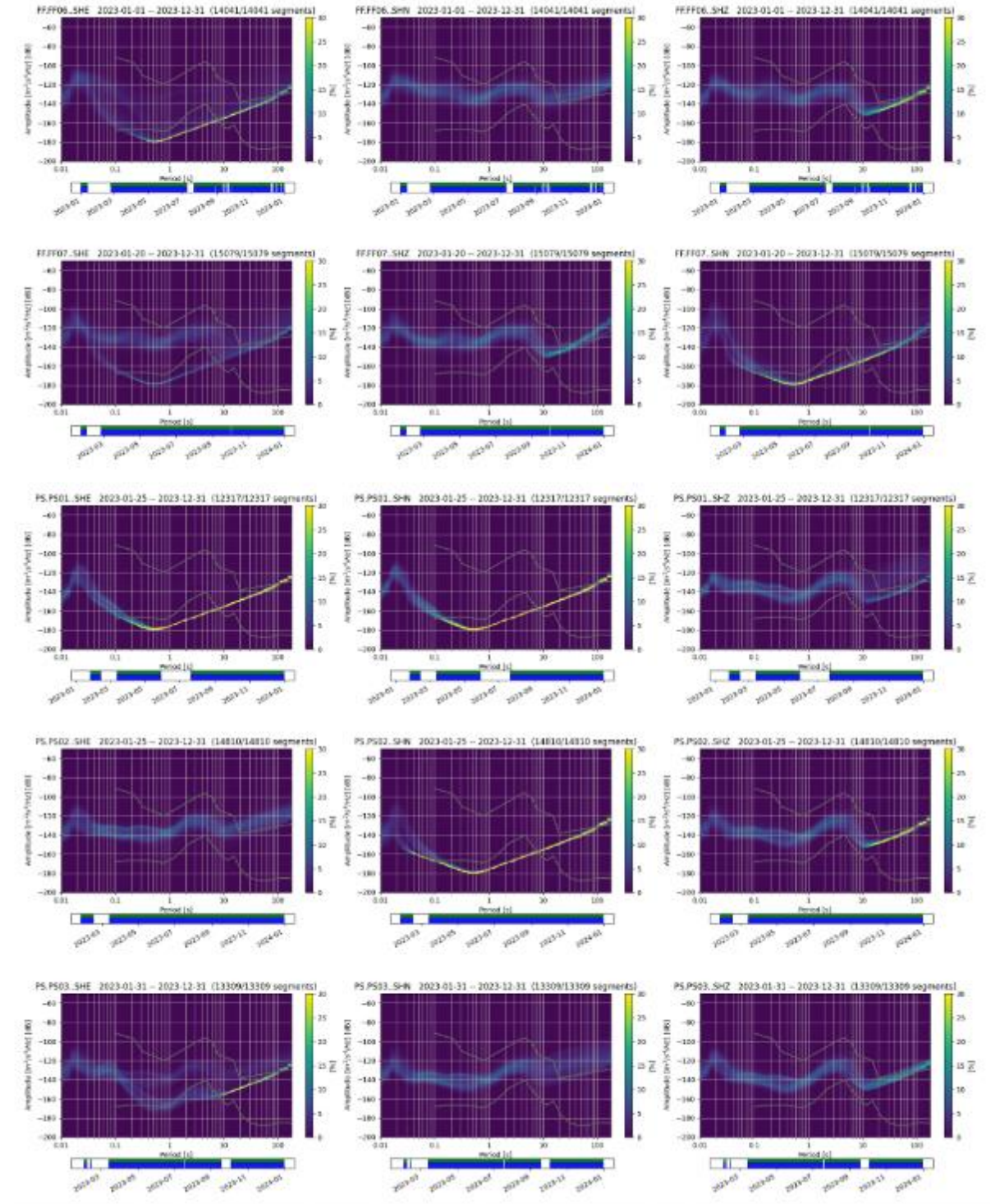

The PilotSTRATEGY project has received funding from the European Union's Horizon 2020 research and innovation programme under grant agreement No. 101022664

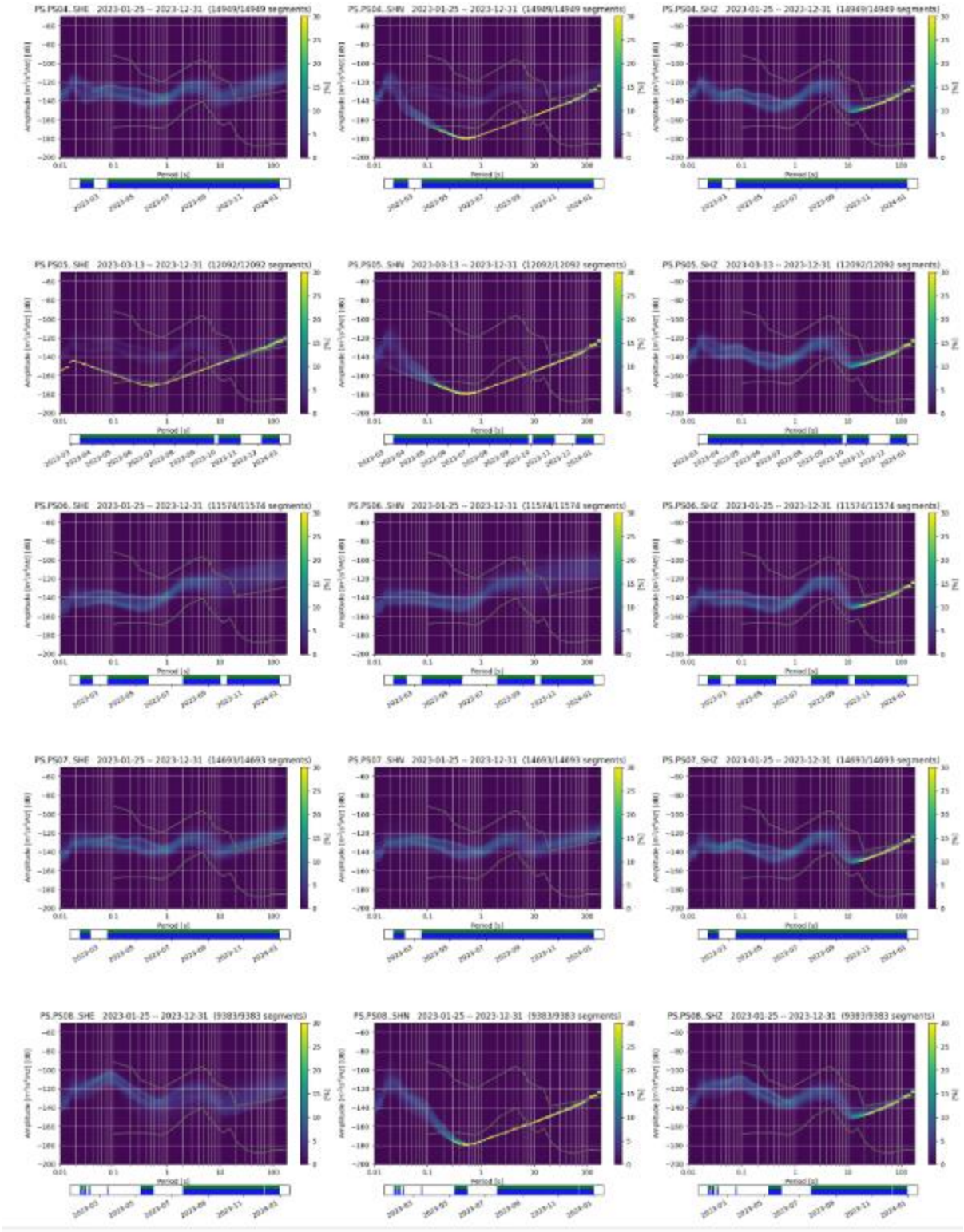

Figure 60. PDFs for the 3 components (SHE, SHN, SHZ) of the offshore seismic. The upper gray line indicates the New High-Noise Model (NHNM) and the lower gray line indicates the New Low-Noise Model (NLNM). The black line corresponds to the mode of the PDF for each period. Colors correspond to the level of the PDF.

3.3.7 Processing

The manual process of detection and picking is extremely time-consuming, which is why we used to automatic detection using the Deep Learning-based picker PhaseNet (Zhu and Beroza, 2018).

After the automatic picking, data association is carried out to eliminate false detections. A minimum of six components was used as a criterion to validate each detection. Following this process, human validation of the detections is performed. This chain of procedures allows for the removal of approximately 90% of false detections.

After picking, the data is entered into a SEISAN database, and in cases where there are matches with events detected by the network, event association is carried out. Event location is the next phase, which takes place within the SEISAN program.

Offshore events are located using an inversion process that employs a Bayesian methodology (Tarantola and Valete, 1982), which combines the product of a probability density function derived from classical HYPO inversion (a priori information) with the probability density function obtained through a beamforming methodology (parameters involved include the azimuth and slowness of the ray).

The 1D base velocity-depth model used in the process is derived from PRISM3D for the study area (Table 17).

Depth of the top of the layer (km)	Velocity P (km/s)
0.0	6.0
11.0	6.5
24.0	8.0
31.0	8.0
Half space	8.0

Table 17. IGN 1D velocity model derived from PRISM3D for the studied area.

3.3.8 The new catalog

After the location and calculation of the magnitude MLM_LML (Maximum Likelihood Method – Log Marginal Likelyhood) of the new events, a new catalog is generated. All events detected by IPMA that are included in their catalog were also identified by the Offshore network. In addition to these, a significant number of low-magnitude events were detected by the Offshore network. Figure 61 displays the epicenters, differentiated by color. The conclusions presented here are based solely on the networks focusing on the offshore area, which operated during the year 2023. Data collected in 2022 were disregarded, as the PilotSTRATEGY project selected the offshore region as the potential CO_2 storage site, rather than the onshore region. Appendix 3 includes the catalog of events detected by the network deployed in the PilotSTRATEGY project.

The PilotSTRATEGY project has received funding from the European Union's Horizon 2020 research and innovation programme under grant agreement No. 101022664

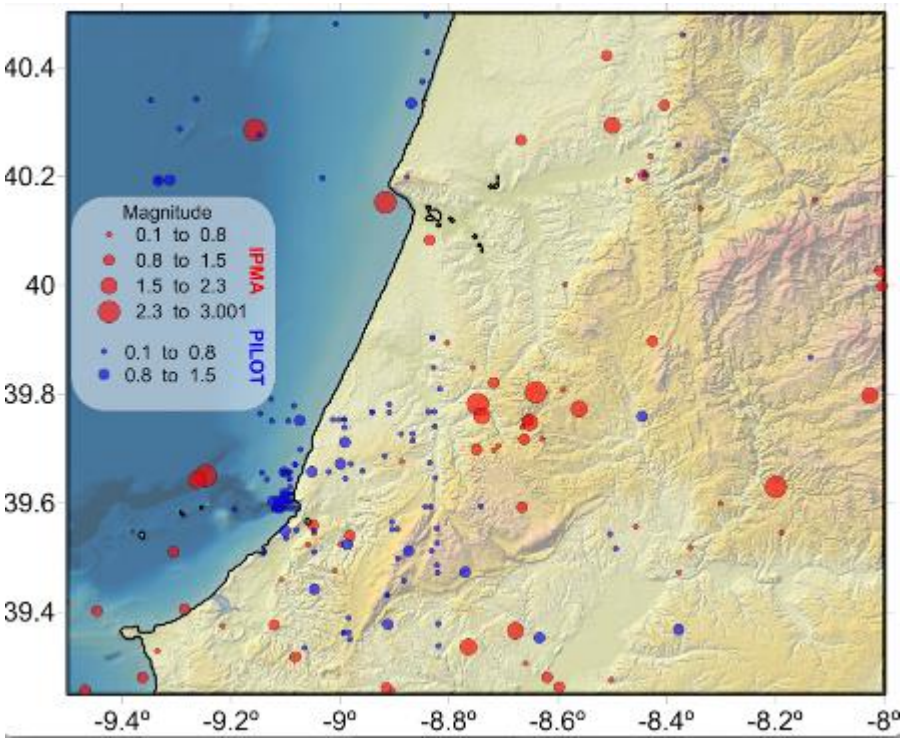

Figure 61. Map of the epicenters located in this study. Red circles represent the epicenters of earthquakes located by both networks (IPMA and Offshore), while blue circles indicate the epicenters of events detected exclusively by the Offshore network.

4. Conclusions

In both the Spanish (Lopin, Ebro Basin) and the Portuguese (offshore Lusitania Basin) area, a successful campaign of passive seismic acquisition was completed. For both areas, catalogues of existing seismic activity were compiled and reviewed. In both areas, a local seismic detection network specially designed for the purpose of local monitoring the area has provided information on local seismic activity.

Collecting seismic data is a logistically complex operation that depends upon the correct operation of installed equipment. For the Lusitania Basin, data gaps occurred during collection due to various contingencies. Although the offshore network's performance fell slightly below expectations due to numerous data gaps, the quality of the recordings remains satisfactory, as confirmed by noise analysis. The dataset collected in the Ebro basin was more complete. In both areas, a robust set of waveform data was obtained, which do not compromise the quality of the catalogue.

In the Lusitania Basin, 183 seismic events (earthquakes) were detected during 12 months of recording with 117 coinciding with events listed in the IPMA catalog. The remaining events are predominantly of magnitude less than 1 and are located in the offshore region. In the Ebro basin, only 5 tectonic earthquakes were detected, 4 within the area of the network and another one nearby. The focal depths are between 5 and 8 km, which indicates that they occur in the basement underneath the sediments of the Ebro basin. The LOPIN network also detected explosions (from quarries) and earthquakes that occurred outside the area. The depth of events was greater than 4.9 km.

The PilotSTRATEGY project has received funding from the European Union's Horizon 2020 research and innovation programme under grant agreement No. 101022664

For the Lusitanian Basin, the epicenter map reveals a concentration of events in the southern part of the region, a pattern that was also observed in the epicenter map for events between 2000 and 2022. The events listed in the current catalog have magnitudes (Ml) ranging from 0.5 to 3, with epicentral depths not exceeding 30 km. For events in the offshore region, an event location process was implemented that combines HYP (SEISAN) locations with beamforming. This methodology made it possible to constrain the locations of events occurring in the offshore region.

For the Ebro basin, the 1D velocity model used by the IGN for the location of earthquakes in the Iberian Peninsula does not represent well the seismic structure in the Ebro basin as the velocities used are too fast for the study area. Therefore shallower focal depth are obtained than when using a more realistic slower velocity model corresponding to a sedimentary basin. Thus, it is necessary to use a more appropriate velocity model to obtain reliable locations, in particular for focal depth. A specific 3D velocity model for the area such as the one used in this study is highly recommended for local seismic monitoring. The velocity model used is critical for the reliable estimation of the focal depth. There is no obvious geographic pattern to the Ebro Basin events, at least partly due to the very low numbers detected.

For any seismic monitoring, it is not possible to obtain focal mechanisms for the detected earthquakes if the magnitude of seismicity in the area is low, and the density of available seismic stations is limited.

The level of seismic activity around Lopín is relatively low, primarily concentrated in the mountain ranges surrounding the Ebro Basin. The maximum calculated magnitude by IGN is 4.1 for an event located 30 km to the south of the Lopín area. For the Lusitanian area, the number of events is higher, though the maximum magnitude is less at 3.0. For both areas, the level of activity is now well characterized, and does not pose a threat to the proposed underground storage of CO_2.

The PilotSTRATEGY project has received funding from the European Union's Horizon 2020 research and innovation programme under grant agreement No. 101022664

5. References

Benz, H.M., Chouet, B.A., Dawson, P.B., Lahr, J.C., Page, R.A. & Hole, J.A., 1996. Three-dimensional P and S wave velocity structure of Redoubt Volcano, Alaska, *J. geophys. Res.*, 101, 8111–8128.

Boaz, R. I., and D. E. McNamara (2008). PQLX: A data quality control system: Uses and applications. ORFEUS Newsletter 8 (1);

Borges, J.F.; Fitas, A.J.; Bezzeghoud, M.; Teves-Costa, P (2001). Seismotectonics of Portugal and its adjacent Atlantic area. Tectonophysics 2001, 331, 373–387. https://doi.org/10.1016/s0040-1951(00)00291-2.

Carrilho, Fernando and more 20 authors (2021). The Portuguese National Seismic Network—Products and Services (2021). Seismological Research Letters (2021) 92 (3): 1541–1570.

de Vicente, G., Cloetingh, S., Muñoz-Martín, A., Olaiz, A., Stich, D., Vegas, R., Galindo-Zaldívar, J. & Fernández-Lozano, J. (2008) Inversion of moment tensor focal mechanisms for active stresses around the microcontinent Iberia: Tectonic implications, Tectonics, 27(TC1009), doi:10.1029/2006TC002093.

Ferrão, C., M. Bezzeghoud; B. Caldeira, J. F. Borges (2016). The Seismicity of Portugal and Its Adjacent Atlantic Region from 1300 to 2014: Maximum Observed Intensity (MOI) Map. Seismological Research Letters (2016) 87 (3): 743–750.

García, J.E, Fernández-Prieto, L.M., Villaseñor, A., Sanz, V., Ammirati, J.B., Díaz Suárez, E.A. and García, C. (2022). "Performance of Deep Learning Pickers in Rou/ne Network Processing Applications." Seismological Research Letters 93 (5): 2529–42. hsps:// doi.org/10.1785/0220210323.

Heidbach, O., Custodio, S., Kingdon, A., Mariucci, M. T., Montone, P., Müller, B., Pierdominici, S., Rajabi, M., Reinecker, J., Reiter, K., Tingay, M., Williams, J., and Ziegler, M.: Stress Map of the Mediterranean and Central Europe, GFZ Data Service, hsps://doi.org/10.5880/WSM.Europe2016, 2016.

Herrmann, R. B., Benz, H. and Ammon, C. J. (2011). "Monitoring the Earthquake Source Process in North America." Bulle/n of the Seismological Society of America 101 (6): 2609–25. hsps://doi.org/ 10.1785/0120110095.

Lomax, A., Virieux, J., Volant, P. and Berge, C. (2000). Probabilistic earthquake location in 3D and layered models: Introduction of a Metropolis-Gibbs method and comparison with linear locations, in Advances in Seismic Event Loca/on Thurber, C.H., and N. Rabinowitz (eds.), Kluwer, Amsterdam, 101-134.

McNamara, D. E., and Buland, R. P. (2004). Ambient Noise Levels in the Continental United States. Bulletin of the Seismological Society of America, 94(4), 1517–1527.

McNamara, D. E., Hutt, C. R., Gee, L. S., Benz, H. M., & Buland, R. P. (2009). A Method to Establish Seismic Noise Baselines for Automated Station Assessment. Seismological Research Letters, 80(4), 628–637. http://doi.org/10.1785/gssrl.80.4.628.

Mousavi, S. M, Ellsworth, W. L., Zhu, W., Chuang, L.Y. and Beroza, G.C. (2020). "Earthquake Transformer—an Asentive Deep-Learning Model for Simultaneous Earthquake Detec/on and

The PilotSTRATEGY project has received funding from the European Union's Horizon 2020 research and innovation programme under grant agreement No. 101022664

Phase Picking." Nature Communications 11 (1): 3952. hsps://doi.org/10.1038/ s41467-020-17591-w.

Olaiz, A.J., Muñoz-Martín, A., de Vicente, G., Vegas, R. and Cloetingh, S. (2009). European continuous active tectonic strain–stress map. Tectonophysics, 474, 33–40

Palomeras, I., Villaseñor, A., Thurner, S., Levander, A., Gallart, J. and Harnafi, M. (2017). "Lithospheric Structure of Iberia and Morocco Using Finite-Frequency Rayleigh Wave Tomography from Earthquakes and Seismic Ambient Noise." *Geochemistry, Geophysics, Geosystems* 18 (5): 1824– 40. hsps://doi.org/10.1002/2016GC006657.

Pereira, N., Carneiro, J.F., Araújo, A., Bezzeghoud, M. & Borges, J. (2014). Seismic and structural geology constraints to the selection of CO2 storage sites—The case of the onshore Lusitanian basin, Portugal. Journal of Applied Geophysics 102 (2014) 21–38.

Peterson (1993). Observation and modeling of seismic background noise, U.S. Geol. Surv. Tech. Rept. 93-322, 1–95.

Podvin, P. and Lecomte, I. (1991). Finite difference computation of travel times in very contrasted velocity models: a massively parallel approach and its associated tools. Geophysical Journal International, 105, 271-284.

Tarantola, A. and Valese, B. (1982). Inverse Problems=Quest for information. Journal of Geophysical Research, 50, 159–170.

Tryggvason, A., Rögnvaldsson, S.ð.T. and Flóvenz, Ó.G. (2002), Three-dimensional imaging of the *P*- and *S*-wave velocity structure and earthquake locations beneath Southwest Iceland. Geophysical Journal International, 151: 848-866. https://doi.org/10.1046/j.1365-246X.2002.01812.x

Villaseñor, A., Herrmann, R. B., Gaite, B. and Ugalde, A. (2020). "Fault Reactivation by Gas Injection at an Underground Gas Storage off the East Coast of Spain." Solid Earth 11 (1): 63– 74. https://doi.org/10.5194/se-11-63-2020.

Zhang, M., W. L. Ellsworth, and G. C. Beroza (2019). Rapid earthquake association and location, Seism. Res. Lett. 90, no. 6, 2276–2284 https://doi.org/10.1785/0220190052.

Zhu, W. and Beroza, G. C. (2019). PhaseNet: A Deep-Neural-Network-Based Seismic Arrival Time Picking Method. Geophysical Journal International, 216(1), 261–273. hsp://doi.org/10.1093/gji/ggy423

The PilotSTRATEGY project has received funding from the European Union's Horizon 2020 research and innovation programme under grant agreement No. 101022664

6. Appendices

The PilotSTRATEGY project has received funding from the European Union's Horizon 2020 research and innovation programme under grant agreement No. 101022664

APPENDIX I – CATALOG OF QUARRY EXPLOSIONS DETECTED BY LOPIN NETWORK USING 1D VELOCITY MODEL IN HYPOCENTER SOFTWARE

Date	Time	Latitude (°N)	Longitude (°E)	Depth (*)(km)
2023-09-01	10:19:50.40	41.4320	-0.399	0.0
2023-09-06	10:03:50.00	41.4780	-0.424	0.0
2023-09-21	10:28:21.70	41.4300	-0.406	0.0
2023-10-05	09:00:51.90	41.4220	-0.796	0.0
2023-10-09	11:00:28.30	41.4340	-0.398	0.0
2023-10-09	12:17:43.60	41.4870	-0.962	0.0
2023-10-19	08:54:53.00	41.3910	-0.807	0.0
2023-11-08	10:33:27.80	41.3950	-0.749	0.0
2023-11-20	11:18:40.10	41.4360	-0.401	0.0
2023-11-24	15:10:24.50	41.4740	-0.933	0.0
2023-11-29	10:32:48.90	41.4140	-0.845	0.0
2023-12-01	11:30:50.50	41.4280	-0.398	0.0
2023-12-05	11:15:22.50	41.4620	-0.847	0.0
2023-12-21	12:30:25.30	41.4490	-0.394	0.0
2024-01-16	11:45:04.70	41.3710	-0.912	0.0
2024-01-18	11:06:39.60	41.3710	-0.773	0.0
2024-01-23	09:40:58.30	41.2980	-0.898	0.0
2024-01-25	10:40:47.20	41.3950	-0.764	0.0
2024-01-25	13:01:59.70	41.4350	-0.386	0.0
2024-01-30	10:19:49.70	41.3470	-0.815	0.0
2024-02-21	10:05:16.10	41.3870	-0.850	0.0
2024-02-22	11:05:44.00	41.4460	-0.238	0.0
2024-03-04	12:18:40.20	41.4500	-0.270	0.0
2024-03-07	13:58:23.50	41.4990	-0.952	0.0
2024-03-13	11:40:45.10	41.4370	-0.397	0.0
2024-03-18	11:43:48.20	41.3910	-0.801	0.0
2024-03-19	12:15:27.00	41.4430	-0.428	0.0
2024-04-09	10:00:04.50	41.4100	-0.876	0.0
2024-04-22	09:57:41.00	41.4650	-0.425	0.0
2024-04-24	11:00:01.20	41.4280	-0.422	0.0
2024-05-03	11:35:30.00	41.4350	-0.411	0.0
2024-05-10	12:34:13.50	41.4300	-0.396	0.0
2024-05-15	10:00:14.80	41.3720	-0.867	0.0
2024-05-22	09:32:12.70	41.3540	-0.848	0.0
2024-05-23	09:57:39.10	41.4310	-0.392	0.0
2024-05-31	13:29:38.20	41.4910	-0.976	0.0
2024-06-03	10:26:49.60	41.4260	-0.437	0.0
2024-06-12	10:04:35.80	41.3550	-0.836	0.0

The PilotSTRATEGY project has received funding from the European Union's Horizon 2020 research and innovation programme under grant agreement No. 101022664

2024-06-17	09:48:13.30	41.4570	-0.369	0.0
2024-06-19	10:10:24.00	41.3550	-0.866	0.0
2024-06-27	09:11:18.20	41.3520	-0.812	0.0
2024-01-25	13:01:59.70	41.4350	-0.386	0.0
2024-01-30	10:19:49.70	41.3470	-0.815	0.0
2024-02-21	10:05:16.10	41.3870	-0.850	0.0
2024-02-22	11:05:44.00	41.4460	-0.238	0.0
2024-03-04	12:18:40.20	41.4500	-0.270	0.0
2024-03-07	13:58:23.50	41.4990	-0.952	0.0
2024-03-13	11:40:45.10	41.4370	-0.397	0.0
2024-03-18	11:43:48.20	41.3910	-0.801	0.0
2024-03-19	12:15:27.00	41.4430	-0.428	0.0
2024-04-09	10:00:04.50	41.4100	-0.876	0.0
2024-04-22	09:57:41.00	41.4650	-0.425	0.0
2024-04-24	11:00:01.20	41.4280	-0.422	0.0
2024-05-03	11:35:30.00	41.4350	-0.411	0.0
2024-05-10	12:34:13.50	41.4300	-0.396	0.0
2024-05-15	10:00:14.80	41.3720	-0.867	0.0
2024-05-22	09:32:12.70	41.3540	-0.848	0.0
2024-05-23	09:57:39.10	41.4310	-0.392	0.0
2024-05-31	13:29:38.20	41.4910	-0.976	0.0
2024-06-03	10:26:49.60	41.4260	-0.437	0.0
2024-06-12	10:04:35.80	41.3550	-0.836	0.0
2024-06-17	09:48:13.30	41.4570	-0.369	0.0
2024-06-19	10:10:24.00	41.3550	-0.866	0.0
2024-06-27	09:11:18.20	41.3520	-0.812	0.0
2024-07-01	09:26:29.90	41.5470	-0.857	0.0
2024-07-02	09:09:26.30	41.4330	-0.436	0.0
2024-07-02	10:41:04.50	41.3950	-0.753	0.0
2024-07-03	08:47:46.40	41.3200	-0.817	0.0
2024-07-05	10:43:25.90	41.4510	-0.934	0.0
2024-07-09	09:31:02.60	41.4020	-0.755	0.0
2024-07-09	10:23:47.10	41.4510	-0.849	0.0
2024-07-10	09:22:06.20	41.3670	-0.759	0.0
2024-07-11	09:39:44.80	41.4010	-0.795	0.0
2024-07-11	10:39:01.60	41.4410	-0.430	0.0
2024-07-16	10:14:18.40	41.4890	-0.439	0.0
2024-07-17	09:43:39.30	41.3630	-0.799	0.0
2024-07-18	09:22:07.60	41.4970	-0.418	0.0
2024-07-18	09:38:41.10	41.4640	-0.412	0.0
2024-07-22	10:09:14.30	41.4400	-0.412	0.0
2024-07-31	10:09:05.60	41.3770	-0.807	0.0
2024-08-26	09:37:20.30	41.4630	-0.414	0.0

The PilotSTRATEGY project has received funding from the European Union's Horizon 2020 research and innovation programme under grant agreement No. 101022664

APPENDIX II – CATALOG OF QUARRY EXPLOSIONS DETECTED BY LOPIN NETWORK USING 3D VELOCITY MODEL IN NonLinLoc SOFTWARE

Date	Time	Latitude (°N)	Longitude (°E)	Depth (*)(km)
2023-09-01	10:19:49.13	41.4260	-0.384	-2.8
2023-09-06	10:03:48.16	41.4640	-0.383	-2.5
2023-09-21	10:28:20.52	41.4290	-0.400	3.5
2023-10-05	09:00:50.83	41.3830	-0.781	0.1
2023-10-09	11:00:27.09	41.4320	-0.406	3.3
2023-10-09	12:17:43.00	41.4690	-0.913	2.3
2023-10-19	08:54:52.54	41.4040	-0.744	-1.7
2023-11-08	10:33:26.74	41.3910	-0.737	2.0
2023-11-20	11:18:38.90	41.4310	-0.400	4.1
2023-11-24	15:10:23.26	41.4680	-0.906	4.0
2023-11-29	10:32:47.97	41.3920	-0.806	3.7
2023-12-01	11:30:49.12	41.4320	-0.400	3.6
2023-12-05	11:15:21.27	41.4450	-0.823	1.7
2023-12-21	12:30:23.94	41.4370	-0.373	4.4
2024-01-16	11:45:04.59	41.3770	-0.827	5.2
2024-01-18	11:06:39.13	41.3980	-0.698	2.8
2024-01-23	09:40:58.62	41.3430	-0.831	4.9
2024-01-25	10:40:46.43	41.3910	-0.737	6.1
2024-01-25	13:01:58.48	41.4370	-0.395	3.6
2024-01-30	10:19:49.91	41.4090	-0.732	2.4
2024-02-21	10:05:15.03	41.3730	-0.810	2.4
2024-02-22	11:05:44.03	41.4330	-0.334	10.5
2024-03-04	12:18:40.20	41.4340	-0.357	8.8
2024-03-07	13:58:22.72	41.4580	-0.934	5.2
2024-03-13	11:40:43.85	41.4320	-0.366	-2.9
2024-03-18	11:43:47.39	41.3880	-0.770	3.1
2024-03-19	12:15:25.41	41.4310	-0.388	-2.9
2024-04-09	10:00:03.33	41.3660	-0.804	-2.8
2024-04-22	09:57:39.87	41.4600	-0.370	-2.6
2024-04-24	10:59:59.82	41.4320	-0.391	4.5
2024-05-03	11:35:28.36	41.4250	-0.397	3.5
2024-05-10	12:34:12.28	41.4320	-0.397	2.7
2024-05-15	10:00:14.11	41.3690	-0.823	4.5
2024-05-22	09:32:12.44	41.3700	-0.793	4.0
2024-05-23	09:57:37.76	41.4250	-0.388	4.1
2024-05-31	13:29:37.43	41.4680	-0.934	2.4
2024-06-03	10:26:48.37	41.4270	-0.414	3.7
2024-06-12	10:04:35.67	41.3840	-0.771	4.0
2024-06-17	09:48:12.20	41.4550	-0.391	4.9

The PilotSTRATEGY project has received funding from the European Union's Horizon 2020 research and innovation programme under grant agreement No. 101022664

2024-06-19	10:10:23.47	41.3590	-0.821	3.2
2024-06-27	09:11:17.94	41.3900	-0.761	4.5
2024-07-01	09:26:28.62	41.4470	-0.822	2.4
2024-07-02	09:09:25.16	41.4380	-0.416	3.3
2024-07-02	10:41:03.75	41.4060	-0.722	3.7
2024-07-03	08:47:46.60	41.3810	-0.765	5.2
2024-07-05	10:43:24.84	41.4610	-0.906	2.4
2024-07-09	09:31:01.92	41.4050	-0.732	3.6
2024-07-09	10:23:46.09	41.4440	-0.822	2.8
2024-07-10	09:22:05.06	41.3770	-0.754	4.0
2024-07-11	09:39:44.26	41.4090	-0.715	0.4
2024-07-11	10:39:00.54	41.4330	-0.412	3.2
2024-07-16	10:14:17.46	41.4850	-0.444	-2.9
2024-07-17	09:43:38.74	41.3910	-0.754	4.8
2024-07-18	09:22:07.03	41.4790	-0.429	0.0
2024-07-18	09:38:39.94	41.4550	-0.385	0.5
2024-07-22	10:09:13.12	41.4370	-0.401	4.0
2024-07-31	10:09:04.44	41.3760	-0.781	3.5
2024-08-26	09:37:18.81	41.4370	-0.378	-2.0

The PilotSTRATEGY project has received funding from the European Union's Horizon 2020 research and innovation programme under grant agreement No. 101022664

The PilotSTRATEGY project has received funding from the European Union's Horizon 2020 research and innovation programme under grant agreement No. 101022664

Year	mon	day	hour	min	sec	Lat (ºN)	Lon(ºE)	Depth (km)	Magn (Ml)
2023	2	1	11	42	42.49	39.656	-9.144	7	0.5
2023	2	4	18	0	47.3	39.459	-9.108	16	0.7
2023	2	4	19	4	32.9	39.897	-8.426	10	0.8
2023	2	5	1	4	45.2	40.294	-8.5	0	1.5
2023	2	6	13	50	46.77	39.378	-8.82	9	0.3
2023	2	8	15	4	28.13	39.337	-8.819	1	0.5
2023	2	10	0	0	0.49	39.51	-9.048	21	0.5
2023	2	14	23	12	17.2	39.518	-8.357	2	0.6
2023	3	9	13	48	38.1	39.402	-9.447	2	1.2
2023	3	10	3	38	19.1	39.676	-8.887	4	0.7
2023	3	15	14	28	31.17	39.55	-9.08	4	0.4
2023	3	15	16	0	5.35	40.192	-9.334	18	0.8
2023	3	15	16	0	5.35	40.192	-9.334	18	0.5
2023	3	16	10	38	59.72	39.349	-8.983	7	0.5
2023	3	16	14	28	53.13	39.727	-8.888	18	0.8
2023	3	19	12	55	33.03	39.368	-8.378	7	0.8
2023	3	19	12	55	33.1	39.262	-8.597	5	1.0
2023	3	19	19	19	46.19	39.362	-8.994	7	0.5
2023	3	20	12	20	26.2	39.405	-9.286	1	1.1
2023	3	20	19	31	27.3	39.336	-8.764	6	2.1
2023	3	21	14	28	32.32	39.727	-8.867	20	0.7
2023	3	24	12	18	8.1	39.51	-9.306	12	0.9
2023	3	30	1	46	51.3	40.331	-8.404	6	0.9
2023	4	4	13	29	5.39	39.671	-9.083	0	0.5
2023	4	4	23	19	30	39.782	-8.747	22	2.6
2023	4	5	9	0	8.29	40.428	-8.84	7	0.8
2023	4	6	13	32	3.55	39.672	-8.98	16	0.5
2023	4	6	22	18	48.2	40.422	-8.51	7	1.2
2023	4	7	5	39	36.4	40.237	-8.43	8	0.7

The PilotSTRATEGY project has received funding from the European Union's Horizon 2020 research and innovation programme under grant agreement No. 101022664

2023	4	8	16	25	34.2	39.276	-8.502	3	0.5
2023	4	9	5	41	29.2	39.473	-8.377	10	0.2
2023	4	9	17	31	33.26	39.903	-8.83	6	0.5
2023	4	10	15	25	54.8	39.28	-9.363	0	1.0
2023	4	11	1	45	38.5	39.718	-8.629	14	0.7
2023	4	12	3	58	10.4	40.202	-8.442	16	0.9
2023	4	13	13	29	33.42	39.565	-8.905	21	0.5
2023	4	13	21	51	13.1	39.54	-8.982	12	1.3
2023	4	17	13	29	31.27	39.714	-8.867	18	0.7
2023	4	20	16	50	42.6	40.285	-9.156	11	2.4
2023	4	23	22	6	22.81	39.512	-8.874	5	0.8
2023	4	25	3	11	40.85	39.779	-9.085	18	0.5
2023	4	26	13	6	11.32	39.767	-8.941	25	0.6
2023	4	27	3	7	25.7	39.821	-8.718	6	0.8
2023	4	27	6	18	10.31	39.752	-9.074	11	0.8
2023	4	30	0	0	4.69	39.55	-9.049	0	0.5
2023	4	30	15	28	58.79	39.658	-9.052	11	0.8
2023	5	1	5	27	59.67	39.552	-8.895	22	0.8
2023	5	1	9	24	53.6	39.773	-8.561	14	1.5
2023	5	3	0	0	9.30	39.512	-8.832	25	0.5
2023	5	4	9	57	56.98	39.458	-8.883	24	0.3
2023	5	4	10	46	50.80	39.849	-8.829	13	0.5
2023	5	4	13	28	48.26	39.712	-8.991	14	0.9
2023	5	12	12	55	42.21	39.657	-9.103	0	0.8
2023	5	14	15	44	10.6	39.999	-8.004	13	1.3
2023	5	16	10	50	23.61	40.334	-8.869	7	0.8
2023	5	16	17	26	38.74	40.495	-8.841	6	0.4
2023	5	17	10	35	30.52	39.516	-8.493	0	0.5
2023	5	20	10	0	22.87	40.374	-8.849	7	0.5
2023	5	22	13	29	41.00	39.59	-9.091	0	0.5

The PilotSTRATEGY project has received funding from the European Union's Horizon 2020 research and innovation programme under grant agreement No. 101022664

2023	5	23	1	50	14.2	40.267	-8.668	3	0.8
2023	5	24	3	17	50.93	39.594	-8.741	0	0.6
2023	5	25	7	0	41.51	39.645	-8.99	12	0.5
2023	5	25	22	49	53.05	39.473	-8.77	13	0.9
2023	5	26	20	12	47.7	40.193	-8.471	21	0.7
2023	5	27	22	12	57.5	39.894	-8.803	5	0.6
2023	5	29	6	56	13.40	39.658	-9.021	12	0.8
2023	5	29	10	15	28.07	40.48	-9.008	55	0.6
2023	5	30	12	38	5.86	40.199	-8.877	0	0.5
2023	5	30	18	2	2.30	40.287	-9.295	17	0.8
2023	6	1	0	2	18.6	40.002	-8.586	12	0.3
2023	6	1	7	39	45.05	39.751	-9.126	7	0.5
2023	6	2	3	9	5.6	39.849	-8.756	8	0.7
2023	6	3	17	2	59.96	39.552	-8.905	14	0.8
2023	6	7	14	27	39.11	39.759	-8.445	0	0.8
2023	6	16	12	55	39.56	39.698	-9.073	4	0.5
2023	6	17	13	20	5.61	39.753	-8.992	6	0.5
2023	6	17	13	27	20.54	39.674	-8.835	22	0.5
2023	6	18	2	57	1.69	39.353	-8.634	32	0.9
2023	6	18	2	57	2.4	39.317	-9.083	15	1.0
2023	6	19	15	0	4.07	40.46	-8.371	7	0.8
2023	6	19	19	3	53.48	40.34	-9.348	7	0.6
2023	6	20	0	0	4.67	39.686	-8.918	18	0.5
2023	6	20	7	27	40.59	39.741	-8.826	4	0.5
2023	6	21	15	32	4.00	40.231	-8.295	21	0.7
2023	6	22	8	49	58.66	39.362	-8.984	4	0.5
2023	6	24	5	56	52.5	39.717	-8.662	14	1.4
2023	6	25	7	6	11.6	40.157	-8.128	11	0.7
2023	6	25	13	46	16	39.256	-8.905	13	0.7
2023	6	26	10	48	34.85	39.739	-8.992	21	0.6

The PilotSTRATEGY project has received funding from the European Union's Horizon 2020 research and innovation programme under grant agreement No. 101022664

2023	6	27	13	26	17.52	39.753	-8.992	5	0.5
2023	7	7	10	31	14.15	40.197	-9.033	0	0.5
2023	7	11	10	32	27.44	39.764	-9.147	7	0.5
2023	7	17	4	40	15.4	39.599	-8.301	18	0.3
2023	7	20	0	10	32.9	40.027	-8.008	15	0.9
2023	7	26	13	28	53.40	39.671	-9.083	2	0.5
2023	7	27	11	18	23.1	39.63	-8.199	10	3.0
2023	7	30	0	20	21.3	39.559	-9.05	21	0.9
2023	8	2	13	26	41.94	39.63	-9.092	0	0.5
2023	8	4	9	53	2.97	39.643	-9.134	0	0.5
2023	8	4	10	53	54.58	39.781	-8.91	23	0.5
2023	8	4	14	28	8.6	39.376	-9.122	3	0.9
2023	8	5	1	37	4.7	39.803	-8.641	11	2.7
2023	8	7	13	31	28.03	39.603	-9.102	0	0.5
2023	8	11	12	37	37.26	39.659	-8.959	29	0.5
2023	8	12	9	7	12.76	39.553	-8.823	7	0.5
2023	8	12	10	21	28.18	39.498	-8.894	0	0.5
2023	8	14	10	36	19.19	39.486	-8.822	4	0.5
2023	8	14	13	31	12.02	39.603	-9.112	0	0.5
2023	8	16	9	18	32.21	39.588	-9.194	0	0.5
2023	8	16	13	27	19.50	39.59	-9.112	0	0.9
2023	8	17	13	30	40.50	39.657	-9.103	0	0.6
2023	8	18	12	52	53.22	39.549	-9.101	7	0.9
2023	8	18	16	31	41.5	39.524	-8.999	8	0.7
2023	8	19	0	49	15.9	39.305	-8.659	13	0.5
2023	8	19	11	13	26.32	39.903	-8.83	15	0.8
2023	8	21	13	27	18.53	39.603	-9.102	0	0.8
2023	8	21	17	22	8.34	39.672	-9	22	0.9
2023	8	22	7	10	13	39.76	-8.74	11	2.2
2023	8	22	8	7	46.09	39.751	-9.095	9	0.5

The PilotSTRATEGY project has received funding from the European Union's Horizon 2020 research and innovation programme under grant agreement No. 101022664

2023	8	22	11	53	23.74	39.472	-8.821	20	0.6
2023	8	22	13	30	41.57	39.603	-9.092	0	0.3
2023	8	23	13	25	2.71	39.644	-9.093	0	0.5
2023	8	24	10	29	6.56	39.524	-8.987	35	1.0
2023	8	25	12	55	16.76	39.603	-9.102	0	0.5
2023	8	25	18	45	59.3	39.697	-8.718	13	0.7
2023	8	28	2	27	22.53	39.431	-8.913	12	0.8
2023	8	28	10	29	2.43	39.526	-8.822	12	0.8
2023	8	29	13	29	53.59	39.603	-9.102	0	0.5
2023	8	30	13	27	3.06	39.617	-9.102	1	0.5
2023	8	30	17	43	31.90	39.389	-8.984	11	0.5
2023	8	31	8	8	16.38	39.593	-8.834	0	0.8
2023	8	31	13	29	38.34	39.603	-9.102	0	0.8
2023	8	31	15	54	28.19	39.768	-8.837	21	0.3
2023	8	31	17	43	42.09	39.809	-8.817	32	0.5
2023	8	31	19	45	4.7	39.705	-8.71	13	0.7
2023	9	1	12	58	53.05	39.657	-9.093	2	0.4
2023	9	3	7	24	36.52	39.791	-9.127	0	0.4
2023	9	4	13	28	3.03	39.657	-9.093	2	0.6
2023	9	11	13	28	18.82	39.753	-9.002	3	0.5
2023	9	12	13	26	47.87	39.603	-9.102	0	0.5
2023	9	13	1	58	38.73	39.868	-8.136	45	0.5
2023	9	14	13	29	22.06	39.59	-9.112	0	0.8
2023	9	15	12	39	24.84	39.543	-8.504	0	0.8
2023	9	15	12	55	24.14	39.644	-9.093	1	0.5
2023	9	15	13	57	50.5	39.557	-8.457	18	0.7
2023	9	18	13	26	35.47	39.603	-9.092	0	0.8
2023	9	19	13	21	8.30	40.276	-9.149	17	0.5
2023	9	23	11	51	21.8	39.752	-8.654	11	1.2
2023	9	23	11	52	8	39.74	-8.665	11	0.3

The PilotSTRATEGY project has received funding from the European Union's Horizon 2020 research and innovation programme under grant agreement No. 101022664

2023	9	23	12	35	3.6	39.748	-8.652	13	1.7
2023	9	28	13	25	5.67	39.589	-9.122	0	0.8
2023	10	7	15	51	38.16	39.334	-9.065	10	0.5
2023	10	9	5	23	25.5	39.546	-8.188	12	0.4
2023	10	9	13	21	21.75	39.59	-9.081	0	0.5
2023	10	11	5	24	21.64	39.431	-8.913	11	0.8
2023	10	11	13	27	28.69	39.657	-9.103	0	0.7
2023	10	11	22	44	11.39	40.342	-9.265	2	0.5
2023	10	12	13	24	52.09	39.442	-9.047	0	0.8
2023	10	13	12	57	8.42	39.617	-9.102	0	1.0
2023	10	24	2	37	49.2	39.698	-8.749	12	1.0
2023	10	25	8	10	24.69	39.362	-8.994	0	0.8
2023	10	27	12	54	23.11	39.603	-9.102	0	0.8
2023	10	31	13	55	51.4	40.083	-8.835	12	0.9
2023	10	31	14	20	39.58	39.768	-8.827	25	0.8
2023	10	31	14	28	49.92	39.617	-9.092	0	0.8
2023	11	2	20	42	48.5	40.152	-8.917	7	2.9
2023	11	3	10	37	21.2	39.365	-8.678	20	2.1
2023	11	3	13	53	46.53	39.603	-9.092	0	0.8
2023	11	3	15	42	23.1	39.808	-8.59	14	0.6
2023	11	6	8	17	44.02	39.767	-8.91	25	0.3
2023	11	6	14	28	59.92	39.603	-9.102	0	0.8
2023	11	30	0	57	54.5	39.476	-9.01	8	0.4
2023	12	5	14	29	25.50	39.603	-9.102	0	0.7
2023	12	5	22	22	50.8	39.26	-8.915	11	1.0
2023	12	6	14	27	47.58	39.59	-9.112	0	0.7
2023	12	7	14	31	15.35	39.59	-9.112	0	0.6
2023	12	8	21	15	43.18	39.647	-8.825	25	0.8
2023	12	15	13	58	55.49	39.657	-9.103	0	0.5
2023	12	15	23	46	24.44	39.377	-8.912	10	0.9

The PilotSTRATEGY project has received funding from the European Union's Horizon 2020 research and innovation programme under grant agreement No. 101022664

2023	12	18	3	38	41.9	39.642	-9.263	5	1.5
2023	12	18	22	9	10.5	39.65	-9.247	11	2.3
2023	12	18	23	28	8.9	40.141	-8.338	12	0.1
2023	12	19	19	15	45.94	40.193	-9.313	8	0.8
2023	12	26	10	7	12.74	39.536	-9.1	18	0.8
2023	12	26	15	39	41.98	39.593	-8.844	0	0.5
2023	12	27	15	4	27.6	39.797	-8.027	0	1.5
2023	12	29	13	59	25.66	39.657	-9.093	1	0.5